Syntheses, Reactivity and Thermochemistry of some Organoplatinum and Organopalladium Complexes.

by

Robin Kapadia, B. Sc., A.R.C.S.

A Thesis Submitted for the Degree of Doctor of Philosophy in the University of London and for the Diploma of Imperial College.

Department of Chemistry
Imperial College of Science, Technology and Medicine
London SW7 2AZ
United Kingdom

January 1990

To my parents and my sister.

ABSTRACT

A series of complexes *cis*-$L_2Pd(CH_2CMe_2Ph)_2$ (L_2 = bipy, Me_2bipy, phen), *cis*-$L_2Pd(CH_2SiMe_2Ph)_2$ (L_2 = bipy, Me_2bipy, phen, dppe), *trans*-$(Ph_2MeP)_2Pd(CH_2SiMe_2Ph)(Cl)$ and *cis*-dppePd$(CH_2SiMe_3)_2$ have been synthesised by alkylation of L_2PdX_2 (X = Cl or Br) using organomagnesium reagents. These complexes were characterised by ^1H and, in some cases, ^{31}P and ^{13}C NMR spectroscopy.

Similar reaction of (bipym)$PdCl_2$ with RMgCl (R = CH_2SiMe_2Ph, CH_2SiMe_3, CH_2CMe_2Ph) gave species whose NMR characteristics indicated nucleophilic attack on one of the bipyrimidyl rings as well as substitution of at least one of the chloride ligands. The complex produced when R = CH_2SiMe_2Ph was characterised by 2D ^1H COSY NMR.

Thermochemical and kinetic studies on a pair of organoplatinum complexes, *trans*-$(Me_3P)_2Pt(R)(Cl)$ (R = CH_2SiMe_3, CH_2CMe_3) have shown the neopentyl ligand to have a greater Pt-C bond strength, *trans*-effect and *trans*-influence than the analogous trimethylsilylmethyl substituent. The order of Pt-C bond strengths is opposite to that in all the previously determined bond strenghts in pairs of neopentyl and trimethylsilylmethyl complexes and the reverse of that expected on the basis of the kinetic labilities of neopentyl and trimethylsilylmethyl complexes in general. These labilities may derive from the relative *trans*-effects of the two alkyl groups.

ACKNOWLEDGEMENTS

I should like to thank Dr. G. Brent Young for his support, guidance and friendship over the past three years.

I should also like to mention Steve, Rob, Debbie, Louise, Katie, Bernardeta, Vic, Andy, Vahé, Steve, Peter, Hussein, Debbie, Greg and John, some of whom were members of the GBY group and all of whom were friends. Special thanks must go to Brian, Chris and Sanjoy for making my time at college so enjoyable.

Most of my NMR spectra were run by Dick Sheppard and Sue Johnson.

The research was carried out with the aid of a S.E.R.C. Studentship; Johnson Matthey provided a loan of palladium and Dr. Pedley supplied the calorimeter together with helpful advice.

Finally, I have to thank my family without whose support, both moral and financial, this work would not have been possible.

CONTENTS

	Page
Title Page	1
Abstract	3
Acknowledgements	4
Contents	5
List of Figures	7
List of Tables	10
Abbreviations	12
Numbering Conventions	13
Chapter One; Synthesis and Spectroscopy of Dineophyl- and Disila-neophylpalladium (II) Complexes with Bidentate Nitrogen and Phosphorus Donor Ligands	14
1.1. Introduction	15
1.2. Experimental	20
1.3. Discussion	25
1.3.1. Complexes with Bidentate Nitrogen Donor Ligands	25
1.3.2. Complexes with Phosphorus Donor Ligands .	33
1.3.3. Thermal Rearrangement of (bipy)Pd($CH_2CMe_2Ph)_2$	39
Chapter Two; Nucleophilic Attack of Carbanionic Reagents on 2,2'-Bipyrimidyl Coordinated to Palladium . . .	42
2.1. Introduction	43
2.2. Experimental	45
2.3. Discussion	50

Chapter Three; Relative Platinum-Carbon Bond Strengths in Organoplatinum Complexes with β-Carbon and Silicon Atoms . . . 68

3.1. Introduction 69

3.2. Syntheses of Reagents 78

3.3. Apparatus 82

3.4. Results 93

3.5. Discussion 95

Chapter Four; The relative *Trans*- Effects and *Trans*-Influences of the Neopentyl and Trimethylsilylmethyl Ligands in $(Me_3P)_2Pt(CH_2SiMe_3)Cl$ and $(Me_3P)_2Pt(CH_2CMe_3)Cl$. 104

4.1. Introduction 105

4.2. Experimental 105

4.3. Results 111

4.4. Discussion 117

References 121

LIST OF FIGURES

		Page
1.1.	β-Hydride Elimination from Transition Metal Alkyl Complexes.	15
1.2.	α-Hydrogen Transfer, Intramolecular Reductive Elimination, γ-, δ– and ε-Hydrogen Transfers in Transition Metal Alkyl Complexes . . .	16
1.3.	Proposed Mechanism for the Thermal Cyclisation of $L_2Pt(CH_2CMe_2Ph)_2$. (L=PEt_3) . . .	17
1.4.	Isolated Ir(III)Hydridoalkyl Complex . .	18
1.5.	^1H NMR of (bipy)$Pd(CH_2SiMe_2Ph)_2$ . . .	30
1.6.	^1H NMR of (bipy)$Pd(CH_2CMe_2Ph)_2$ . . .	31
1.7.	^{13}C NMR of (Me_2bipy)$Pd(CH_2CMe_2Ph)_2$ . .	34
1.8.	^1H NMR of (dppe)$Pd(CH_2SiMe_2Ph)_2$ . . .	38
2.1.	Nucleophilic 1,6-addition of PhH to a 2,4-disubstituted pyrimidine . . .	43
2.2.	Reaction of RMgCl with (bipym)$PdCl_2$ where R= -CH_2SiMe_2Ph and -CH_2SiMe_3 and X is unknown.	44
2.3.	^1H NMR spectrum of **2a**.	51
2.4.	Decoupling experiments on **2a** . . .	53
2.5.	Proposed structure of **2a**	55
2.6.	Newman Projection along the H_2C-C_6' bond of **2a**	57
2.7.	^1H NMR resonances for H11a, H11b and H21a in complex **2a**	58
2.8.	^1H NMR spectrum of **2b**.	59

2.9.	Proposed structure of **2b**	61
2.10.	Calculated Charges (x 1000) on Ring in Free Ligands and in $[FeL(CN)_4]^{2-}$ Complexes . .	64
3.1.	Reversible Cyclometallation in *cis*-L_4OsRH where L=PMe_3 and E=Si or C . .	69
3.2.	Reaction of $[Ir(PMe_3)_4]Cl$ with $LiCH_2CMe_3$ and $LiCH_2SiMe_3$ with Subsequent Cyclometallations	70
3.3.	Cyclometallation of Thorium Dialkyls . .	70
3.4.	Alkylation of $[(h^5\text{-}C_5Me_5)(PPh_3)RhCl_2]$ by Me_3SiCH_2MgCl and Me_3CCH_2MgCl. . .	71
3.5.	Proposed Mechanism for the Thermal Cyclisation of $Pt(CH_2CMe_3)(PEt_3)_2$ . . .	72
3.6.	Proposed Mechanism for the Thermal Rearrangement of $Pt(CH_2SiMe_3)_2(PEt_3)_2$ . .	73
3.7.	Cyclometallation of $L_2Pt(CH_2CMe_2Ph)_2$ (where L_2=cod, bipy, bipym, Ph_2phen or L=PEt_3, PPh_3)	74
3.8.	Cyclometallation of $(Me_3P)_2Ni(CH_2CMe_2Ph)_2$ produced from $(Me_3P)NiCl_2$ or $(tmed)Ni(CH_2CMe_2Ph)_2$	75
3.9.	Mechanism for the Protonolysis of *trans*-$(Et_3P)_2Pt(CH_2CMe_3)Cl$	77
3.10.	Calorimeter	83
3.11.	Electrical Circuit used to Measure the Resistance of the Thermistor . . .	84
3.12.	Temperature Characteristics of Thermistor .	85
3.13.	Apparatus for sealing bulbs	87

3.14.	Typical Plots of Thermistor and Wall Temperatures against Time for a Reaction Step	89
3.15.	Typical Plot of T versus Time for a Reaction Step	91
3.16.	Comparative NMR Characteristics for (cod)Pt(CH_2CMe_2Ph)$_2$ and (cod)Pt(CH_2SiMe_2Ph)$_2$	99
3.17.	^{13}C-{^1H} NMR of methylene carbon for *trans*-(Me_3P)$_2$Pt(CH_2CMe_3)Cl in $CDCl_3$ . .	101
3.18.	^{13}C-{^1H} NMR of methylene carbon for *trans*-(Me_3P)$_2$Pt(CH_2SiMe_3)Cl in $CDCl_3$ . .	102
4.1.	Reaction of *trans*-(Me_3P)$_2$Pt(CH_2CMe_3)Cl with OMe^- in MeOH	112
4.2.	Reaction of *trans*-(Me_3P)$_2$Pt(CH_2SiMe_3)Cl with OMe^- in MeOH	113
4.3.	Graph of 10^4k_{obsd} against [$^-$OMe] for the Reaction with (Me_3P)$_2$Pt(CH_2SiMe_3)Cl . .	115
4.4.	Graph of 10^3k_{obsd} against [$^-$OMe] for the Reaction with (Me_3P)$_2$Pt(CH_2CMe_3)Cl . .	116

LIST OF TABLES

		Page
1.1.	Elemental Analyses of L_2PdBr_2 where L_2=bipy, Me_2bipy and phen . . .	22
1.2.	^1H NMR Data for Dineophylpalladium Complexes (**1a-1c**)	27
1.3.	^1H NMR Data for Disila-neophylpalladium Complexes (**1d-1f**)	28
1.4.	^1H NMR Chemical Shifts of Methylene Resonances in L_2MR_2 . . .	29
1.5.	^{31}P NMR Characteristics of **1g**, **1h**, **1i** and Comparable Complexes . . .	35
1.6.	^1H NMR Data for **1g**, **1h** and **1i** . . .	37
1.7.	^{13}C NMR Data for **1g**, **1h**, (dppe)Pt(CH_2-$CMe_3)_2$ and (dppe)Pt($CH_2SiMe_3)_2$ . . .	39
2.1.	Comparison of pyrimidine ring resonances in ^1H NMR spectra of **2a**, **2b** and**2c**. . .	46
2.2.	Comparison of methylene and methyl resonances in ^1H NMR spectra of **2a**, **2b** and **2c** .	47
2.3.	Comparison of phenyl resonances in ^1H NMR spectra of **2a**, **2b** and **2c** . . .	48
3.1.	ΔlnR Values Measured for Individual Reaction Steps	94
3.2.	Previously Determined Metal-Carbon Bond Strengths for Neopentyl and Trimethylsilylmethyl Complexes	96

3.3. Comparison of Steric Hindrance in Analagous Neopentyl and Trimethylsilylmethyl Complexes. 98

4.1. Measured Values for k_{obsd} for the Reaction of MeO^- with *Trans*-$(Me_3P)_2(CH_2EMe_3)Cl$ (where E=Si or C) at 20±1°C 110

4.2. Measured k_1 and k_2 Values and their Standard Deviations at 20±1°C for the Reaction of MeO^- with *Trans*-$(Me_3P)_2Pt(CH_2EMe_3)Cl$ (where E=Si or C) 117

4.3. Platinum-Chlorine Stretching Frequencies in various *Trans*-Organoplatinum Complexes . 118

ABBREVIATIONS

ABS	Absorbance
acac	2,4-pentanedionato
adme	tricyclo[3.3.1,1]dec-1-ylmethyl
bipy	2,2'-bipyridine
bipym	2,2'-bipyrimidine
cod	1,5-cyclooctadiene
COSY	Correlation Spectroscopy
Cp	h^5-C_5H_5
Cp*	h^5-C_5Me_5
δ	NMR Chemical Shift Relative to Tetramethylsilane
DMC	1,1-dimethylcyclopropane
dmpe	1,2-bis(dimethylphosphino)ethane
dppe	1,2-bis(diphenylphosphino)ethane
ε	Molar Extinction Coefficient
FT	Fourier Transform
HOMO	Highest Occupied Molecular Orbital
IR	Infrared
LUMO	Lowest Unoccupied Molecular Orbital
M	Mole dm^{-3}
Me_2bipy	4,4'-dimethyl-2,2'-bipyridine
neopentyl	2,2-dimethylpropyl
neophyl	2-methyl-2-phenylpropyl
nm	Nanometre (10^{-9}m)
NMR	Nuclear Magnetic Resonance
phen	1,10-phenanthroline
Ph_2phen	4,7-diphenyl-1,10-phenanthroline

ppm	parts per million
py	pyridine
saloph	N,N'-bis(salicylidene)-o-phenylenediamine
sila-neophyl	dimethyl(phenyl)silylmethyl
THF	tetrahydrofuran
tmed	N,N,N',N'-tetramethylethylenediamine
UV-vis	Ultra-Violet-Visible
2D	Two-Dimensional

NUMBERING CONVENTIONS

Bipy, Me_2bipy, phen, all other heterocyclic ligands, together with substituted phenyl rings, were numbered throughout according to the IUPAC conventions. Where the IUPAC conventions do not apply, diagrams showing the numberings are inserted.

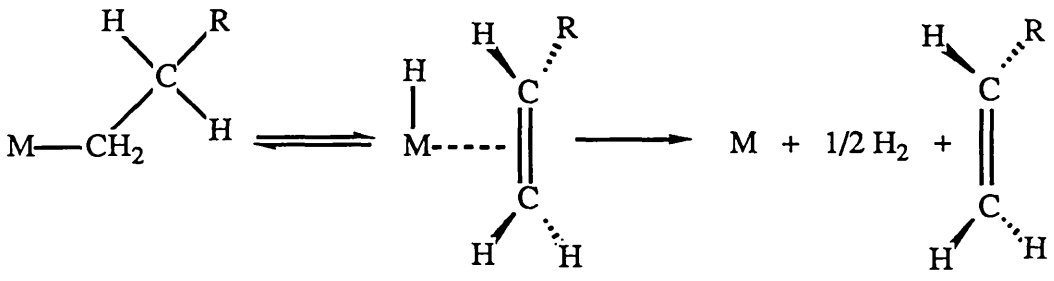
CHAPTER ONE

Synthesis and Spectroscopy of Dineophyl- and Disilaneophylpalladium (II) Complexes with Bidentate Nitrogen and Phosphorus Donor Ligands.

1.1. INTRODUCTION

The most common mode of decomposition of transition metal alkyls is by β-hydride transfer followed by elimination of the alkene produced (Fig. 1.1.)

Fig. 1.1. **β-Hydride Elimination from Transition Metal Alkyl Complexes.**



Examples of this reaction mode are common in the literature[1-3] and the mechanism is well understood. If, however, this rearrangement pathway can be blocked, either by using elimination stabilised alkyls which are unable to undergo such a hydrogen transfer, or by filling the coordination sphere of the metal (as the hydride and alkene groups produced by the rearrangement of one alkyl ligand require two coordination sites in which to bind) other less common reaction modes may become predominant. Examples of these other reaction modes which may take over include intramolecular reductive elimination, α–, γ-, δ–, and ε-hydrogen transfers (Fig. 1.2.)

We decided to take the former approach; using elimination stabilised alkyls without any β-hydrogens, such as the neopentyl- (Me_3CCH_2-), trimethylsilylmethyl- (Me_3SiCH_2)-, neophyl-

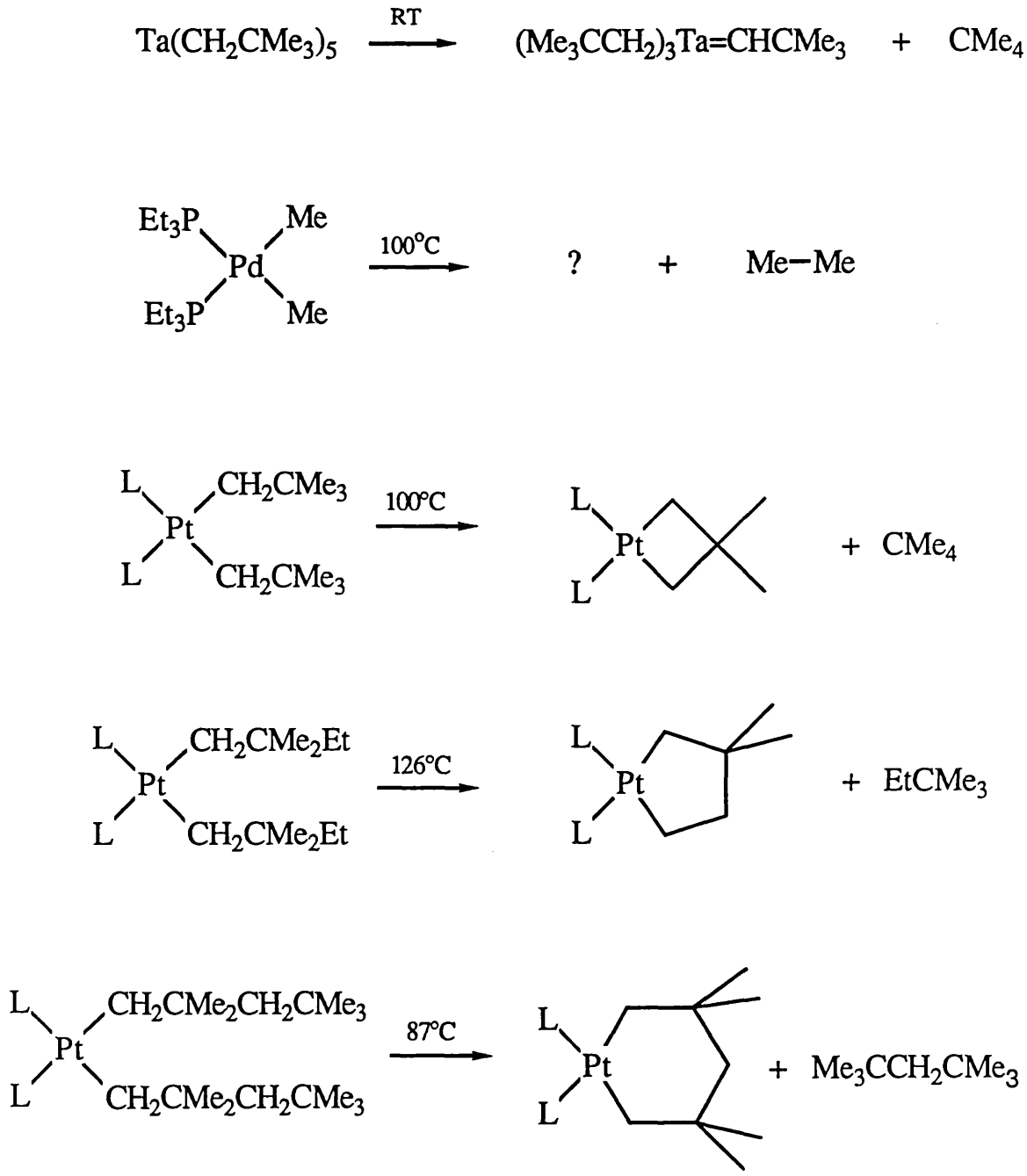


Fig. 1.2. **α-Hydrogen Transfer, Intramolecular Reductive Elimination, γ–, δ- and ε-Hydrogen Transfers in Transition Metal Alkyl Complexes.**

($PhMe_2CCH_2$-) and silaneophyl- ($PhMe_2SiCH_2$-) ligands, in order to prevent the β-hydride elimination process.

A range of di- and monoalkynickel[4-10] and -platinum[1-3,11-13] complexes with such alkyl ligands have been synthesised and characterised. While the di- and monoalkylplatinum, monoalkylnickel[5] and a few of the dialkylnickel complexes are thermally inert, most of the dialkylnickel complexes are labile[6] and rearrange at room temperature so that in some cases only the rearranged product is observed e.g. $NiCl_2(PMe_3)_2$ and $NiCl_2(PMe_2Ph)_2$ react with two equivalents of $(PhMe_2CCH_2)MgCl$ in Et_2O at ambient temperature to give $(Me_3P)_2Ni(CH_2CMe_2\text{-}o\text{-}C_6H_4)$[9] and $(PhMe_2P)_2Ni\text{-}(CH_2CMe_2\text{-}o\text{-}C_6H_4)$[10] respectively. In contrast dineophylplatinum (II) complexes in solution in toluene undergo an intramolecular hydrogen transfer from an aromatic δ-carbon to give a metallacycle and *tert*-butyl benzene (Fig. 1.3.) usually at elevated temperatures.[1-3]

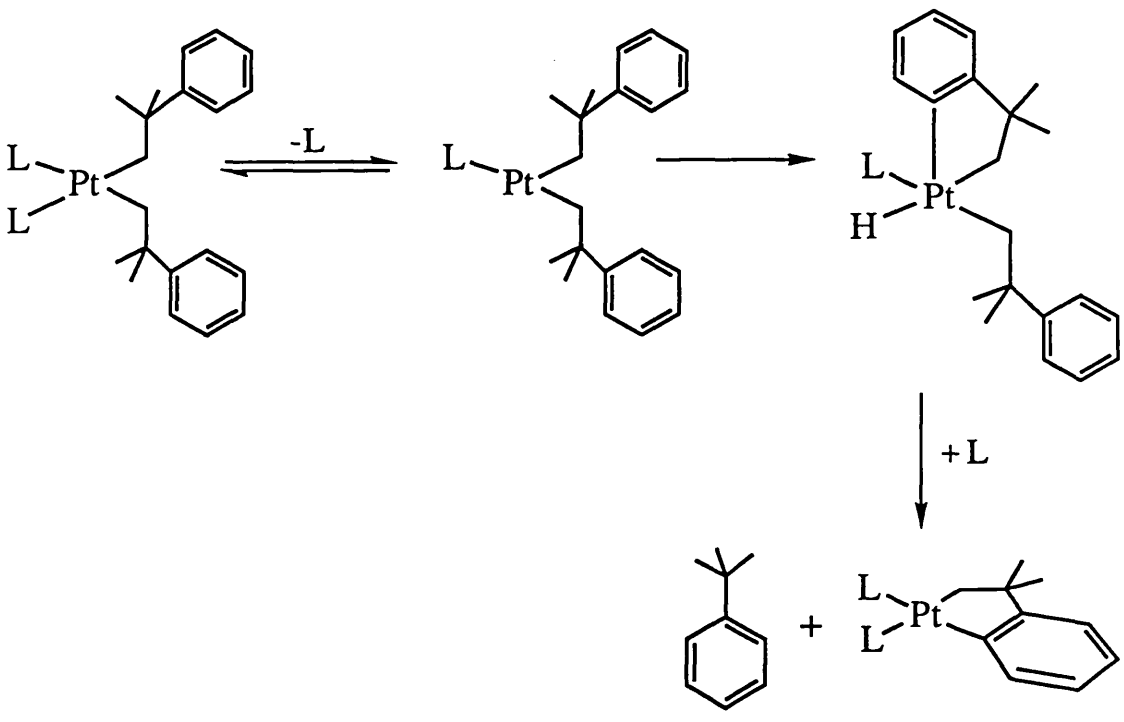


Fig. 1.3. **Proposed Mechanism for the Thermal Cyclisation of $L_2Pt(CH_2CMe_2Ph)_2$. (L=PEt_3)**

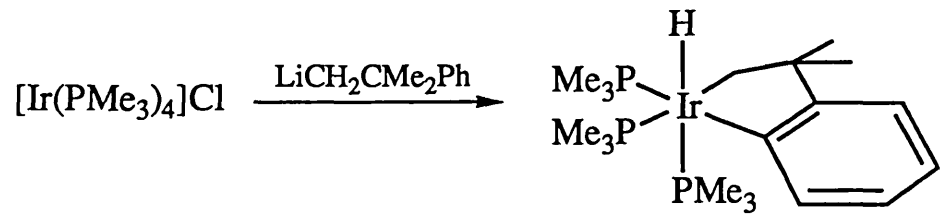


Fig. 1.4. **Isolated Ir(III) Hydridoalkyl Complex.**[15]

Although the platinum(IV) intermediate in Fig. 1.3. was not isolable, support for the mechanism below is provided by the formation of a similar iridium(III) hydrido-alkyl by the reaction of $LiCH_2CMe_2Ph$ with $[Ir(PMe_3)_4]Cl$ in hexane (Fig. 1.4.)[15]

The rate at which the cyclometallation of the dineophylplatinum complex occured was dependent upon the nature of the supporting ligands, L_2. The reaction is fastest for bulky monodentate ligands (e.g. PPh_3) and slower for chelating ligands.

The rearrangement reactions are also much more complicated for nickel complexes e.g. dineophylnickel complexes have been shown to give not only the nickelacyclopentene and *tert*-butylbenzene, but also dineophyl[4]. This is because both dialkylnickel (II) and dialkylpalladium (II) complexes more readily undergo intramolecular reductive elimination than dialkyl-platinum (II) complexes.[16]

Although the thermal rearrangements of dialkylplatinum (II) and dialkylnickel (II) complexes have been well studied, the same cannot be said of the corresponding dialkylpalladium (II) complexes, due to the greater difficulty of synthesising and handling the latter (the dialkylpalladium (II) complexes synthesised by us so far have shown themselves to be air-sensitive and thermally labile in solution at room temperature).

So it was decided to attempt to synthesise a new group of dialkylpalladium (II) complexes with neophyl and sila-neophyl ligands. Various bidentate N- and P-donors were envisaged as supporting ligands (L_2 in Fig. 1.3.) because they seem to increase the thermal inertness of the product.

A number of neutral, mononuclear mono- and dialkylbis-(phosphine)palladium (II) and mono- and dialkyl(bispyridine)-palladium (II) complexes have been synthesised to date, although apart from the multitude of methyl- and phenylpalladium (II) complexes so far characterised, few other simple organo-palladium (II) complexes have been found. Exceptions include the bis(heptafluoro-n-propyl)(bipy)palladium (prepared from the dimethyl complex)[17], a range of simple diethyl, di-n-propyl and di-n-butyl complexes (many prepared from $Pd(acac)_2$ and alkylaluminium reagents)[18-23], and several dicyanomethanide complexes.[24] Also notable are *cis*-$(Et_3P)_2Pd(CH_2SiMe_3)_2$,[25] *trans*-$(Et_3P)_2Pd(CH_2SiMe_3)Cl$[25] (both synthesised from the dichlorobis-(triethylphosphine)palladium (II)), *trans* - $(Me_3P)_2Pd(CH_2Si-Me_3)_2$[26], $(dmpe)Pd(CH_2SiMe_3)_2$[26] (both synthesised by the alkylation of palladium (II) acetate), *cis*- $(bipy)Pd(adme)_2$[27] and *trans*- $(Ph_3P)_2Pd(CH_2SMe)Cl$ (synthesised by the oxidative addition of chloromethylmethyl sulphide to $(Ph_3P)_4Pd$.[28,29]) It was decided to attempt the synthesis of similar organopalladium complexes by direct alkylation of the dichlorobis(phosphine)palladium or dibromo(bispyridine)pall-adium. This is the method used by Diversi et al[30] in their synthesis of the dineopentylpalladium (II) complexes $L_2Pd(CH_2CMe_3)_2$ where L_2 = dppe, bipy and L = PMe_2Ph.

1.2. EXPERIMENTAL

General and Instrumental.

Elemental analyses were performed by Imperial College Microanalytical Laboratories. NMR spectra were recorded on Bruker WM250 (^{1}H, 250.13MHz; ^{13}C, 62.9MHz) and Jeol FX90Q (^{13}C, 22.51MHz; ^{31}P, 36.21MHz) spectrometers. IR data were collected as Nujol mulls using CsI plates on a Perkin-Elmer 1720 FT spectrometer.

All reactions were carried out under an argon atmosphere using standard anaerobic techniques, except for the syntheses of L_2PdBr_2 (where L_2 is a bidentate nitrogen donor ligand) and (dppe)$PdCl_2$. Solvents were distilled under nitrogen prior to use; diethyl ether, hexane and tetrahydrofuran from sodium/ benzophenone and toluene from sodium.

Diphenylmethylphosphine and dppe were used as supplied by Strem Chemicals. Hydrobromic acid (49%), d- chloroform, 2,2'-dipyridyl, 4,4'-dimethyl-2,2'-dipyridyl and 1,10-phenanthroline monohydrate were used as supplied by the Aldrich Chemical Company. d_6-benzene and d_6-acetone were also supplied by the Aldrich Chemical Company but were predistilled (from sodium and potassium carbonate respectively) and stored under nitrogen. Acetone (AnalaR Grade) and lithium bromide were used as supplied by BDH Chemicals Ltd. Lithium chloride was used as supplied by Rose Chemicals Ltd.

Synthesis of (dppe)$PdCl_2$.

To a deep red acetone solution of $(PhCN)_2PdCl_2$[31] (0.40g, 1.04mmol in 25mL) was added dppe in toluene (0.42g, 1.05mmol in

15mL), with stirring to immediately give a pale-pink solid. This solid was filtered off, washed with cold acetone (5mL) and dried *in vacuo.* The complex was purified by Soxhlet extraction with acetone to give a pale yellow crystalline solid. I.R. (cm^{-1}) 3056(w), 3077(m), 1437(s), 1184(w), 1100(s), 999(m), 881(m), 821(s), 758(s), 745(s), 723(s), 718(s), 706(s), 696(s), 688(s), 657(m), 533(s), 492(s), 481(s), 461(w), 436(w), 395(w), 315(m), 296(m) and 251(m).

Anal. Calcd: C, 54.23; H, 4.21. Found: C, 54.18; H, 4.05.

Synthesis of $(Ph_2MeP)_2PdCl_2$.

$(PhCN)_2PdCl_2$[31] (0.40g, 1.04mmol) was dissolved in acetone (25mL) to give a red solution. To this solution was added Ph_2MeP (0.42g, 2.10mmol) in toluene (10mL) to give a pale yellow-green solid, which was washed with cold acetone (5mL) and dried *in vacuo* . I.R. (cm^{-1}) 3058(w), 1478(m), 1439(s), 1434(s), 1313(w), 1288(w), 1279(w), 1178(w), 1104(s), 1001(w), 906(s), 891(s), 841(w), 756(s), 750(m), 745(m), 738(s), 723(s), 708(w), 698(s), 688(w), 517(s), 507(m), 494(s), 479(s), 455(s), 413(w), 316(s), 295(s) and 254(m).

Anal. Calcd: C, 54.04; H, 4.54. Found: C, 53.89; H, 4.50.

Synthesis of $(bipy)PdBr_2$, $(Me_2bipy)PdBr_2$, and $(phen)PdBr_2$.

LiCl (0.424g, 10mmol) and $PdCl_2$ (0.866g, 5mmol) were fused together in a silica crucible over a Bunsen flame. The resulting dark-brown Li_2PdCl_4 was dissolved in water (100mL) and LiBr (1.74g, 20mmol) added to the red solution. Next HBr (1.30mL of a 49% solution, 10mmol) was added, the deep red

solution filtered, the free bidentate ligand (5mmol) added all at once (0.76g of bipy, 0.92g of Me_2bipy or 0.90g of phen) and the mixture stirred for one hour. Golden orange precipitates were produced almost immediately (although when L_2 = phen it had a pinkish tinge), which were filtered off, washed with water (20mL) and dried *in vacuo.* These compounds were purified by Soxhlet extraction with acetone. Elemental analyses are shown in Table 1.1.

Table 1.1.

Elemental Analyses of L_2PdBr_2 where L_2 = bipy, Me_2bipy and phen.

	Calcd.			Found		
L_2	%C	%H	%N	%C	%H	%N
bipy	28.43	1.91	6.63	29.03	1.83	6.76
Me_2bipy	31.99	2.69	6.22	30.69	2.62	5.95
phen	32.28	1.81	6.28	32.58	1.78	6.20

General synthesis of $L_2Pd(CH_2CMe_2Ph)_2$ and $L_2Pd(CH_2$-$SiMe_2Ph)_2$

To a suspension of L_2PdBr_2 (0.40g), where L_2 = bipy, Me_2bipy or phen, in THF (50mL) at -30° C was added 2.1 equivalents of $Mg(CH_2CMe_2Ph)Cl$ or $Mg(CH_2SiMe_2Ph)Cl$ in solution in Et_2O with stirring. The mixture was allowed to warm up to -15° C, stirred at this temperature for one hour, and then quenched with saturated aqueous NH_4Cl solution (5mL). All further manipulations

were carried out below -15°C. The dark orange organic layer was filtered off, the frozen aqueous layer washed with THF (2 x 10mL), and the combined washings and filtrate stirred over $MgSO_4$ and activated charcoal. The solution was filtered and the solvent removed *in vacuo* to give an orange oil which was recrystallised from acetone/hexane to give the desired product as an orange solid.

All six combinations of the above ligands were prepared, (bipy)Pd(CH_2CMe_2Ph)$_2$ (**1a**), (Me_2bipy)Pd(CH_2CMe_2Ph)$_2$ (**1b**), (phen)Pd(CH_2CMe_2Ph)$_2$ (**1c**), (bipy)Pd(CH_2SiMe_2Ph)$_2$, (**1d**) (Me_2bipy)Pd(CH_2SiMe_2Ph)$_2$ (**1e**) and (phen)Pd(CH_2SiMe_2Ph)$_2$ (**1f**), and characterised by ^{1}H NMR (although **1c** was impure despite repeated recrystallisations). The temperature and oxygen-sensitivities of these six complexes precluded elemental analysis.

Reaction of (dppe)$PdCl_2$ with Mg(CH_2SiMe_2Ph)Cl and Mg(CH_2SiMe_3)Cl.

To a suspension of (dppe)$PdCl_2$ (0.40g, 0.69mmol) in THF (50mL) at 0° C were added Mg(CH_2SiMe_2Ph)Cl or Mg(CH_2SiMe_3)Cl (1.42mmol) in solution in Et_2O, and the mixture stirred at 0° C for one hour and then at ambient temperature for two hours. The mixture was quenched with saturated aqueous NH_4Cl (5mL), the aqueous layer frozen, and the pale yellow organic layer filtered off. The ice layer was washed with THF (2 x 10mL), the combined filtrate and washings stirred over $MgSO_4$ and activated charcoal and the solvent removed *in vacuo* to give a yelow-green solid.

This solid was recrystallised from acetone/water to give a crystalline pale yellow solid, (dppe)Pd(CH_2SiMe_2Ph)$_2$ (**1g**) or

(dppe)Pd(CH_2SiMe_3)$_2$ (**1h**). These were characterised by ^{31}P NMR, ^1H NMR, ^{13}C NMR and elemental analysis.

Anal.

Calcd. [**1g**]: C, 65.77; H, 6.29. Found: C, 65.70; H, 6.26.

Calcd. [**1h**]: C, 60.12; H, 6.83. Found: C, 60.08; H, 6.88.

Reaction of (Ph_2MeP)$_2PdCl_2$ with Mg(CH_2SiMe_2Ph)Cl.

To a pale yellow suspension of (Ph_2MeP)$_2PdCl_2$ (0.180g, 0.312mmol) in THF (50mL) at -30°C was added Mg(CH_2SiMe_2Ph)Cl (0.64mmol) in solution in Et_2O (2.78mL, 0.23M), the mixture allowed to warm up to -15°C and stirred for 15 minutes to give a clear pale yellow solution. The mixture was quenched, and the crude product extracted as for **1g** and **1h**.

The pale yellow solid remaining was dissolved up in cold (-10°C) acetone (5mL), the solution filtered and a layer of cold (-10°C) hexane (20mL) floated on top. After one week at -15°C a small quantity of the product *trans*- (Ph_2MeP)$_2$Pd(CH_2SiMe_2Ph)Cl (**1i**) was obtained as pale yellow blocks, which were filtered off with cold hexane (2mL) and dried *in vacuo* . **1i** was only slightly soluble in acetone and chloroform and was characterised by elemental analysis, ^{31}P NMR and ^1H NMR.

Anal. Calcd. [**1i**]: C, 60.78; H, 5.68. Found: C, 60.41; H, 5.65.

Thermolytic Studies on (bipy)Pd(CH_2CMe_2Ph)$_2$.

Preliminary studies on **1a** showed it to be stable for short periods of time under N_2 at room temperature in the solid state.

A sample of the orange crystalline solid was dissolved in d_6-benzene in a sealable NMR tube with a Teflon tap, and was allowed to rearrange at room temperature for several days. After

only one hour, the solution had become cloudy and after ten hours, a pale orange precipitate had settled out. After three days the supernatant was still orange and a ^1H NMR spectrum was almost identical to that of **1a** (only weaker) with the exception of the appearance of four singlets at 1.12, 1.15, 1.17 and 1.21 p.p.m. (three of them having low integrals relative to the largest peak at 1.17 p.p.m.), another weak singlet at 0.49 p.p.m. and at least three weak multiplets centred at 7.42, 7.33 and 7.21 p.p.m. Also appearing was a doublet centred at 3.35 p.p.m.

Leaving the sample at room temperature for a further three days resulted in only slight further rearrangement of the remaining **1a** as there were only small increases in the integrals of the newly appeared peaks and no observable change in the intensity of the supernatant or of the amount of pale orange powder produced.

The smallest of the four new peaks at 1.1-1.21 p.p.m. was assigned as *tert-* butylbenzene (δ 1.21 p.p.m.) by comparison to an authentic sample of that compound. The *tert-* butylbenzene is also responsible for the two multiplets centred at 7.21 and 7.33 p.p.m. The other new peaks in the spectrum could not be assigned.

1.3. DISCUSSION

1.3.1. **Complexes with Bidentate Nitrogen Donor Ligands.**

The air-sensitive complexes **1a-1f** were all synthesised by the simple alkylation of the corresponding dibromide complexes. As expected they were thermally labile, with thermal stabilities intermediate between those of the analogous organoplatinum and -nickel complexes, rearranging in solution at room temperature to

give insoluble solids.

1d-1f were more thermolytically inert than **1a-1c**. For this reason, recrystallised samples of **1d-1f** were cleaner (by ^1H NMR) than the analagous dineophyl complexes, some of which had rearranged slightly in solution.

1d-1f also tended to be more soluble in organic solvents than **1a-1c**. Indeed the ^1H NMR spectrum of **1c** was noisy and of poor quality whereas that of **1f** was relatively noise-free. In this way palladium is similar to nickel where it was possible to obtain the ^1H NMR spectrum of (phen)Ni($CH_2SiMe_2Ph)_2$ but not of (phen)Ni($CH_2CMe_2Ph)_2$ because of the low solubility of the latter.

Spectroscopy.

a) **^1H NMR.**

The ^1H NMR data for **1a-1f** are shown in Table 1.2. and 1.3. The spectra for **1a** and **1d** are shown in Figs. 1.6. and 1.5. respectively and are typical of the dialkylpalladium complexes synthesised with bidentate nitrogen donor ligands.

The aromatic resonances were assigned on the basis of their multiplicities and by analogy with the organoplatinum complexes (where couplings to ^{195}Pt are of assistance in the assignments). Several general guidelines emerge from these assignments. In **1a-1f** the most downfield resonance is always H6 (or H2(9) in phen) for the nitrogen donor ligand. The most upfield of the resonances for nitrogen donor ligand hydrogens is always H5 (or H3(8) in phen). Also the alkyl group H2 is usually observable as a double-doublet at around 7.7 ppm.

These six compounds all contain magnetically equivalent Si

Table 1.2. **^{1}H NMR Data for Dineophylpalladium Complexes (1a-1c).**

	δ ^{1}H ppm *N-Donor Ligands*	δ ^{1}H ppm *Alkyl*	δ ^{1}H ppm *Aromatic*
1a (d_6-benzene)	8.43(d, $^3J_{(H6-H5)}$=5.0Hz) [H6] 6.38(m, $^3J_{(H5-H4)}$=7.0Hz) [H5] 6.78(dd, $^3J_{(H3-H4)}$=8.0Hz, $^4J_{(H3-H5)}$=1.6Hz) [H3] 6.84(m) [H4]	2.43(s) [CH_2] 1.97(s) [CH_3]	7.95(dd, $^4J_{(H2-H4)}$=1.3Hz) [H2] 7.11(t, $^3J_{(H2-H3)}$=8.4Hz) [H3] 6.93(tt, $^3J_{(H4-H3)}$=7.2Hz) [H4]
1b (d_6-acetone)	8.52(d, $^3J_{(H6-H5)}$=5.7Hz) [H6] 6.91(d) [H5] 8.20(s) [H3] 1.48(s) [CH_3]	2.46(s) [CH_2] 2.30(s) [CH_3]	7.58(dd, $^3J_{(H2-H3)}$=8.3Hz, $^4J_{(H2-H4)}$= 1.3 Hz) [H2] 6.86-7.27(m) [H3 & H4]
1c (d_6-benzene)	8.47(dd, $^3J_{(H2(9)-H3(8)}$=7.3Hz, $^4J_{(H2(9)-H4(7)}$=1.5Hz) [H2(9)] 8.29(dd, $^3J_{(H4(7)-H3(8)}$=7.6Hz) [H4(7)]	2.11(s) [CH_2] 2.02(s) [CH_3]	7.04-7.30(m) [H2, H3 & H4]

Table 1.3. **^{1}H NMR Data for Disila-neophylpalladium Complexes (1d-1f).**

	δ ^{1}H ppm *N-Donor Ligands*	δ ^{1}H ppm *Alkyl*	δ ^{1}H ppm *Aromatic*
1 d	8.61(dd, $^3J_{(H6-H5)}$= 5.4Hz, $^4J_{(H6-H4)}$=0.9Hz) [H6]	0.32(s) [CH_2]	7.60-7.65(m) [H2]
(d_6-acetone)	7.53(m, $^3J_{(H5-H4)}$=7.6Hz) [H5]	0.24(s) [CH_3]	7.12-7.17(m) [H3 & H4]
	8.11(m, $^3J_{(H4-H3)}$=8.0Hz) [H4]		
	8.40(dd, $^4J_{(H3-H5)}$=1.0Hz) [H3]		
1 e	9.14(d, $^3J_{(H6-H5)}$=5.5Hz) [H6]	0.34(s) [CH_2]	7.58-7.64(m) [H2]
(d_6-acetone)	8.24(s) [H3], 1.17(s) [CH_3]	0.34(s) [CH_3]	7.13-7.18(m) [H3 & H4]
	7.49(d) [H5]		
1 f	8.92(dd, $^3J_{(H2(9)-H3(8))}$=5.0Hz, $^4J_{(H2(9)-H4(7))}$	0.49(s) [CH_2]	7.84-7.90(m) [H2]
(d_6-acetone)	=1.5Hz) [H2(9)] 8.14(s) [H5(6)]	0.28(s) [CH_3]	7.08-7.11(m) [H3 & H4]
	7.87(dd) [H3(8)]		
	8.69(dd, $^3J_{(H4(7)-H3(8))}$=8.3Hz) [H4(7)]		

Table 1.4. **^{1}H NMR Chemical Shifts of Methylene Resonances in L_2MR_2[3,4,12].**

δ ^{1}H ppm [CH_2]	R=neophyl			R=sila-neophyl		
M	M=Ni	M=Pd	M=Pt	M=Ni	M=Pd	M=Pt
(bipy)MR_2	1.62[b]	2.43[a]	2.78[b]	0.40[b]	0.32[d]	1.41[b]
(Me_2bipy)MR_2	1.58[b]	2.67[a]	2.94[a]	0.37[b]	0.34[d]	1.37[b]
		2.46[d]				
(phen)MR_2		2.11[a]	2.52[b]		0.49[d]	1.60[b]
(dppe)MR_2				0.85[b]	0.74[d]	1.32[a]

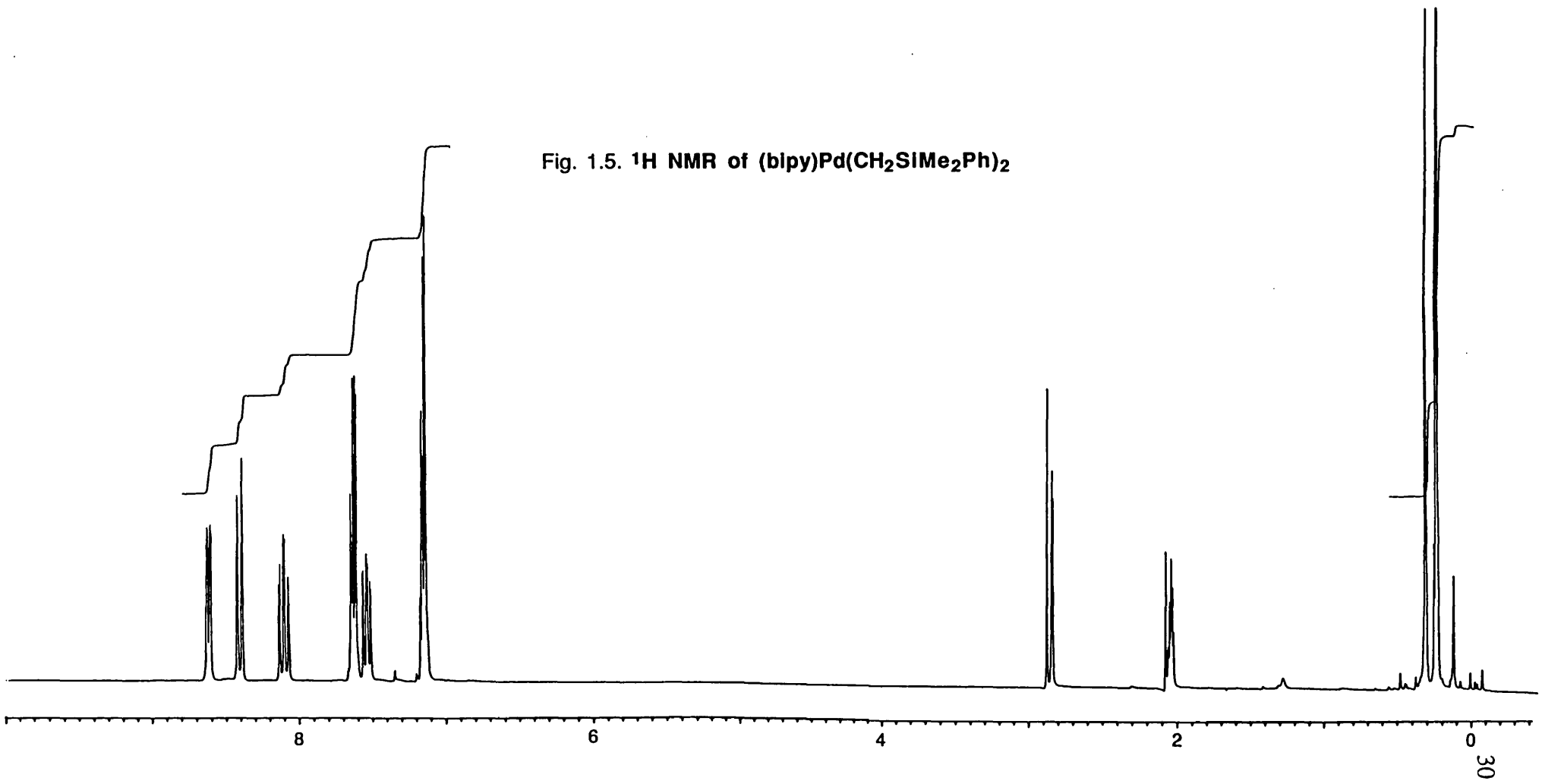
(a) Recorded in d_6-benzene

(b) Recorded in d_8-toluene

(c) Recorded in d_2-dichloromethane

(d) Recorded in d_6-acetone

Fig. 1.5. ^{1}H NMR of (bipy)Pd($CH_2SiMe_2Ph)_2$



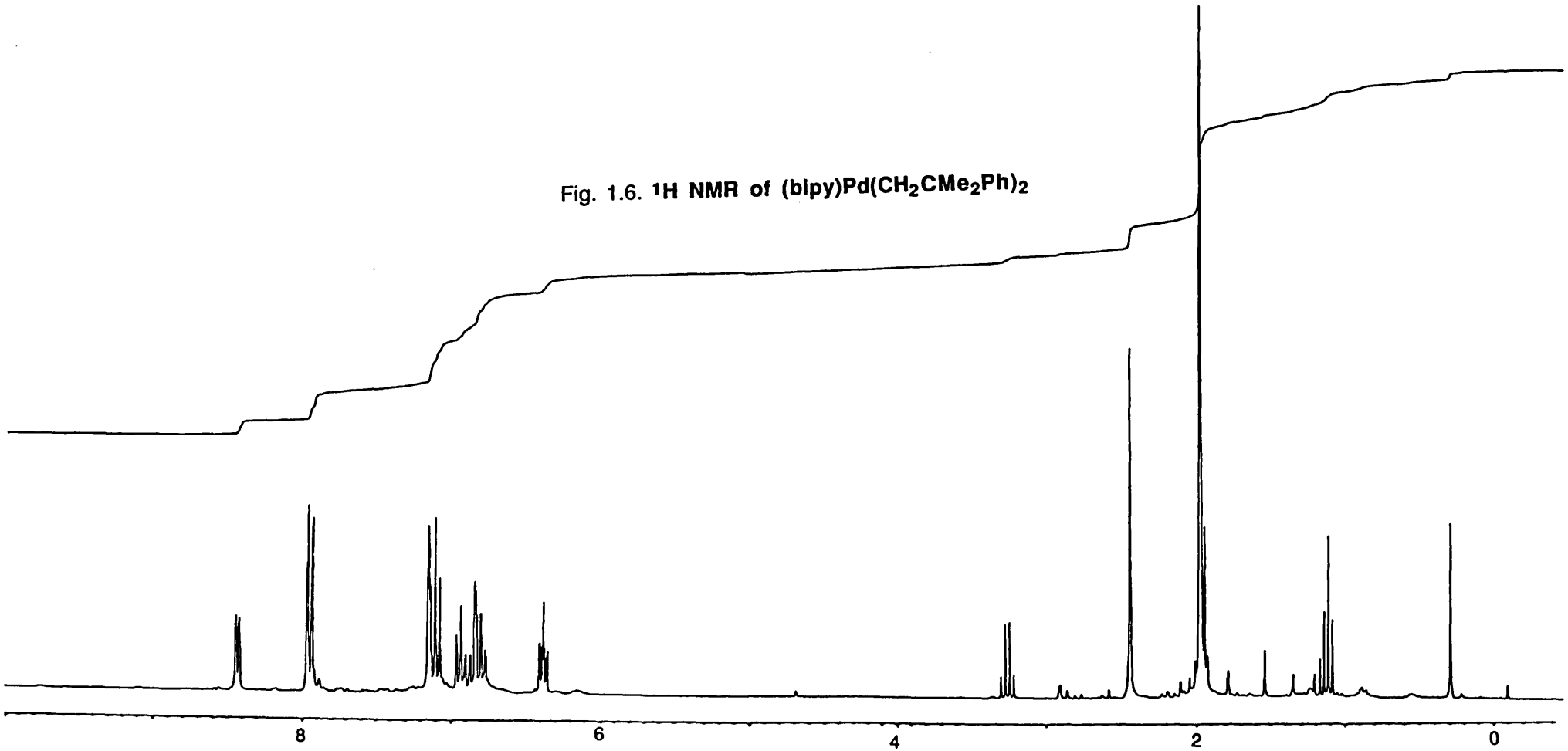


Fig. 1.6. ^1H NMR of (bipy)Pd(CH_2CMe_2Ph)$_2$

Me or C-Me groups and magnetically equivalent methylene groups. For **1d-1f**, these resonances all occur at around 0 ppm.

An interesting exercise is to compare the chemical shifts of the methylene protons in various dineophyl and disila-neophyl complexes of nickel[4], palladium and platinum[3,12] with bidentate nitrogen donors and dppe (Table 1.4.) Although these spectra were measured in different solvents which might contribute to an extent to the shift differences, several trends emerge. To begin with, the methylene resonances in disila-neophyl complexes tend to be shifted further upfield by 1.1-2.1 ppm than the same resonances for dineophyl complexes. This is due to Si having a lower electronegativity than C and the β-Si atom being better able to shield the methylene protons than the β-C atom.

A more interesting observation comes from comparing the methylene proton shifts on varying the metal within a complex. The methylene resonances in dineophylpalladium complexes have a chemical shift that is closer to the same resonances in the analogous platinum complexes than to those in the analogous nickel complexes. The converse is true for the disila-neophylpalladium complexes. It is difficult to explain the theory behind these observations as these chemical shifts depend upon the electronegativities of both the metal and the β-atom as well as upon the different magnetic environments around the metal atoms caused by the different spatial extension of their orbitals. But it is another example of the way in which neophyl and sila-neophyl complexes differ in their behaviour.

b) **^{13}C NMR.**

The thermal labilities of complexes **1a-1f** meant that any

measurement of ^{13}C NMR spectra, which requires the species to remain in solution for several hours, would have to be carried out at sub-ambient temperatures. However sub-ambient temperatures limit the solubility of these compounds in any solvent. In practise we were only able to obtain the ^{13}C NMR spectrum of **1b** (Fig. 1.7.) This was measured at -15°C at 62.86MHz in solution in d_6-acetone.

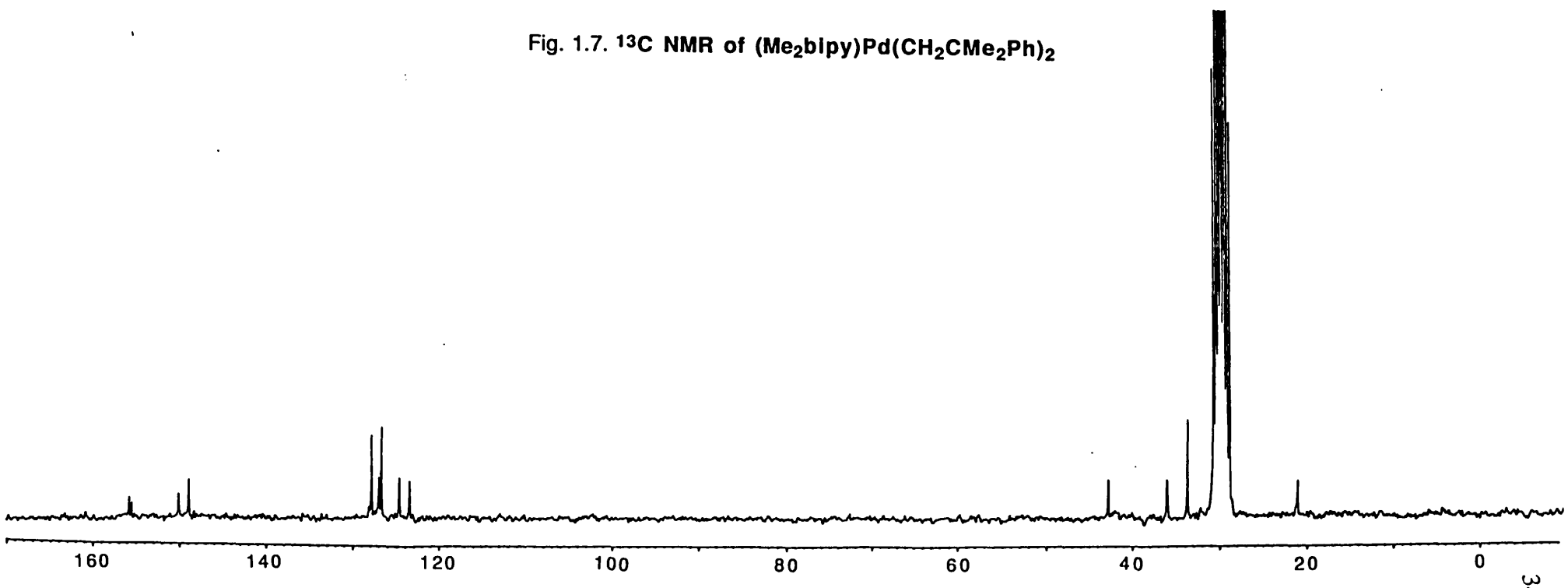
^{13}C NMR of **1b**:-

δ ^{13}C ppm (CH_2CMe_2Ph)		δ ^{13}C ppm (Me_2bipy)	
21.1 (s) [CH_2]	33.7 (s) [CH_3]	36.1 (s) [CH_3]	123.4 (s) [C5]
150.0 (s) [C1]	127.8 (s) [C2]	124.6 (s) [C3]	148.9 (s) [C6]
126.6 (s) [C3]	126.9 (s) [C4]	155.4 (s) [C4]	155.7 (s) [C2]
42.7 (s) [C_{quart}]			

1.3.2. **Complexes with Phosphorus Donor Ligands.**

We have shown that it is possile to synthesise a range of organopalladium (II) complexes containing phosphine ligands. These complexes are more inert than the organopalladium (II) complexes described above with nitrogen donor ligands. The dppe complexes **1g** and **1h** are analogues of the already prepared (dppe)Pt($CH_2SiMe_2Ph)_2$[13] (dppe)Pt($CH_2SiMe_3)_2$[11] and (dppe)Ni(CH_2-$SiMe_2Ph)_2$[4]. The platinum and nickel analogues of **1i** have not as yet been synthesised (althugh several similar monoalkylnickel complexes have[4]) and in fact, very few monoalkylpalladium complexes are known. Exceptions to this include monomethylpalladium complexes, *trans*-($Ph_3P)_2$Pd(CH_2SMe)Cl and

Fig. 1.7. ^{13}C NMR of $(Me_2bipy)Pd(CH_2CMe_2Ph)_2$



trans-$(Et_3P)_2Pd(CH_2SiMe_2)Cl$. The latter was a yellow sticky solid which could not be purified.

Spectroscopy.

a) **^{31}P NMR.**

The ^{31}P NMR spectra of our three new bis(phosphine)alkyl-palladium (II) complexes **1g**, **1h** and **1i** contain just a single peak, due to the two phosphorus atoms. All ^{31}P NMR spectra were measured with broad band ^{1}H decoupling (in the absence of the decoupling the two phosphorus atoms would be chemically equivalent but magnetically inequivalent, but the decoupler removes any couplings to hydrogens which cause this magnetic inequivalence, resulting in chemically and magnetically equivalent phosphorus atoms). The spectroscopic data are shown in Table 1.5. together with comparable data for $(dppe)Pt(CH_2SiMe_3)_2$, $(dppe)Ni(CH_2SiMe_2Ph)_2$ and $(PhMe_2P)_2Ni(CH_2SiMe_2Ph)(Cl)$.

Table 1.5. **^{31}P NMR Characteristics of 1g, 1h, 1i and Comparable Complexes.**

Complex	δ ^{31}P ppm	Solvent
$(dppe)Pd(CH_2SiMe_2Ph)_2$ (**1g**)	42.26	d_6-acetone
$(dppe)Pd(CH_2SiMe_3)_2$ (**1h**)	42.94	d_6-acetone
$(MePh_2P)_2Pd(CH_2SiMe_2Ph)(Cl)$ (**1i**)	12.22	d-chloroform
$(dppe)Pt(CH_2SiMe_3)_2$[11]	43.61	d-chloroform
$(dppe)Ni(CH_2SiMe_2Ph)_2$[4]	49	d_6-benzene
$(PhMe_2P)_2Ni(CH_2SiMe_2Ph)(Cl)$[4]	12	d_6-benzene

b) **^{1}H NMR**

The alkyl hydrogen resonances of **1g**, **1h** and **1i** share some common characteristics. Like **1d-1f**, these three compounds all contain magnetically equivalent Si-Me groups and at least one Pd-CH_2-Si group, which resonate near 0 ppm (Table 1.6.) For the *cis*-complexes, **1g** and **1h**, this methylene resonance is a double-doublet with a large coupling to the *trans*- phosphorus (10.4 and 10.8Hz respectively) and a smaller coupling to the *cis*-phosphorus (8.5 and 8.7Hz respectively). For the *trans*- complex, **1i**, a triplet is observed for this resonance with a coupling constant of 8.1Hz, due to coupling to two magnetically equivalent phosphorus atoms.

Further evidence for the *trans*- stereochemistry of **1i** is the presence of a triplet for the P-Me resonance. This is due to virtual coupling which is often observed in *trans*- complexes. Measurement of the relative integrals of the Si-Me and P-Me peaks supports our assertion that the complex is only the monoalkyl and not the dialkyl complex.

The ^{1}H NMR spectrum of **1g** is shown in Fig. 1.8. and is very similar to the ^{1}H NMR spectrum of **1h**. The methylene resonances are complex in both spectra due to coupling to two magnetically inequivalent phosphorus atoms.

The ^{1}H NMR spectrum of **1i** was measured in both d_6-acetone and d-chloroform as the P-Me resonance was obscured by solvent peaks in the former.

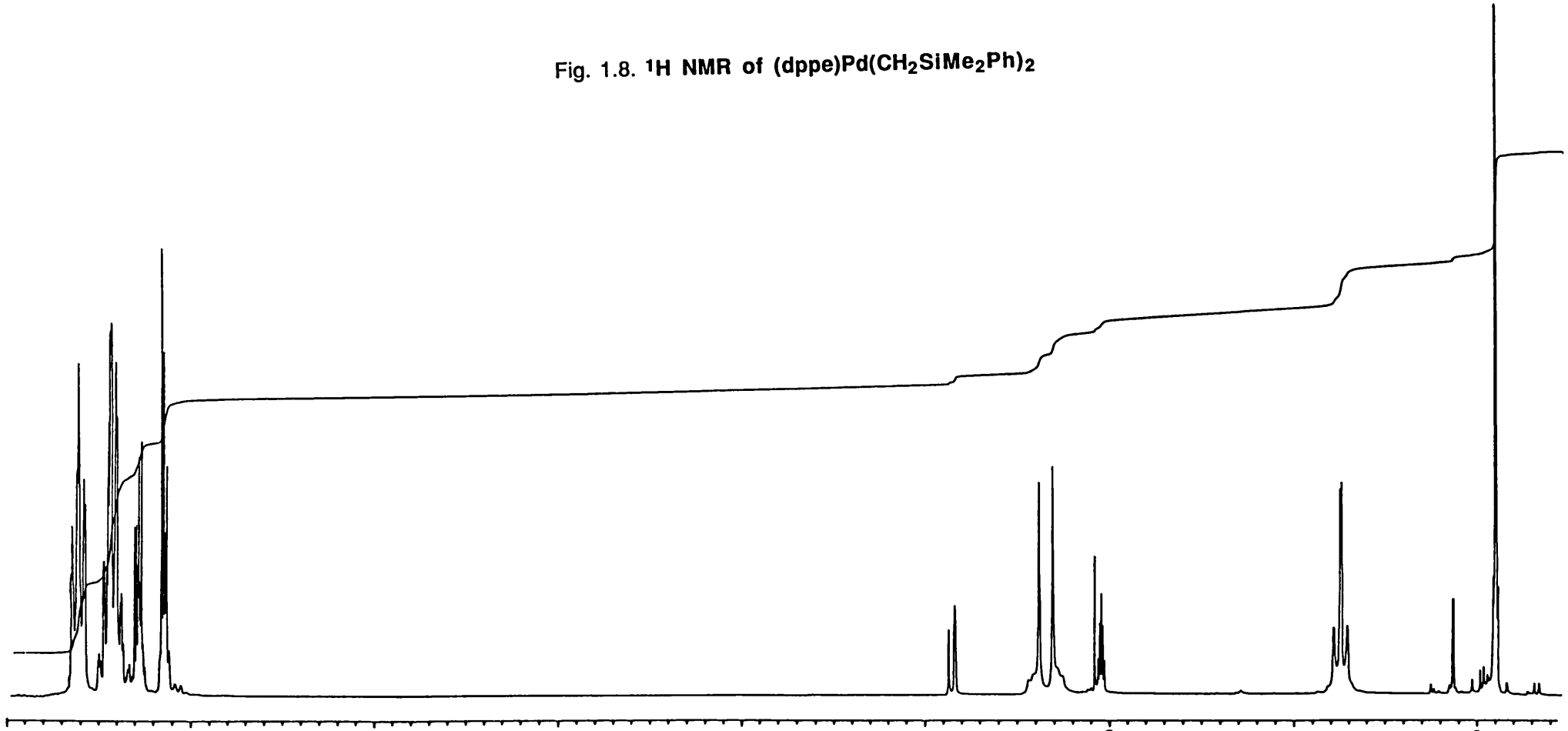
Table 1.6. **^{1}H NMR Data for 1g, 1h and 1i.**

Complex	δ ppm *Alkyl*			δ ppm *P-Donor Ligands*	
	δ CH_3	δ CH_2	δ *Aromatic*	δ CH_2 or CH_3	δ *Aromatic*
1 g (d_6-acetone)	-0.10(s)	0.74(dd, $^3J_{(P-H)trans}$= 10.4Hz, $^3J_{(P-H)cis}$=8.5Hz)	7.12-7.15(m) [H3&H4] 7.25-7.29(m) [H2]	2.34(d*, $^2J_{(P-H)}$=18.2Hz)	7.36-7.47 (m) [H3&H4] 7.56-7.64 (m) [H2]
1 h (d_6-acetone)	-0.30(s)	0.56(dd, $^3J_{(P-H)trans}$= 10.8Hz, $^3J_{(P-H)cis}$=8.7Hz)	N/A	2.31(d*, $^2J_{(P-H)}$=18.3Hz)	7.39-7.48 (m) [H3&H4] 7.60-7.68(m) [H2]
1 i (d_6-acetone)	-0.16(s)	0.58(t, $^3J_{(P-H)cis}$=8.1Hz)	7.64-7.74(m) [H2] 7.13-7.45(m) [H3&H4]	Obscured	7.64-7.74(m) [H2] 7.13-7.45(m) [H3&H4]
1 i (d-chloroform)	-0.18(s)	0.55(t, $^3J_{(P-H)cis}$=8.1Hz)	7.54-7.63(m) [H2] 7.11-7.40(m) [H3&H4]	1.98("t", $^2J_{(P-H)}$=3.1Hz)	7.54-7.63(m) [H2] 7.11-7.40(m) [H3&H4]

"t" indicates virtual coupling.

* indicates that the doublets are second order.

Fig. 1.8. ^1H NMR of (dppe)Pd($CH_2SiMe_2Ph)_2$



c) **^{13}C NMR**

The ^{13}C NMR data for **1g** and **1h** are shown in Table1.7. (both measured at 13.26MHz with broad band ^{1}H decoupling) together with the data for (dppe)Pd(CH_2CMe_3)$_2$[19] and (dppe)Pt(CH_2SiMe_3)$_2$[9]. In the main, the spectra were unambiguous, with the exception of the assignment of the two methylene carbon resonances. In contrast to the work of Diversi et al[19], who assigned the triplet at 24.31ppm ($J_{(P-C)}$=17.6Hz) in the ^{13}C NMR spectrum of (dppe)Pd(CH_2CMe_3)$_2$ to the alkyl methylene carbons and the doublet at 34.53ppm ($J_{(P-C)}$=133.2Hz) to the dppe methylene carbons, we have assigned the triplets at 25.4 ($J_{(P-C)}$=20.0Hz) and 26.0 ($J_{(P-C)}$=20.6Hz) ppm in the ^{13}C NMR spectra of **1g** and **1h** respectively to the dppe methylene carbons and the double-doublets at 2.1($J_{(P-C)trans}$=93.5Hz) and 2.9($J_{(P-C)trans}$=93.5Hz) ppm respectively to the alkyl methylene carbons. Our assignments were made by analogy with (dppe)Pt(CH_2SiMe_3)$_2$[11] (where the alkyl methylene carbons may be unambiguously assigned on the basis of Pt-C coupling constants) and on the basis of chemical shifts (the alkyl methylene carbons were in an α-position to a Si atom and would be expected to have a chemical shift close to 0 ppm).

1.3.3. Thermal Rearrangement of (bipy)Pd(CH_2CMe_2Ph)$_2$.

The rearrangement of **1a** in solution in benzene at room temperature resulted in a complicated mixture of soluble organic products and insoluble inorganic produts (produced as a yellow powder). These insoluble products could not be characterised by ^{1}H NMR (although we did observe several very weak doublets at 9.31, 9.07, 8.74, 8.53, 7.74 and 7.62 and two very weak triplets at

Table 1.7. **^{13}C NMR Data for 1g, 1h, (dppe)Pd(CH_2CMe_3)$_2$[19] and (dppe)Pt(CH_2SiMe_3)$_2$.[9]**

Complex	δ ppm *Alkyl*			δ ppm *dppe*	
	δ CH_2	δ CH_3	δ *Aromatic*	δ CH_2	δ *Aromatic*
1g (d_6-benzene)	2.1(dd, $^2J_{(P\text{-}C)trans}$= 93.5Hz, $^2J_{(P\text{-}C)cis}$=8.3Hz)	2.7(s)	127.4-134.9(m)	25.4(t, $J_{(C\text{-}P)}$ =20.0Hz)	127.4-134.9(m)
1h (d-chloroform)	2.9(dd, $^2J_{(P\text{-}C)trans}$= 93.5Hz, $^2J_{(P\text{-}C)cis}$=8.3Hz)	3.7(s)	N/A	26.0(t, $J_{(C\text{-}P)}$ =20.6Hz)	128.3-133.9(m)
(dppe)Pd(CH_2-CMe_3)$_2$ (d_6-benzene)	24.31(t, $J_{(P\text{-}C)}$=17.6Hz)	35.72(d, $J_{(P\text{-}C)}$=8.5Hz)	N/A	34.53(d, $J_{(C\text{-}P)}$ =133.2Hz)	128.17-133.76(m)
(dppe)Pt(CH_2-$SiMe_3$)$_2$ (d-chloroform)	1.94(m, $^2J_{(P\text{-}C)trans}$= 89.3Hz, $^2J_{(P\text{-}C)cis}$=5.5Hz)	3.58(t)	N/A	28.10 (m)	128.30-133.57(m)

6.52 and 6.18p.p.m.) But we were able to characterise *tert*-butylbenzene as one component of the organic product mixture. This was observed as a singlet at 1.20 and two multiplets centred at 7.21 and 7.32 p.p.m.

Unfortunately from our observations we could not discern the nature of the other organic products or the mechanism of rearrangement of **1a**, and further studies are underway in this area.

CHAPTER TWO

Nucleophilic Attack of Carbanionic Reagents on 2,2'-Bipyrimidyl Coordinated to Palladium.

2.1. INTRODUCTION

The past fifteen years have seen growth in the field of nucleophilic attack on coordinated chelating heterocyclic diimines, initiated by the extensive work of Gillard. There have been several reviews[32-34] in the field, which includes some work on nucleophilic attack on coordinated bipyrimidyl[35] in which we are now interested. Although some of this work has since been called into question,[36,37] there is still considerable experimental evidence (together with theoretical calculations and discussions[38-41]) to support the occurrence of such attacks on coordinated diimines.

By contrast, simple uncoordinated pyrimidines have long been known to undergo nucleophilic addition by organomagnesium and organolithium reagents, usually in a 1,2-fashion as shown in Fig. 2.1. Simple 1,2-addition is also the most common regio-

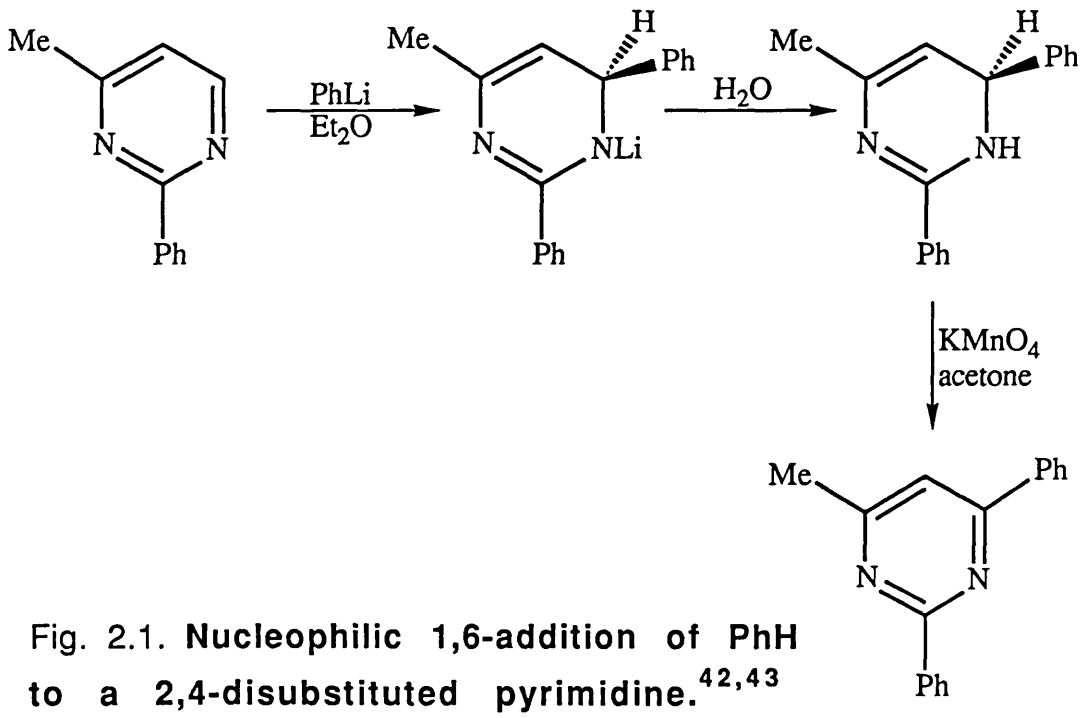


Fig. 2.1. **Nucleophilic 1,6-addition of PhH to a 2,4-disubstituted pyrimidine.**[42,43]

selectivity seen in nucleophilic addition to coordinated diimines.

It has been postulated[33] that coordination of diimines, pyrimidines and bipyrimidines to a metal cation will act, like quarternisation, to activate the heterocyclic rings further towards nucleophilic addition. Such simple analogies fail to take into account back-bonding from the metal to the ring which does not occur upon quarternisation. By including the effects of back-bonding, recent theoretical calculations on the effects of coordination of heterocyclic diimines[38] have shown that coordination to the $Fe(CN)_4^{2-}$ moiety slightly reduces the susceptibility of the diimines to nucleophilic attack (*vide infra*).

The work described here featured the alkylation of (bipym)$PdCl_2$ using $Mg(CH_2SiMe_2Ph)Cl$, in which a species was obtained whose ^1H NMR characteristics can best be explained by nucleophilic attack on one of the heteroaromatic rings of the bipyrimidine ligand (leading to 1,4-addition of RH across the ring; Fig. 2.2.) as well as substitution of at least one of the coordinated chlorides. Alkylations of (bipym)$PdCl_2$ using $Mg(CH_2CMe_2Ph)Cl$ and $Mg(CH_2SiMe_3)Cl$ gave similar products

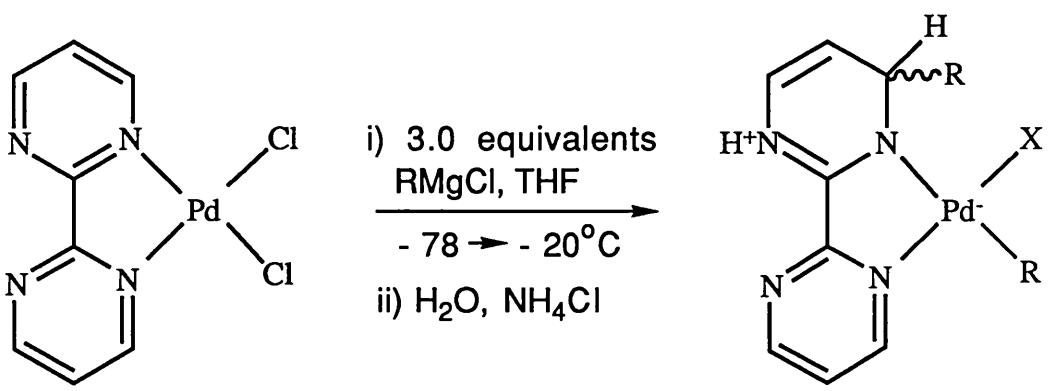


Fig. 2.2. **Reaction of RMgCl with (bipym)$PdCl_2$ where R= -CH_2SiMe_2Ph or -CH_2SiMe_3 and X is unknown.**

although the results were in some respects ambiguous. Attempts to alkylate free bipym with $Mg(CH_2SiMe_2Ph)Cl$ and $Mg(CH_2SiMe_3)Cl$ led only to insoluble polymeric products.

2.2. EXPERIMENTAL

General and Instrumental.

Details of chemical proceedures were as for Chapter One. Elemental Analyses, IR and NMR were also as for Chapter One with the exception of the ^1H NMR data for **2a** which was measured on a Bruker WM 500 (^1H, 500.13MHz.)

Bipyrimidyl was used as supplied by Lancaster Synthesis.

Preparation of (Bipym)$PdCl_2$.

$(C_6H_5CN)_2PdCl_2$[31] (1.00g, 2.61mmol) was dissolved up in acetone (150mL) and the solution filtered. To the deep-red filtrate was added a solution of bipym in acetone (0.53g, 2.61mmol in 150mL) with stirring to give a pale yellow precipitate. This was filtered off, washed with cold acetone (2 x 25mL) and diethyl ether (2 x 25mL) and dried in vacuo to give a pale yellow powder. Yield = 0.77g (88%).

IR (cm^{-1}) 3070(m), 1580(s), 1560(m), 1400(s), 1040(m), 760(s), 680(s), 350(s).

Anal. Calcd: C, 28.64; H, 1.80; N, 16.70. Found: C, 28.99; H, 1.86; N, 16.12.

Reactions of (Bipym)$PdCl_2$ with $Mg(CH_2CMe_2Ph)Cl$, $Mg(CH_2SiMe_2Ph)Cl$ and $Mg(CH_2SiMe_3)Cl$.

To a stirred suspension of (bipym)$PdCl_2$ (0.300g,

0.788mmol) in THF (50mL) at -78° C was added the appropriate organomagnesium reagent (2.40mmol as a ca. 0.4M solution in Et_2O). After warming to -20° C and stirring at this temperature for an hour, a dark orange or black suspension was obtained. All further manipulations were carried out below -20° C.

The suspension was quenched with saturated aqueous NH_4Cl solution (10mL). The orange organic layer was decanted off, stirred over $MgSO_4$ and activated charcoal, and the solvent removed *in vacuo* to give an orange oil. This oil was washed with hexane (10mL) and recrystallised from acetone/hexane to give an orange, thermally-labile, micro-crystalline solid. The product of the reaction of (bipym)$PdCl_2$ with $Mg(CH_2SiMe_2Ph)Cl$ (**2a**), $Mg(CH_2CMe_2Ph)Cl$ (**2b**) and one of the two products from $Mg(CH_2SiMe_3)Cl$ (**2c**) were characterised by ^1H NMR (250 MHz, d_6-acetone, Tables 2.1., 2.2. and 2.3.) and **2a** by ^1H COSY 2D NMR (500MHz, d_6-acetone) as well. Good elemental analyses could not be obtained for any of these compounds, with the exception of **2a**.

Anal. Calcd. [$C_{26}H_{33}N_4Si_2PdCl$ (**2a**)]: C, 52.08; H, 5.55; N, 9.34: Found: C, 51.54; H, 5.43; N, 9.30.

Reactions of (Bipym)$PdCl_2$ with MeLi, Me_2Mg and MeMgBr.

The method used was as for **2a**, but using MeLi (2.40mmol) MeMgBr (2.40mmol) or Me_2Mg (1.20mmol). In each case, on quenching with saturated aqueous NH_4Cl solution (10mL), the supernatant was light orange in colour even though most of the (bipym)$PdCl_2$ remained unreacted (and was recovered and characterised by IR). On working up the orange solutions, however, tarry orange-brown solids were obtained which exhibited complicated ^1H NMR spectra.

Table 2.1. **Comparison of pyrimidine ring resonances in ^{1}H NMR spectra of 2a, 2b and 2c.**

	[H4']	[H5']	[H6']	[H3']
2a	6.35(dd, $^3J_{(H4'-H3')}$=4.4 Hz, $^3J_{(H4'-H5')}$ =7.2 Hz)	4.63(ddd, $^3J_{(H5'-H6')}$=5.1 Hz, $^4J_{(H5'-H11b)}$=1.4 Hz)	3.94(ddd, $^3J_{(H6'-H11b)}$=12.0 Hz, $^3J_{(H6'-H11a)}$=3.1 Hz)	9.46(br)
2b	7.05-7.26(m)[a]	7.05-7.26(m)[a]	N/A	N/A
2c	6.58(br d, $^3J_{(H4'-H3')}$ is small, $^3J_{(H4'-H5')}$=7.3Hz)	5.12(dd, $^3J_{(H5'-H6')}$=5.1 Hz)	4.24(ddd, $^3J_{(H6'-H11b)}$=12.1 Hz, $^3J_{(H6'-H11a)}$=3.0 Hz)	9.62(br)

	[H6]	[H4]	[H5]
2a	9.19(dd, $^3J_{(H6-H5)}$=5.2 Hz, $^4J_{(H6-H4)}$=2.2 Hz)[a]	9.06(dd, $^3J_{(H4-H5)}$=5.0 Hz)[a]	7.89(t)
2b	8.85(dd, $^3J_{(H6-H5)}$=5.2 Hz, $^4J_{(H6-H4)}$=2.3 Hz)[a]	8.42(dd, $^3J_{(H4-H5)}$=5.5 Hz)[a]	5.05(dd)
2c	9.17(dd, $^3J_{(H6-H5)}$=5.1 Hz, $^4J_{(H6-H4)}$=2.1 Hz)[a]	9.07(dd, $^3J_{(H4-H5)}$= 4.9 Hz)[a]	7.89(t)

Table 2.2. **Comparison of methylene and methyl resonances in ^{1}H NMR spectra of 2a, 2b and 2c.**

	[H21a & H21b]	[H11b]	[H11a]
2a	1.56 & 0.41(d, $^2J_{(H21a-H21b)}$=11.0 Hz)	1.28(dd, $^2J_{(H11b-H11a)}$=13.9 Hz, $^3J_{(H11b-H6')}$=12.0 Hz)	1.46(dd, $^3J_{(H11a-H6')}$ =2.9 Hz)
2b	2.45 & 1.76(d, $^2J_{(H21a-H21b)}$=8.8 Hz)[a]	2.66(d, $^2J_{(H11a-H11b)}$=15.0 Hz)	2.79(d)
2c	1.38 & 0.33(d, $^2J_{(H21a-H21b)}$=10.2 Hz)	1.11(dd, $^2J_{(H11b-H11a)}$=13.7 Hz, $^3J_{(H11b-H6')}$=11.9 Hz)	1.31(dd, $^3J_{(H11a-H6')}$ =3.1 Hz)

	[Me]					
2a	N/A	N/A	0.32	0.33	0.33	0.38
2b	N/A	N/A	1.68	1.56	1.48	1.22
2c	-0.06	-0.04	0.04	0.09	0.09	0.13

Table 2.3. **Comparison of phenyl resonances in ^{1}H NMR spectra of 2a, 2b and 2c.**

	[H2o & H2o']	[H1o & H1o']	[H2m, H2m' & H2p]	[H1m, H1m' & H1p]
2a	7.57-7.60(m)[a]	7.51-7.53(m)[a]	7.20-7.23(m)[a]	7.26-7.30(m)[a]
2b	7.62-7.67(m)[a]	7.05-7.26(m)[a]	6.84-6.92(m) [H2p] 6.97-7.04(m) [H2m & H2m']	7.05-7.26(m)[a]
2c	N/A	N/A	N/A	N/A

[a] see text

Reaction of Bipym with $Mg(CH_2SiMe_2Ph)Cl$ and $Mg(CH_2SiMe_3)Cl$.

To a clear, colourless solution of bipym (0.210g, 1.33 mmol) in THF (50mL) at -78° C was added dropwise $Mg(CH_2SiMe_2Ph)Cl$ (1.40mmol) or $Mg(CH_2SiMe_3)Cl$ (1.40mmol) in solution in diethyl ether, with stirring. The first few drops of the added organo-magnesium reagent caused the colourless solution to turn deep red with further addition producing a deep red suspension which, on warming to -15° C, became dark brown in colour. This suspension was allowed to settle out to give a dark brown solid and a pale brown supernatant. This solid was filtered off and dried in vacuo to give a black free-flowing powder.

This powder was sparingly soluble in most of the common organic solvents and water. It was very soluble in pyridine to give a deep brown solution. Removal of the solvent from this solution *in vacuo* gave a red-brown glassy solid.

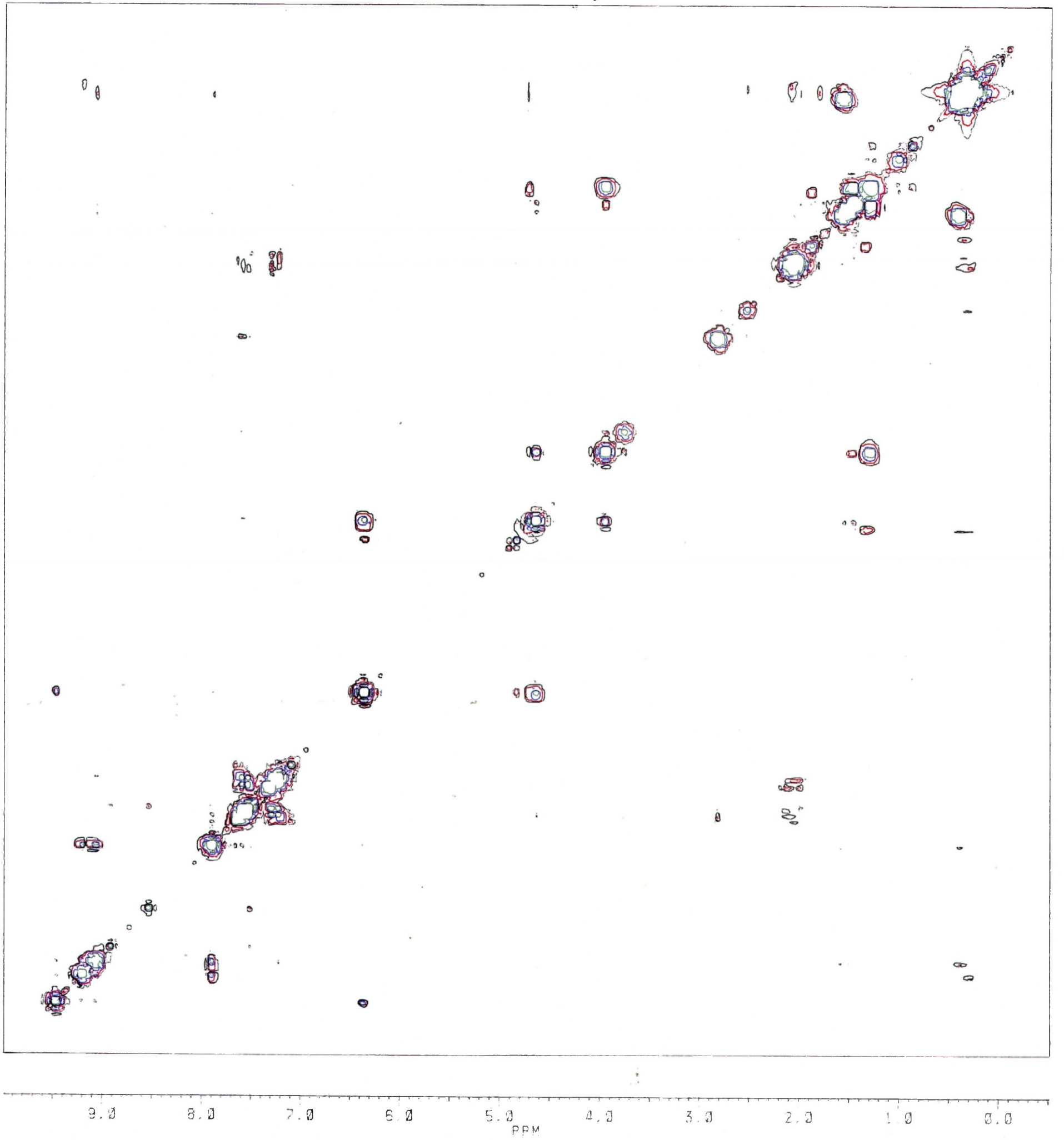
2.3. DISCUSSION

Reaction of $Mg(CH_2SiMe_2Ph)Cl$ with $(Bipym)PdCl_2$.

Detail of the ^1H NMR (500MHz, d_6-acetone) and 2D COSY ^1H NMR (500MHz, d_6-acetone) spectra of **2a** are shown in Figs. 2.3. and 2.7. The resonances at 9.19 [H6], 9.06 [H4] and 7.89 [H5] ppm (see Fig. 2.5. for the labelling convention for **2a**) were assigned on the basis of $(bipym)Pt(CH_2SiMe_2Ph)_2$[12] (H4, H5 and H6 were assigned for **2c** as well on this basis) in which H6, H5 and H4 were at 8.36(dd, $^4J_{(H6\text{-}H4)}$=2.2 Hz), 5.86(dd, $^3J_{(H5\text{-}H6)}$=5.5 Hz) and 8.17(dd, $^3J_{(H5\text{-}H4)}$=4.6 Hz) ppm respectively and Pt-H coupling defines H_6. This is supported by the decoupling experiments on **2a**

Fig.2.3.

COSY 2D ^{1}H NMR spectrum of 2a.



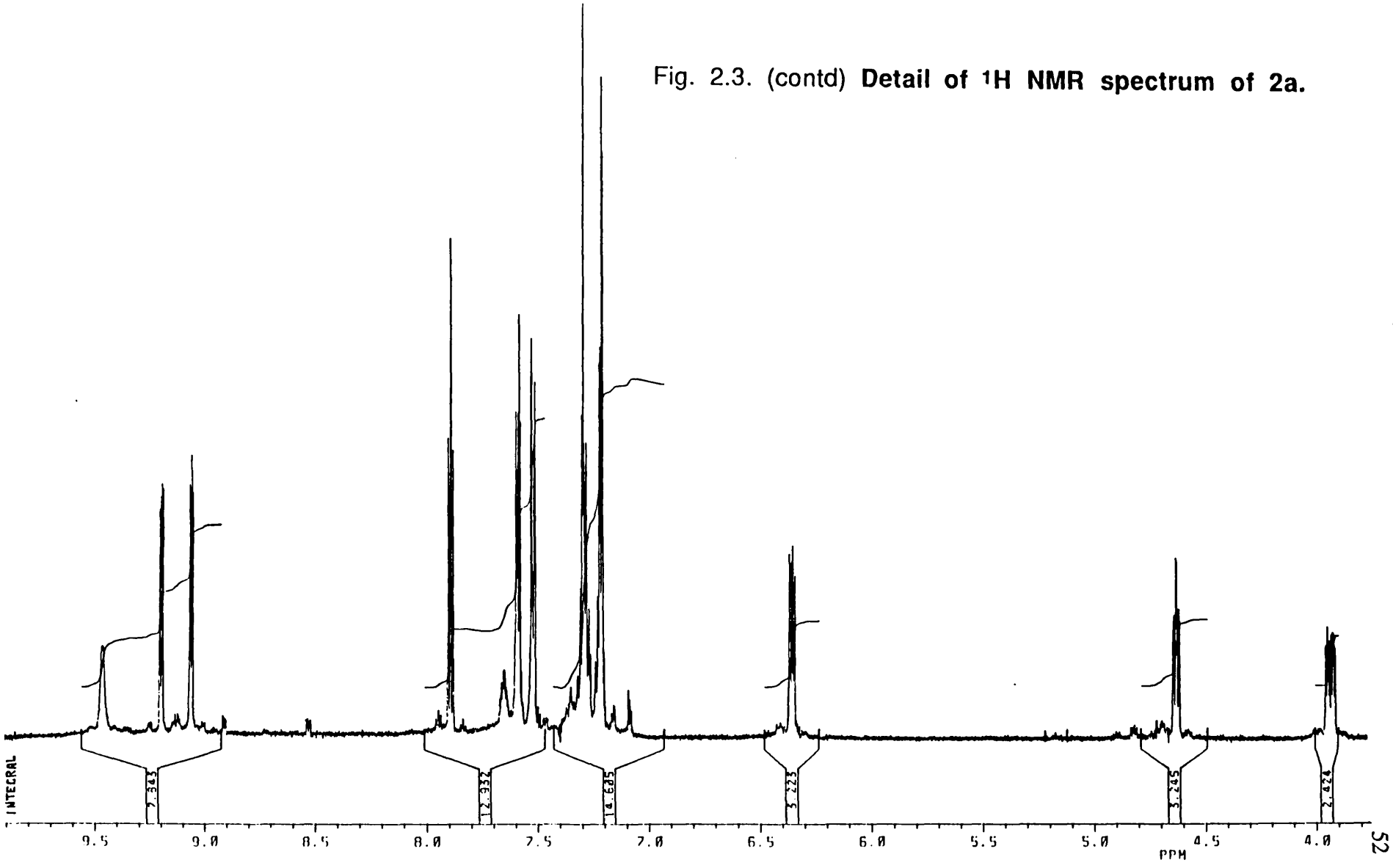


Fig. 2.3. (contd) **Detail of ^{1}H NMR spectrum of 2a.**

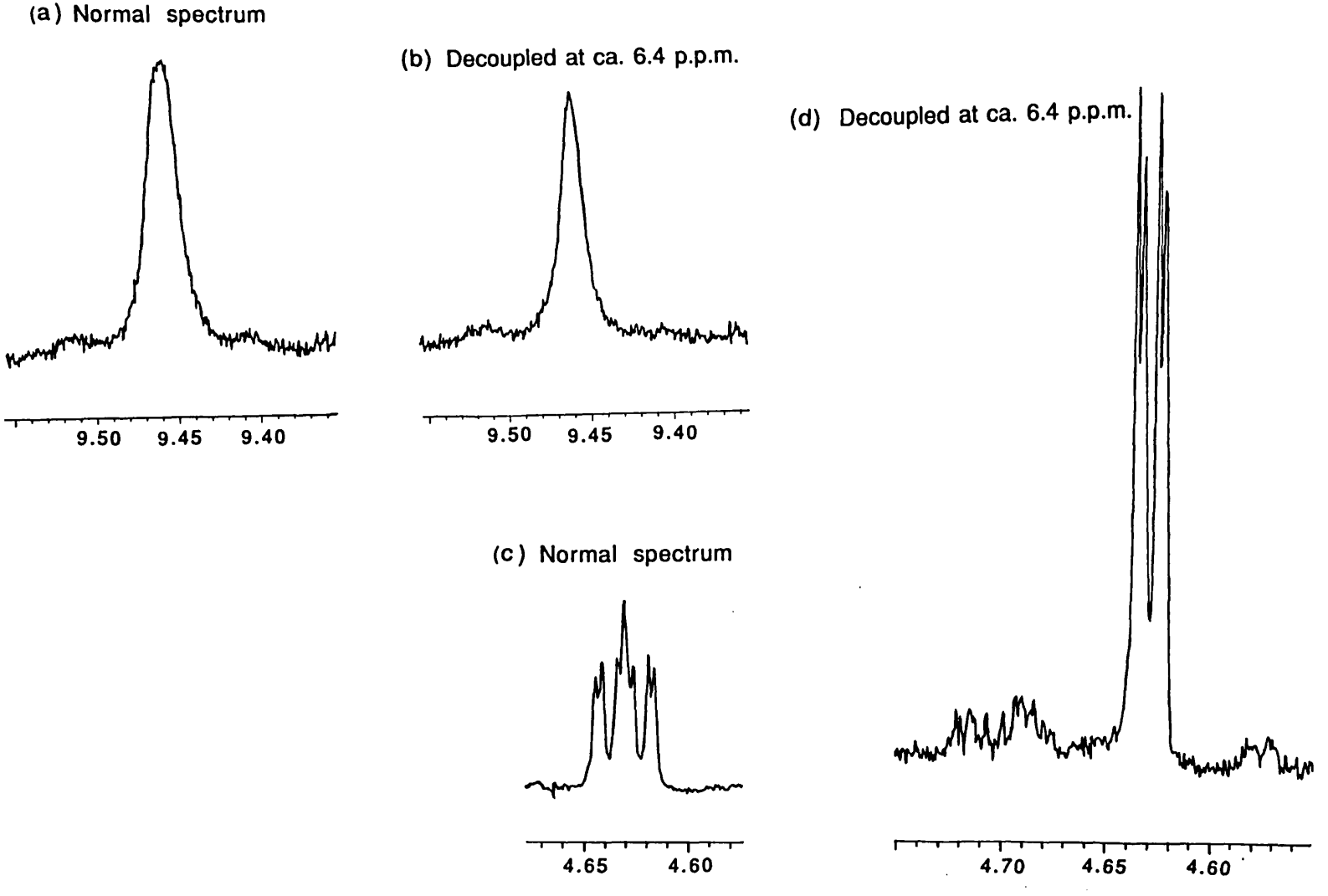


Fig. 2.4. **Decoupling experiments on 2a.**

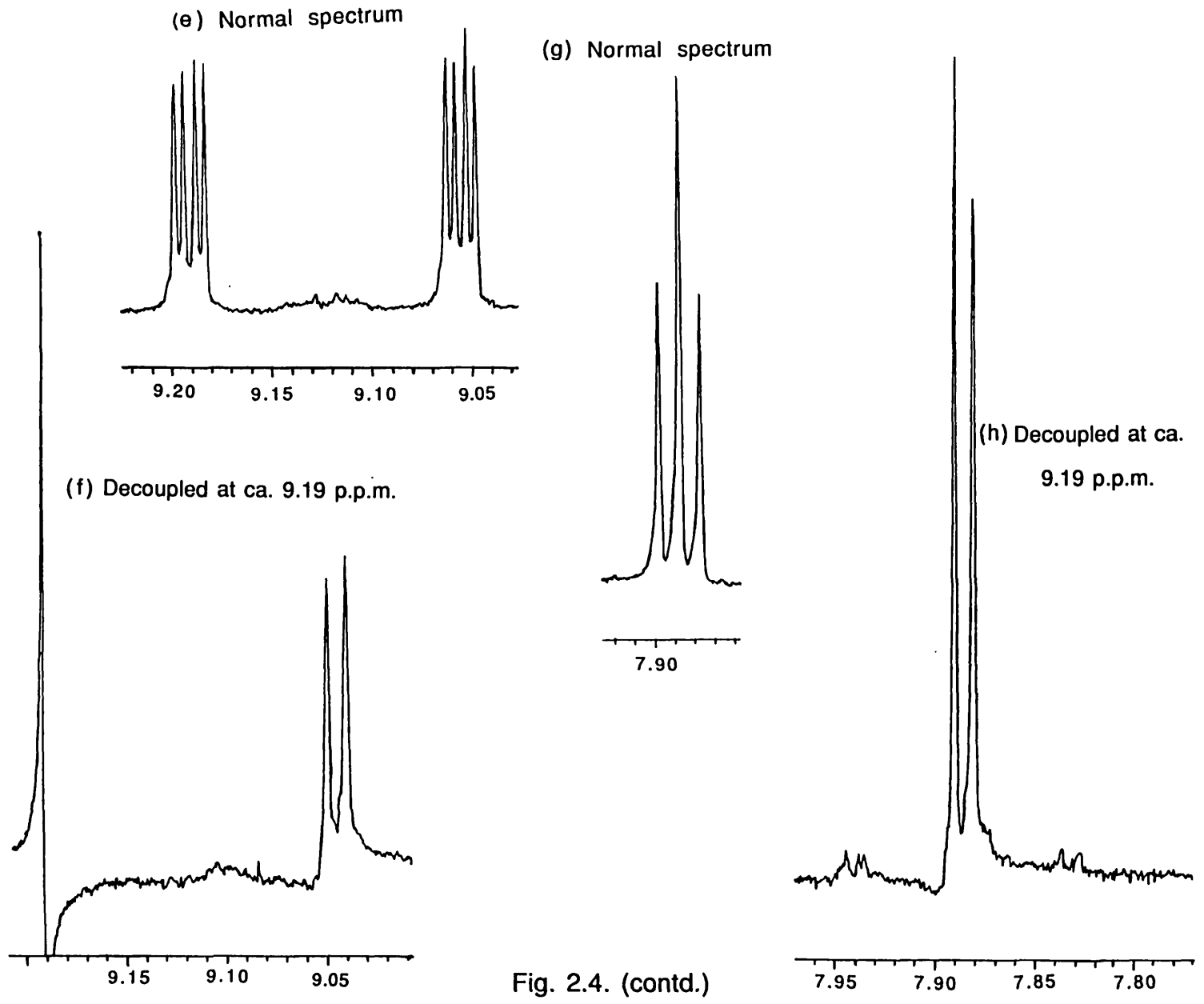

(e) Normal spectrum
9.20
9.15
9.10
9.05
(f) Decoupled at ca. 9.19 p.p.m.
9.15
9.10
9.05
(g) Normal spectrum
7.90
(h) Decoupled at ca.
9.19 p.p.m.
7.95
7.90
7.85
7.80

Fig. 2.4. (contd.)

shown in Figs. 2.4.(e), (f), (g) and (h).

The broad peak centred at 9.46 ppm is coupled to only the double-doublet centred at 6.35 ppm; this was confirmed by the decoupling experiment shown in Figs. 2.4(a) and (b). Despite the decoupling, the peak still remained quite broad. This suggested that this hydrogen may be directly attached to one of the N-atoms of the bipym ligand.

Turning to the aromatic protons on the sila-neophyl groups; each of the multiplets centred at 7.59 and 7.52 ppm (each representing two hydrogens) may be assigned to the two *ortho*-hydrogens of a phenyl ring and each of the multiplets centred at 7.29 and 7.21 ppm (with integrals representing three hydrogens) may be assigned, respectively, to two *meta*- and one *para*-

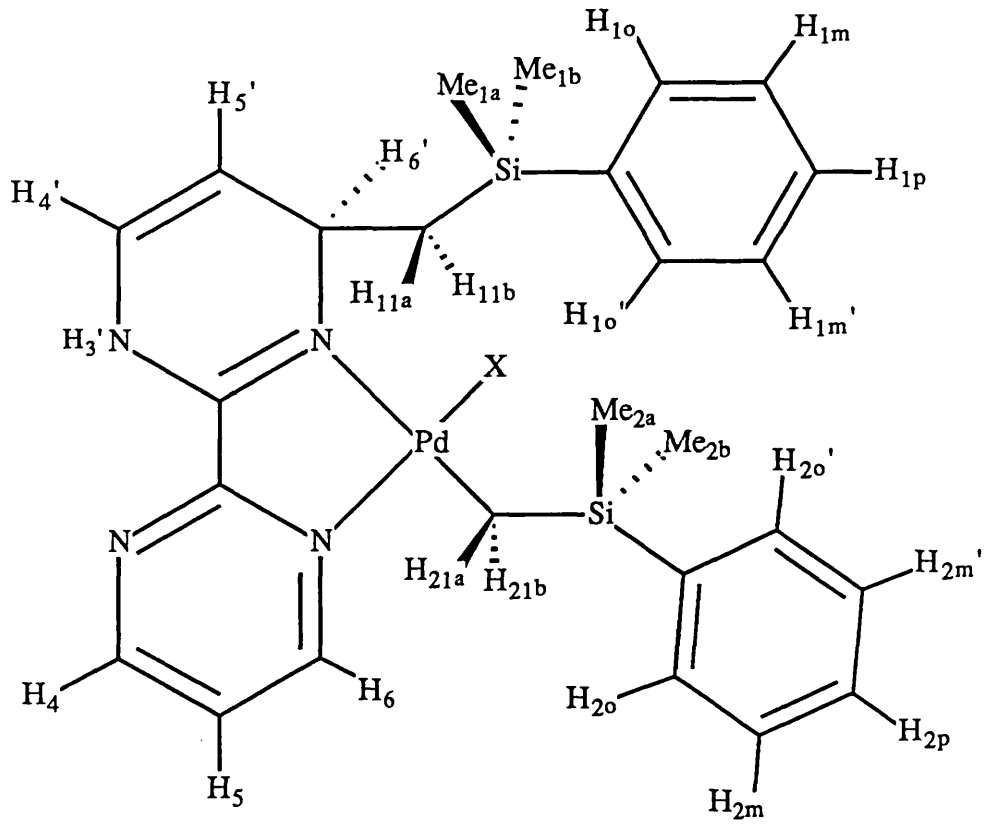


Fig. 2.5. **Proposed structure of 2a.**

hydrogens of a phenyl ring. Assigning the multiplets to the relavent alkyl group was not as straightforward. The multiplet at 7.59 ppm was tentatively assigned to H2o and H2o' on the basis of the equivalent resonances in (bipy)Pd($CH_2SiMe_2Ph)_2$ and (Me_2bipy)Pd($CH_2SiMe_2Ph)_2$[12] (7.60-7.65 and 7.58-7.64 ppm respectively). Likewise the multiplet centred at 7.20-7.22 was attributed to H2m, H2m' and H2p by comparison with (bipy)Pd($CH_2SiMe_2Ph)_2$ (7.12-7.17 ppm) and (Me_2bipy)Pd(CH_2Si-$Me_2Ph)_2$[12] (7.13-7.18 ppm).

The presence of only two sila-neophyl groups in **2a** is further supported by the evidence of four distinguishable methylene hydrogens, two diastereotopic hydrogens on the sila-neophyl group on the pyrimidine ring giving rise to a pair of double-doublets centred at 1.28 and 1.46 ppm and a diastereotopic pair on the sila-neophyl group coordinated to the palladium atom giving a pair of doublets centred at 1.56 and 0.41 ppm. Each of these pairs of diastereotopic protons are coupled strongly to each other, the former pair with a $^2J_{(H-H)}$ of 13.9 Hz and the latter pair with a $^2J_{(H-H)}$ of 11.0 Hz, which may be clearly observed from Fig. 2.7.

From the values of $^3J_{(H-H)}$ between H6' and H11a or H11b (using $^3J_{(H-H)}$=7-cosϕ+5cos2ϕ[44]) we estimate ϕ, the dihedral angles, as being ca. 165° and 65°. These angles not only give the correct coupling constants, but also differ by ca. 130°, which is close to the expected angle (120°) between two H-C-C-H6' planes where the two carbon atoms are sp^3 hybridized (Fig. 2.6.) Fig. 2.6. shows only one of the two possible *anti*-periplanar conformations about the H_2C-C_6' bond. H11a and H11b were labelled arbitrarily. If their labels were reversed another conformation would occur,

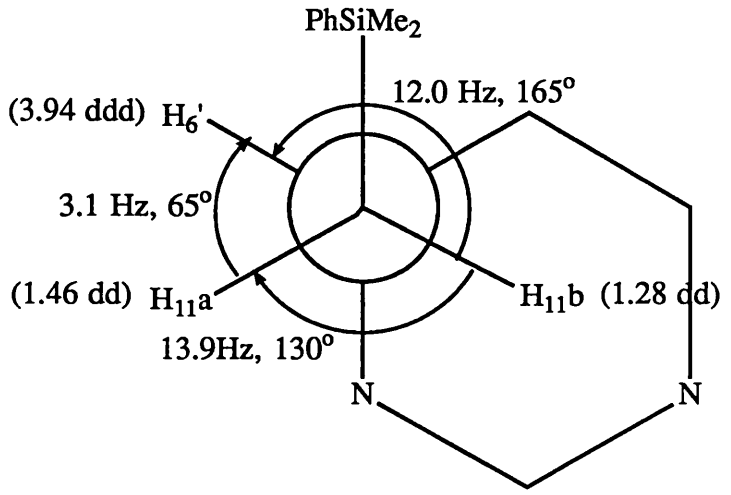


Fig. 2.6. **Newman Projection along the H_2C-C_6' bond of 2a.**

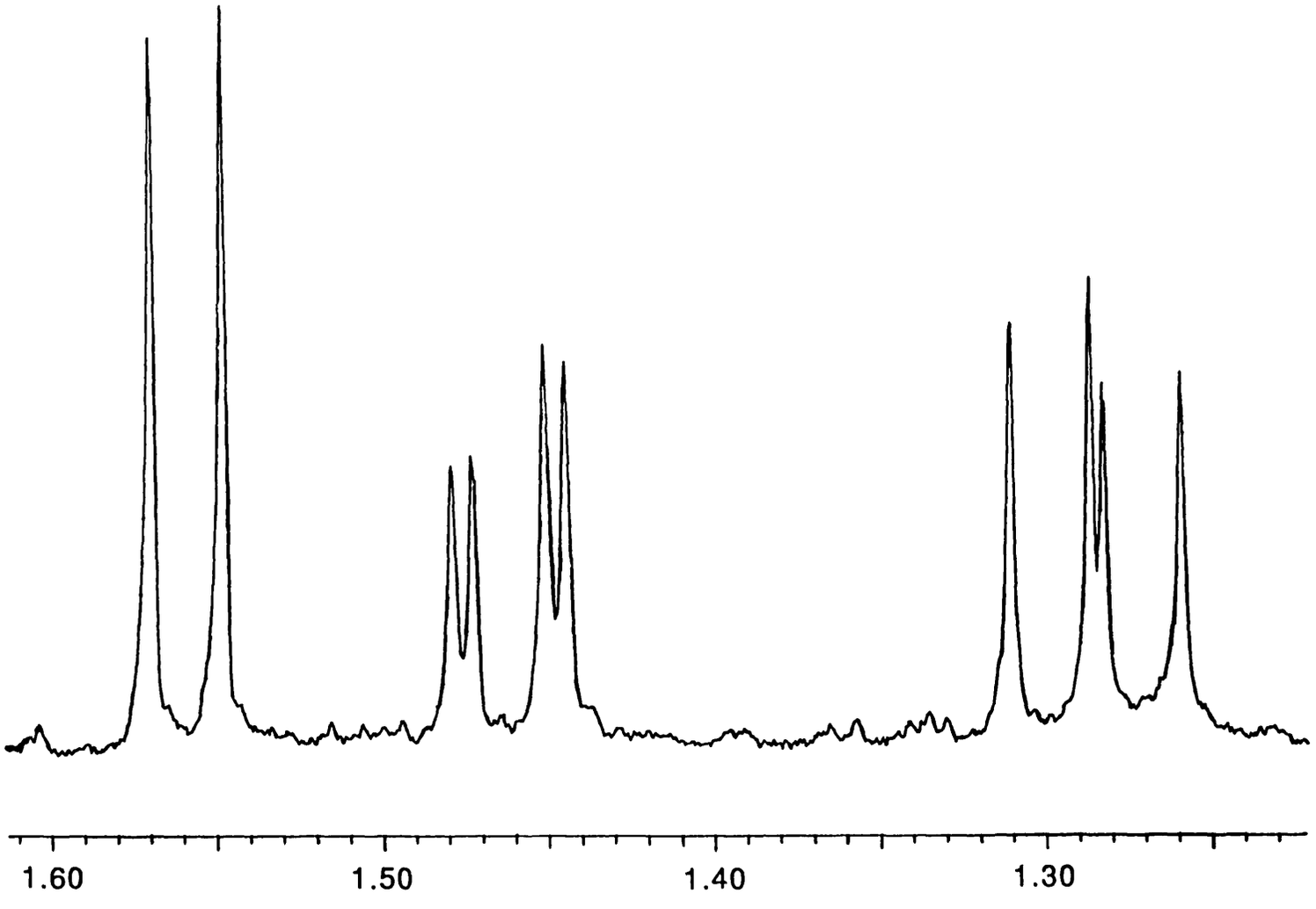
still with H11b *anti-* to H6' but with H11a now *anti-* to N1.

Only twelve hydrogens are present in the Si-Me resonances, showing up as three separate singlets at ca. 0.35 ppm. One of the singlets is broader than the other two and must correspond to two Si-Me groups.

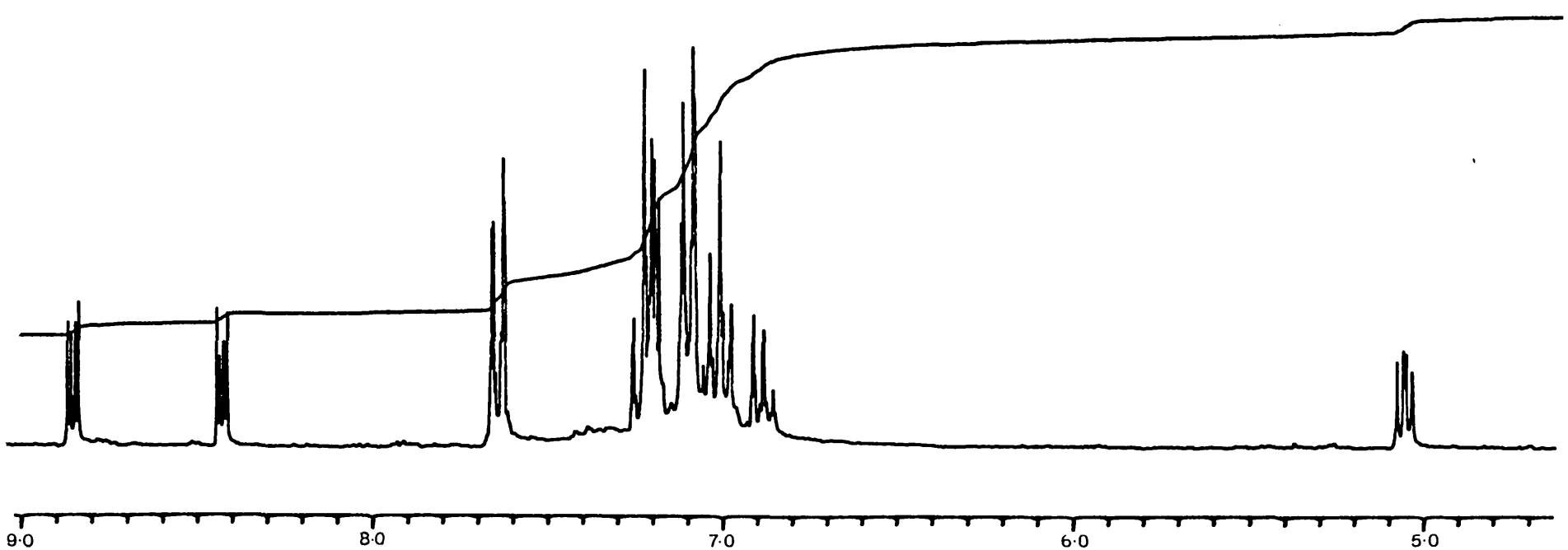
If **2a** were merely (bipym)Pd(CH_2SiMe_2Ph)$_2$ then we would expect only two multiplets for the phenyl hydrogens, one integrating as four hydrogens and the other corresponding to six hydrogens. Also one singlet each is expected for the methyl and methylene hydrogens. This is clearly not the case and the two sila-neophyl groups in **2a** are in completely different environments; one on the pyrimidine ring and one coordinated to the palladium. The tetrahedral geometry around C_6' has lowered the symmetry of **2a** causing magnetic inequivalence between all the methylene resonances and between the methyl groups.

As palladium is four coordinate in most of its complexes

Fig. 2.7. **^{1}H NMR resonances for H11a, H11b and H21a in complex 2a.**



^{1}H NMR Spectrum of **2b**



and only one sila-neophyl ligand is coordinated to it, the nature of the fourth ligand in **2a** is unknown. The most likely candidate is chloride. This is supported by the elemental analysis of the compound.

Reaction of $Mg(CH_2CMe_2Ph)Cl$ with $(Bipym)PdCl_2$.

The ^1H NMR spectrum of **2b** (250 MHz, d_6-acetone) showed four singlets at 1.69, 1.56, 1.48 and 1.22 ppm, each corresponding to three hydrogens. These were assigned to four inequivalent C-Me groups. Also visible were two pairs of doublets; one pair at 1.76 and 2.45 ppm (J=8.8Hz) and the other pair at 2.77 and 2.66 ppm (J=17.7Hz). The former pair are assigned as H21a and H21b on the basis of their similarity to the analogous resonances in **2a**. The aliphatic resonances are very similar to those in **2a**, except that they are shifted downfield by about 1 ppm. It appears that in **2b** there are again two different alkyl groups containing chemically and magnetically inequivalent methylene and methyl hydrogens.

There are, however, no apparent corresponding alkenic or allylic resonances or couplings to the methylene hydrogens at 2.66 and 2.77 ppm associated with these hydrogens in **2a**. In fact, only the resonances attributable to one unsubstituted pyrimidine ring coordinated to the palladium are clearly evident with multiplets centred at 8.85 [H6], 8.42 [H4] and 5.05 [H5] ppm, each of whose relative intensities indicate a single hydrogen (Fig. 2.8.) These multiplets are shifted upfield compared to **2a** by 0.34, 0.64 and notably 2.84 ppm respectively. In fact this part of the spectrum more closely resembles the ^1H NMR spectrum of $(bipym)Pt(CH_2CMe_2Ph)_2$[12] where H4 and H6 generate a multiplet at

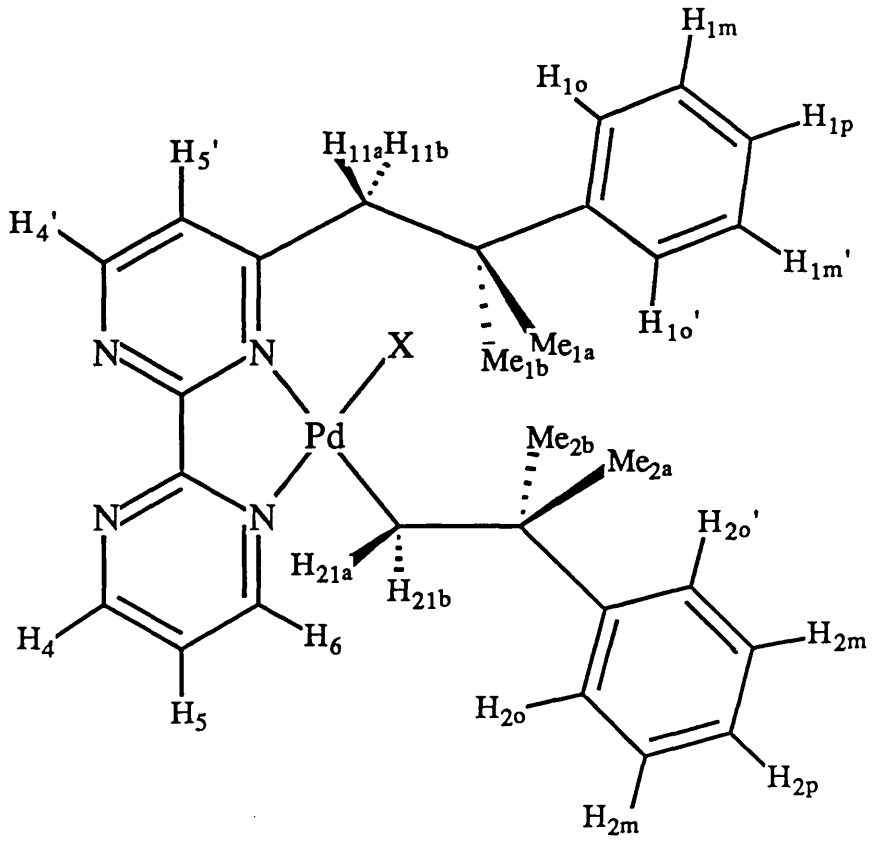


Fig. 2.9. **Proposed structure of 2b.**

8.16 ppm and H5 produces a double-doublet at 5.93 ppm with indistinguishable equal coupling (6 Hz) to H4 and H6.

Although the hydrogens on the second pyrimidine ring are not immediately discernable, the multiplet at 6.84-7.26 ppm contains contributions from 9-10 hydrogens which, together with the H2o and H2o' hydrogens in the multiplet at 7.62-7.67 ppm indicates 11-12 aromatic hydrogens in total. Plausibly, therefore, the other pyrimidine ring *is* neophyl-substituted, but has retained (or regained) its aromaticity and the H4' and H5' resonances are contained in the multiplet at 6.84-7.27 ppm.

The proposed structure of **2b** is shown in Fig. 2.9. Nucleophilic attack of PhLi on 2-phenyl-4-methyl pyrimidine followed by oxidation (Fig. 2.1.) has given a product with a

structure similar to that proposed for **2b**. It seems possible that the production of **2b** occurs via a neophyl analogue of **2a** which was then oxidised (possibly by adventitous dioxygen) to **2b**.

One difficulty with the proposed structure is that the aromatic (sp^2) nature of C_6' (which is no longer tetrahedral) implies magnetic and chemical equivalence between the methylene hydrogens and between the methyl groups within each alkyl group. This is because **2b**, unlike **2a**, contains a mirror plane. This magnetic equivalence could be removed (giving the observed four methylene and four methyl signals) by postulating some form of restricted rotation around the C_6'-CH_2 or Pd-CH_2 bonds.

Reaction of $Mg(CH_2SiMe_3)Cl$ with $(Bipym)PdCl_2$.

^1H NMR analysis suggests that the product of the reaction of $Mg(CH_2SiMe_3)Cl$ with $(bipym)PdCl_2$ is a 70:30 mixture of two compounds **2c** and **2d**, of which at least one, **2c**, has undergone nucleophilic attack at one of its pyrimidine rings. For **2c** the aliphatic region of the spectrum indicates six Si-Me environments at 0.14 to -0.06 ppm. Also present are several methylene resonances including doublets centred at 0.33 and 1.38 ppm, and double-doublets centred at 1.11 and 1.31 ppm.

Table 2.1. shows a comparison of the ^1H NMR data for **2a** and **2c** from which it is clearly evident that the two compounds have very similar ^1H NMR characteristics. An analogous structure for **2c** seems likely.

Nucleophilic Attack on Coordinated Diimines.

In an attempt to rationalise covalent hydrate formation by

nucleophilic attack on coordinated diimine ligands, INDO molecular orbital calculations have been carried out[38] on both free and coordinated (as $[FeL(CN)_4]^{2-}$) pyridine, 1,10-phenanthroline, 2,2'-bipyridyl, 2,2'-bipyrimidyl, 2,2'-bipyrazyl, 3,3'-bipyridazyl and 4,4'-bipyrimidyl. Calculations of the charges at the various ring sites are quite revealing (and are shown in Fig. 2.10. for 2,2'-bipyridyl, 1,10-phenanthroline and 2,2'-bipyrimidine). Of these seven ligands, the free ligand with the greatest positive charge at any single ring site is 4,4'-bipyrimidyl, where the C2 and C6 have charges of +0.299 and +0.203 respectively. These are closely followed by 2,2'-bipyrimidyl where both C6 and C4 have charges of +0.201 and C2 has a charge of +0.235 (the free ligand has a C_2 axis along the C2-C2' bond).

Looking at the effects of coordination of these ligands to the divalent metal in $[FeL(CN)_4]^{2-}$, these calculations show that on coordination to the iron atom most carbons in the complexes suffer a *reduction* in positive charge by about 0.020. This reduction was unexpected as it was thought that coordination to a metal atom, like quarternisation, would result in an increase in positive charge on the ring. But it should be remembered that coordination to a d-block element, unlike quarternisation, may involve retrodative back-bonding. It seems that it is this back-bonding which causes the reduction in positive charge at the ring carbon sites.

The greatest positive charge on any ring site in these coordinated ligands is still for 4,4'-bipyrimidyl (+0.287 at C2), closely followed again by 2,2'-bipyrimidyl (+0.221, +0.187 and +0.167 at C2, C6 and C4 respectively).

If nucleophilic attack at the ring were purely charge-controlled, then coordinated 2,2'-bipyrimidyl would be more likely to undergo attack than either coordinated 2,2'-bipyridyl or 1,10-phenanthroline. Also attack should occur less readily for coordinated 2,2'-bipyrimidyl than for free 2,2'-bipyrimidyl, although the difference should be slight. And finally the most likely sites of attack are at C2 or C6. Because attack occurs at C6

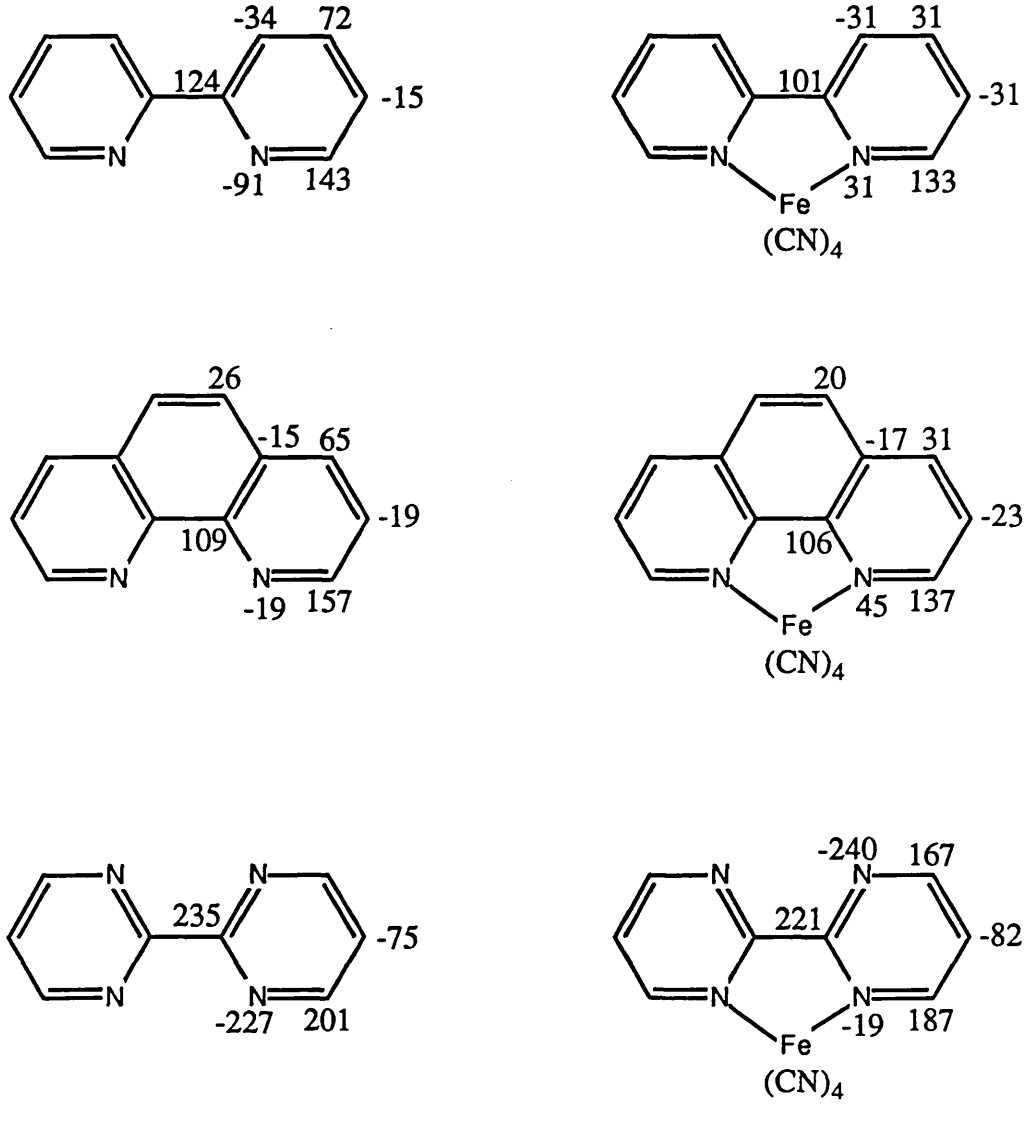


Fig. 2.10. **Calculated Charges (x 1000) on Ring in Free Ligands and in $[FeL(CN)_4]^{2-}$ Complexes.[38]**

and not (as far as we can detect) at C2, we may immediately say that the charge at any site on the ring is not the sole factor controlling the regioselectivity of the reaction. The C2 position is more sterically hindered than the C6 position by the presence of the other pyrimidine ring and this in itself inhibits attack at C2. A third factor which may affect the regioselectivity is the matching of energies and symmetry of the HOMO on the incoming nucleophile and the LUMO of the coordinated pyrimidine ring.

These predictions agree well with the current observations. For the palladium compounds, reaction with $Mg(CH_2SiMe_2Ph)Cl$ resulted in nucleophilic attack on the diimine ligand at C6 for 2,2'-bipyrimidyl but not at all for 2,2'-bipyridyl or 1,10-phenanthroline (Chapter 1). It should be remembered, however, that (bipy)$PdBr_2$ and (phen)$PdBr_2$ were reacted with $Mg(CH_2SiMe_2Ph)Cl$ (in Chapter One) while in this case the metal substrate was (bipym)$PdCl_2$. It has already been mentioned that the degree of back-bonding from the metal will alter the charges on the ring. In (bipym)$PdCl_2$, the degree of back-bonding from the $PdCl_2$ moiety should be different to the degree of back-bonding from the $PdBr_2$ moiety in (bipy)$PdBr_2$ and (phen)$PdBr_2$.

Looking at the calculated charges on the coordinated 2,2'-bipyrimidyl ligand in $[Fe(2,2'\text{-bipym})(CN)_4]^{2-}$, it should be noticed that the N3 position has a charge of -0.240 compared to -0.019 for N1. Although we should again stress that our (bipym)$PdCl_2$ would have different charges on the ring, and that attack by the Grignard reagent at C6 would further alter these charges, we may still say that N3 in the deprotonated form of **2a** would probably have a larger negative charge than N1. This lends further support to our assertion that the N3 position is protonated in preference

to the N1 position. From the 2D ^1H NMR, there is no association of H3' to N3 of the unattacked pyrimidine ring or to either of the two N1 sites. Any such association would be visible in the form of couplings to hydrogens α- to these nitrogens.

The mechanisms of the reactions producing **2a**, **2b**, **2c** and **2d** cannot yet be assigned unequivocally. Reaction of (bipym)$PdCl_2$ with anything between one and four equivalents of $Mg(CH_2SiMe_2Ph)Cl$ produces **2a** as the only observable Pd-containing product (with only one equivalent of $Mg(CH_2SiMe_2Ph)Cl$ unreacted (bipym)$PdCl_2$ remains on quenching the reaction mixture). The second pyrimidine ring is never attacked. This information does not, however, help to determine the sequence of attack on the ring and on the metal.

An interesting future project would be to investigate the possibility of nucleophilic attack on (4,4'-bipyrimidine)$PdCl_2$ and to compare this to the nucleophilic attack on (2,2'-bipyrimidine)$PdCl_2$.

Reaction of 2,2'-Bipyrimidine with Organomagnesium Reagents.

The nature of the dark-coloured compounds formed on reaction of free 2,2'-bipyrimidine with organomagnesium reagents is not known. 1,10-phenanthroline has been used as an indicator in the titration of organomagnesium and organolithium reagents in the past.[44] Addition of a small amount of 1,10-phenanthroline to certain organomagnesium reagents results in a violet coloration in the solution. It is thought that the 1,10-phenanthroline underwent simple reversible coordination with the organomagnesium reagent to give the charge-transfer complex.

2,2'-Bipyrimidine may be working in much the same way, but with the possibility of bidentate coordination to two metal centres; the deep-red insoluble products that we observed may be the binuclear species. It may be significant that the only solvent in which these charge-transfer complexes were reasonably soluble was pyridine, which is highly coordinating. Pyridine could be cleaving the binuclear species into monomeric species which would then be soluble. The ^1H NMR spectra of these charge-transfer complexes in solution in d_5-pyridine were complicated.

It was also thought that the deep-red glassy solid formed on removing pyridine from these solutions *in vacuo* contained coordinated pyridine. ^1H NMR spectra of the glassy deep-red solids in solution in d_5-pyridine showed very large solvent peaks compared to that of the pure solvent; due to rapid exchange of the coordinated undeuterated pyridine with the deuterated solvent

Although we could not determine the exact nature of the products of reaction of organomagnesium reagents with 2,2'-bipyrimidine, our failure to detect any evidence of nucleophilic addition to the free 2,2'-bipyrimidine meant that coordinating the ligand to a metal centre (in our case Pd(II)) caused it to react in a manner unlike that of the free ligand.

CHAPTER THREE

Relative Platinum-Carbon Bond Strengths in Organoplatinum Complexes with β-Carbon and Silicon Atoms.

3.1. INTRODUCTION

Rearrangements of Neopentyl and (Trimethylsilyl)methyl Transition Metal Complexes.

It is often found that neopentyl and (trimethylsilyl)methyl complexes of d-block and f-block transition metals re-arrange similarly, undergoing intramolecular cyclometallation at the γ-C-H site to give substituted metallacyclobutanes (Fig. 3.1.)[45-51]. This rearrangement is usually slower for the trimethylsilyl-methyl derivative than for the corresponding neopentyl derivative (Fig.3.2.[15] and Fig.3.3.[50,51])

However, it was recently shown that such similarities in the chemistry of analogous alkyl complexes with and without β-Si atoms are not universal. Apart from the work already mentioned,[45-51] where platinacyclobutanes were formed from the neopentyl and trimethylsilylmethyl analogues, there have been several instances where the two alkyl groups show distinctly different chemical behaviour when coordinated to a metal centre (Figs. 3.4., 3.5. and 3.6.)[52-57]

For example, the thermolytic rearrangement of $(PEt_3)_2Pt$-

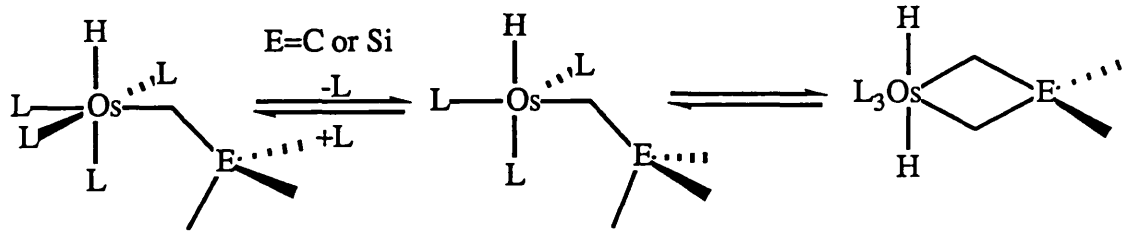


Fig. 3.1. **Reversible Cyclometallation in *cis*- L_4OsRH (where L=PMe_3 and E=Si or C.)**

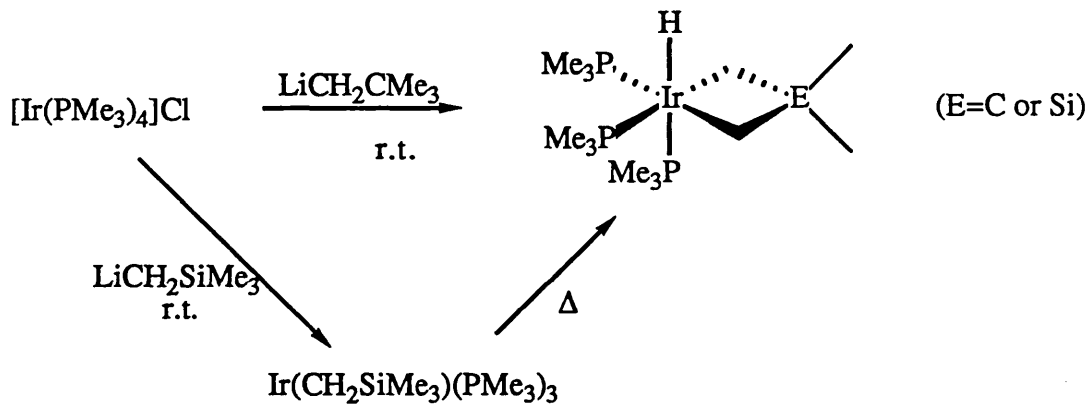


Fig. 3.2. **Reaction of $[Ir(PMe_3)_4]Cl$ with $LiCH_2CMe_3$ and $LiCH_2SiMe_3$ with Subsequent Cyclometallations.[15]**

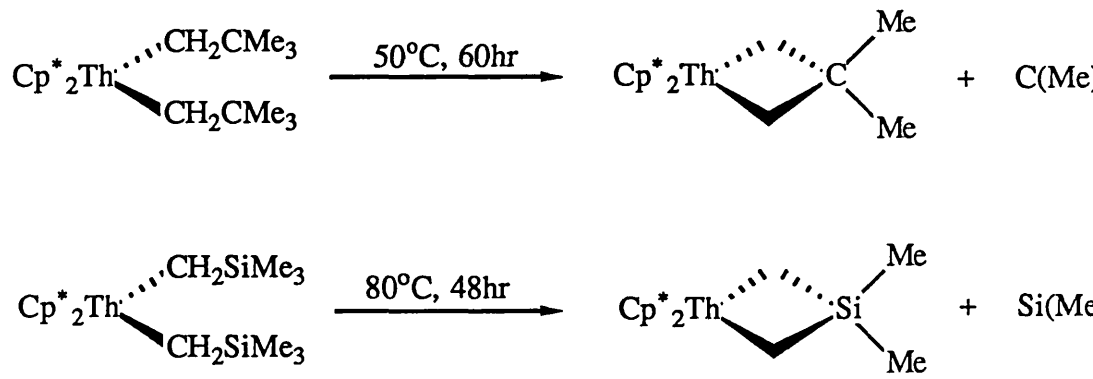


Fig. 3.3. **Cyclometallation of Thorium Dialkyls.[49,50]**

$(CH_2CMe_3)_2$ was shown to proceed as expected, to give the substituted platinacyclobutane (Fig.3.5.)[53,54] In contrast, thermolysis of the corresponding trimethylsilylmethyl compounds[55,56] (where L=PPh_3, PPh_2Me, PMe_3 and PEt_3) in toluene resulted in coupling of the two alkyl groups to give the {[(trimethylsilyl)-methyl]dimethylsilyl}methyl group, via a β-methyl transfer from silicon to platinum. The proposed mechanism for this reaction is

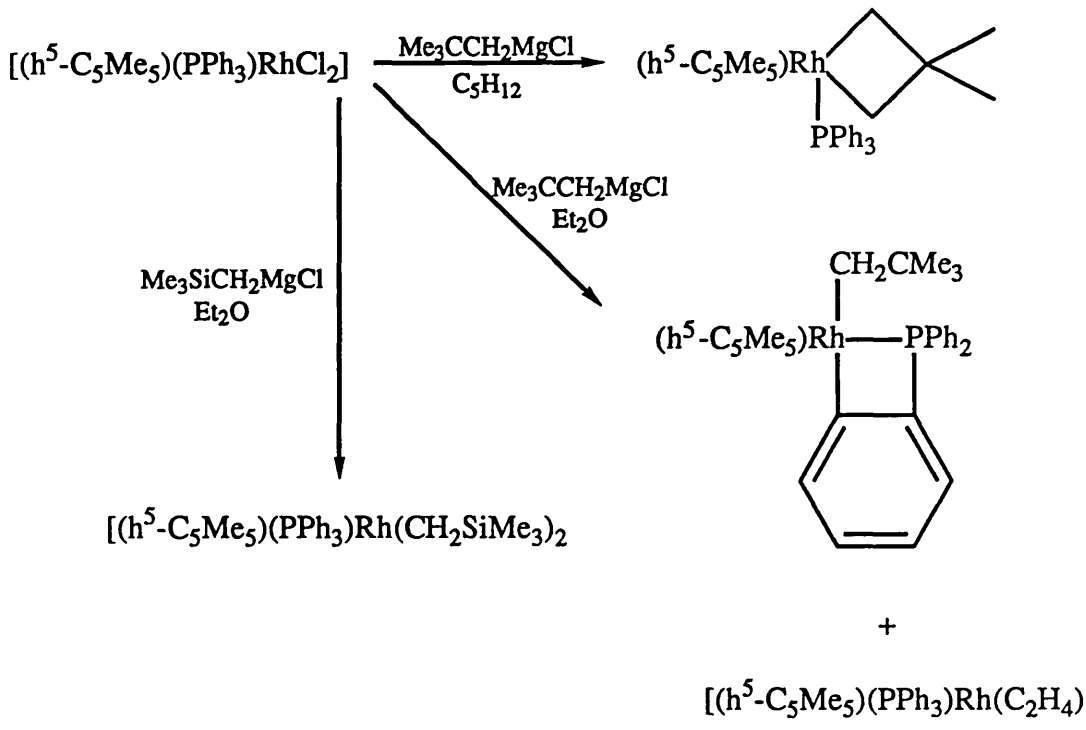


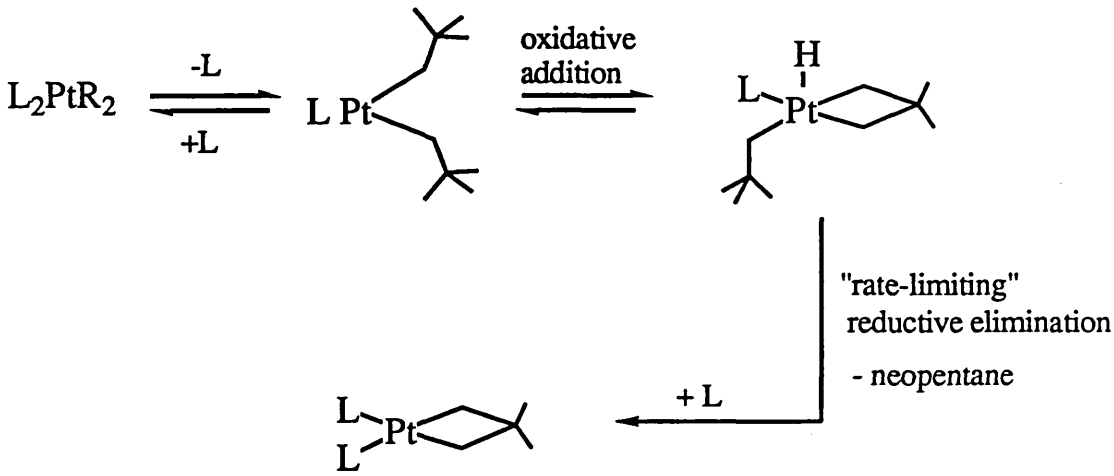
Fig. 3.4. **Alkylation of $[(h^5\text{-}C_5Me_5)(PPh_3)RhCl_2]$ by Me_3SiCH_2MgCl and Me_3CCH_2MgCl.[52]**

shown in Fig. 3.6. Initial loss of phosphine resulted in a T-shaped intermediate which underwent rearrangement, probably via the η^2-silene complex to give the methyl(trimethylsilylmethyldimethylsilylmethyl)platinum(II) complex as the product, which was characterized by X-ray crystallography.

Rearrangements of Neophyl and Sila-neophyl Transition Metal Complexes.

In the same way, neophyl complexes of the transition metals rearrange by intramolecular cyclometallation at the δ-C-H site to give the substituted 1-metallaïndan (Figs. 3.7. and 3.8.)[1,3,6,9] Again the derivative with the β-Si atom turns out to be more kinetically inert[12].

Fig. 3.5. **Proposed Mechanism for the Thermal Cyclisation of $Pt(CH_2CMe_3)_2(PEt_3)_2$.**[53-54]

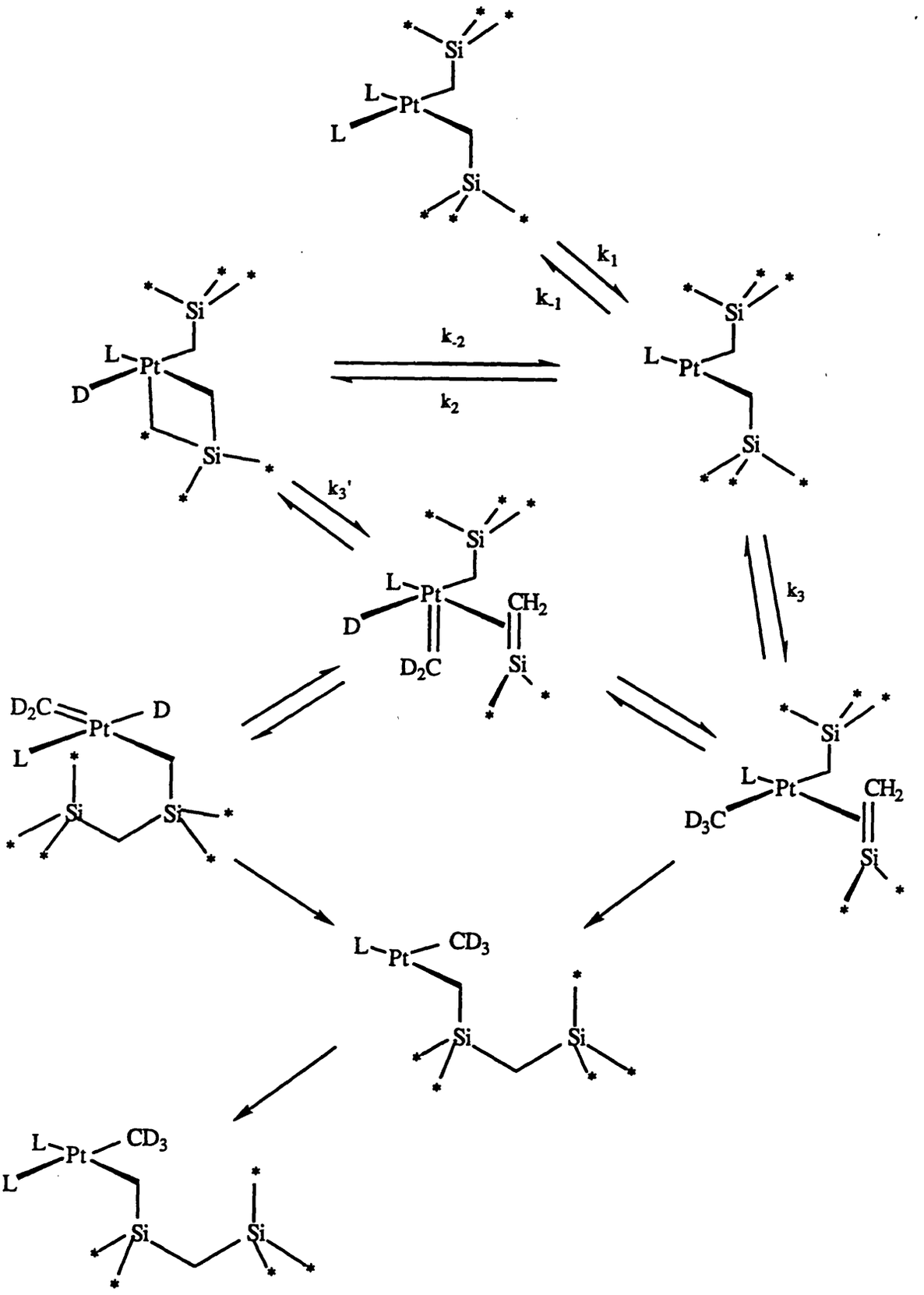


It would be interesting to see whether any differences in the Pt-C bond strengths of organoplatinum complexes with and without β-Si atoms may correlate with differences in reactivities and stabilities, or whether these effects originate in steric or kinetic effects of the alkyl groups.

Calorimetric Measurements of Pt-C Strengths in *trans*-$Pt(CH_2EMe_3)(Cl)(PMe_3)_2$ (where E = C and Si).

In measuring the relative Pt-C bond strengths in a pair of analogous neopentyl and trimethylsilylmethyl complexes we adapted the general methods reported by Marks[58-61], Lappert and Pedley[62,63], and Ashcroft and Mortimer.[64] The first two groups have measured actual M-C bond strengths for thorium and uranium and for titanium group neopentyl and trimethylsilylmethyl complexes. Ashcroft and Mortimer have calculated the Pt-C bond

Fig. 3.6. **Proposed Mechanism for the Thermal Rearrangement of $Pt(CH_2SiMe_3)(PEt_3)_2$.**



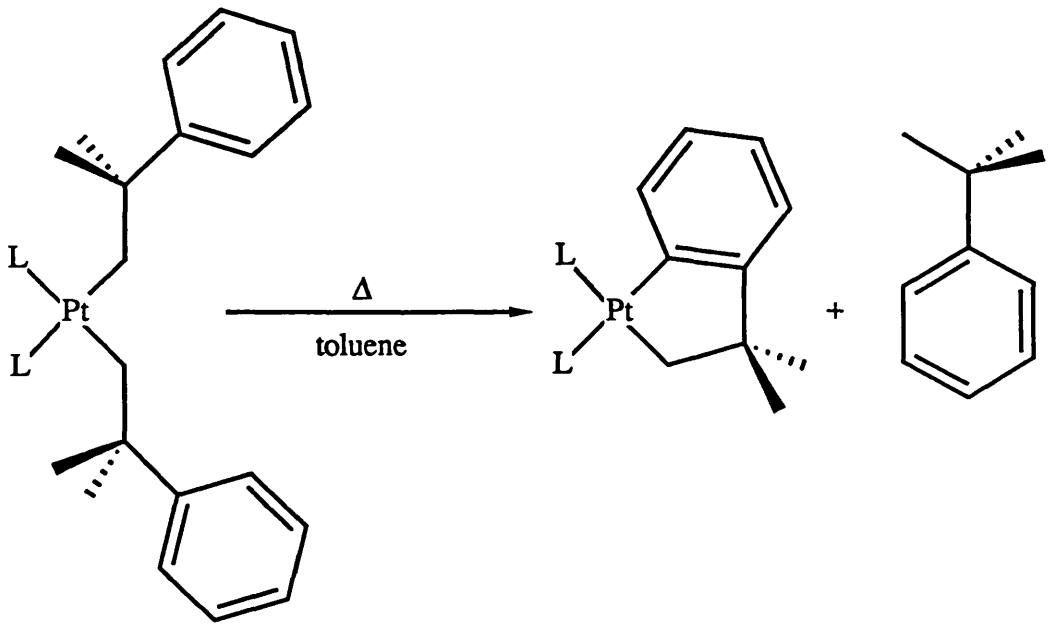


Fig. 3.7. **Cyclometallation of $L_2Pt(CH_2CMe_2Ph)_2$ (where L_2=cod, bipy, bipym, Ph_2phen or L=PEt_3, PPh_3).**

strength in *trans*-$(Et_3P)_2Pt(phenyl)_2$ as being 250 kJ mol^{-1}. This was done by measuring the heat of reaction of *trans* - $(Et_3P)_2Pt(phenyl)_2$with a solution of anhydrous HCl in dioxane giving *trans*- $(Et_3P)_2Pt(phenyl)Cl$ and benzene as the products, and by estimating the platinum-chlorine bond strength in the product complex as being 380 kJ mol^{-1}.

We surmised that a similar approach might be appropriate to the measurement of the bond strengths of platinum-carbon σ-bonds in a pair of structurally similar neopentyl and trimethylsilylmethyl complexes. In order to minimise differences which could arise through the nature and internal arrangement of ligands, a pair of compounds was identified which reacted with retention of stereochemistry about the platinum:-

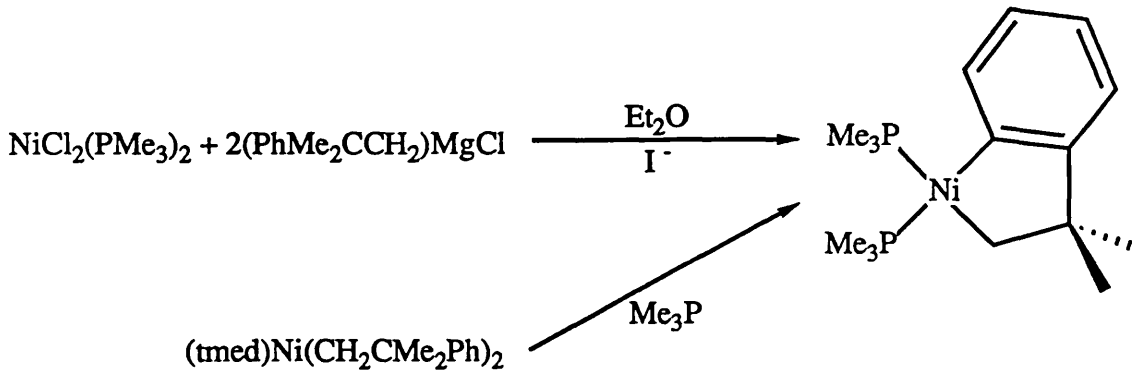


Fig. 3.8. **Cyclometallation of $(Me_3P)_2Ni(CH_2CMe_2Ph)_2$ produced from $(Me_3P)_2NiCl_2$ or (tmed)Ni(CH_2-$CMe_2Ph)_2$.**

$(PR'_3)_2PtR_nCl_{(2-n)} + HCl = (PR'_3)_2PtR_{(n-1)}Cl_{(3-n)} + RH$
where R=neopentyl and trimethylsilylmethyl and n=2,1

It was preferable for only one R group to be cleaved during the reaction, as if $(PR')_2PtR_2$ was reacted with two equivalents of HCl to give $(PR'_3)_2PtCl_2$, then the measured energy change would be the sum of the energy changes for two different reactions, giving only a mean value for the Pt-C bond strength for the dialkylplatinum and monoalkylmonochloroplatinum complexes; a highly unsatisfactory situation.

Preliminary ^{31}P NMR studies indicated that the two complexes *trans*-$(Me_3P)_2Pt(CH_2CMe_3)Cl$ and *trans*-$(Me_3P)_2Pt$-$(CH_2SiMe_3)Cl$ were suitable model compounds. These compounds both reacted with HCl in dioxane at ambient temperature to give *trans*-$(Me_3P)_2PtCl_2$ as sole detectable product. They had the added bonus of the small cone angle of PMe_3 minimising steric interactions between the alkyl and phosphine groups, which have in the past been blamed for the weaker M-C bond strengths in

neopentyl complexes (vide infra). It was also quite important that the model compounds could be obtained free from impurities and in good yield as solids.

There have been several mechanistic studies of interest on reactions of similar *trans*-bis(phosphine)neopentylplatinum(II) complexes.

The probable mechanism of the thermal rearrangement of *trans*- chloroneopentylbis(tricyclopentylphosphine)platinum(II) to *trans*- chlorohydridobis(tricyclopentylphosphine)platinum(II) and 1,1-dimethylcyclopropane (DMC) was elucidated.[65] This reaction proceeded by loss of phosphine followed by intramolecular γ-H-transfer to form the platinacyclobutane, which rearranged to the DMC and *trans*- $(Cy_3P)_2PtHCl$.

Another species very similar to our model neopentyl complex has been shown to undergo intermolecular C-H bond activation with d_6-benzene.[66] *Trans*-neopentyl(trifluoromethanesulfonato)bis(trimethylphosphine)platinum(II) was shown to react with d_6-benzene at 133 ° C to give *trans*- $(Me_3P)_2Pt(C_6D_5)(SO_3CF_3)$ and neopentane-d_1 as products.

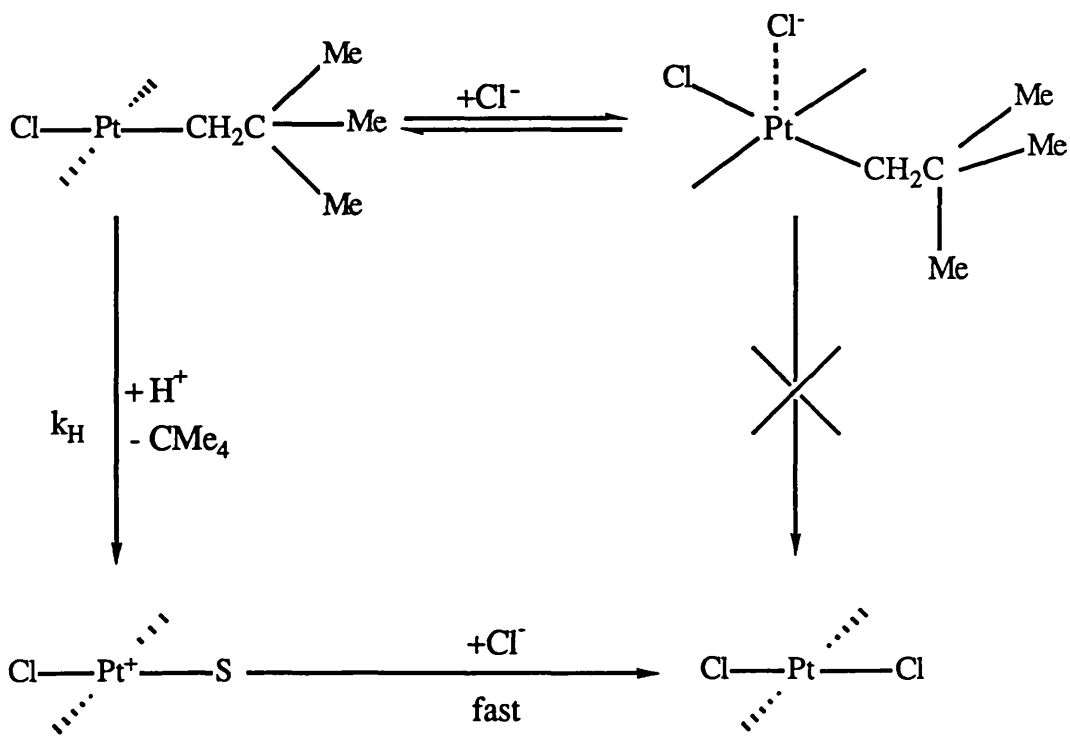
Measurement of the Pt-C bond energies for our model compounds might provide insight into these systems, just as the measurement of Th-C bond energies in the thorium dialkyls of Marks gave an insight into the intermolecular activation of benzene[67], Me_4Si[68,69], cyclopropane[68] and even CH_4[68] by thoracyclobutanes.

It should be remembered, however, that the mechanisms of the C-H activation of the hydrocarbons are different for the platinum and thorium systems. As seen earlier, platinum tends to lose one ligand e.g. a phosphine or, in this case, a triflate group,

to form a T-shaped, tri-coordinate intermediate which may then undergo C-H activation by oxidative addition. The thorium has no labile ligands to lose and is already in a high oxidation state (IV). So the activation mechanism is more likely to be concerted, passing through a highly ordered transition state (as indicated by a negative entropy of activation), with direct transfer of a hydrogen from one alkyl group to the other.

The mechanism of the reaction of *trans*-$(PEt_3)_2Pt(CH_2CMe_3)Cl$ with HCl in aqueous methanol was determined (Fig. 3.9.)[70] Although the mechanism for our reaction may be different due to the difference in the nature of the solvent and of the phosphine, it is interesting to note that the above reaction

Fig. 3.9. **Mechanism for the Protonolysis of *trans*- $(Et_3P)_2Pt(CH_2CMe_3)Cl$.**



(S=solvent)

proceeds by initial rate-limiting protonation of the platinum complex. Reversible attack by chloride on the platinum complex may occur to give a five-centred intermediate, but the reaction proceeds no further.

3.2. SYNTHESES OF REAGENTS

Preparation of $(COD)PtCl_2$

This was prepared by the modified method of McDermott, White and Whitesides[71].

Preparation of $(COD)Pt(CH_2SiMe_3)_2$

To a stirred suspension of $(COD)PtCl_2$ in Et_2O (2.00g, 5.35mmol in 100mL) was added an ethereal solution of $Mg(CH_2SiMe_3)Cl$ (3.00 equivalents, 16.04mmol) dropwise at -78° C. The mixture was allowed to reach ambient temperature and stirred overnight. Next saturated aqueous NH_4Cl solution (60mL) was added dropwise at -20° C and the mixture allowed to warm up to ambient temperature while stirring. The ethereal layer was decanted off, the aqueous layer washed with fresh Et_2O (2 x 50mL) and the combined ethereal solutions dried and decolourised over anhydrous $MgSO_4$ and activated charcoal respectively. Concentration of the colourless solution *in vacuo* yielded white crystals of the product. Yield = 2.42g (95%).

Preparation of $(COD)Pt(CH_2SiMe_3)Cl$

A solution of HCl in dry Et_2O (25.6mL, 0.31M, 7.94mmol, 1.99 equivalents) was added dropwise at -78° C to a stirred solution of $(COD)Pt(CH_2SiMe_3)_2$ in Et_2O (1.90g, 3.98mmol in

50mL), and the mixture allowed to warm up to ambient temperature and stirred overnight. The ether was then removed *in vacuo* to give a white crystalline solid. Yield = 1.60g (94%).

^{1}H n.m.r. (90MHz, $CDCl_3$): 0.1 (s) [-CH_3]; 1.0 (t, $J_{(Pt-H)}$ =76Hz) [Pt-CH_2]; 2.3 (m) [COD -C**H**$_2$-]; 4.5 (m, $J_{(Pt-H)}$ =76Hz) [COD C=C**H**- (*trans* - to Cl)]; 5.4 (m, $J_{(Pt-H)}$ =38Hz) [COD C=C**H**- (*trans* - to R)].

Preparation of (COD)Pt(CH_2CMe_3)$_2$

This was prepared in the same way as (COD)Pt(CH_2SiMe_3)$_2$ except using Mg(CH_2CMe_3)Cl (3.00 equivalents, 18.92mmol). The product was obtained as pale yellow crystals. Starting with 2.36g (6.31mmol) of (COD)$PtCl_2$, yield = 2.63g (93%).

Preparation of (COD)Pt(CH_2CMe_3)Cl

A solution of HCl in dry Et_2O (20.3mL, 0.31M, 6.29mmol, 2.00 equivalents) was added dropwise at -78° C to a stirred solution of (COD)Pt(CH_2CMe_3)$_2$ in Et_2O (1.40g, 3.14mmol in 50mL), and the mixture allowed to warm up to ambient temperature and stirred overnight. The ether was then removed *in vacuo* to give the product as an off-white solid. Yield = 1.17g (91%).

^{1}H n.m.r. (90MHz, $CDCl_3$): 1.1 (s) [CH_3]; 1.8 (t, $J_{(Pt-H)}$ =76Hz) [Pt-C**H**$_2$]; 2.3 (m) [COD -C**H**$_2$-]; 4.5 (m, $J_{(Pt-H)}$ =76Hz) [COD C=C**H**- (*trans* - to Cl)]; 5.5 (m, $J_{(Pt-H)}$ =34Hz) [COD C=C**H**- (*trans* - to R)].

Preparation of (Me_3P)$_2$Pt(CH_2SiMe_3)Cl and (Me_3P)$_2$Pt-(CH_2CMe_3)Cl

To a stirred solution of (COD)PtRCl (where R= -CH_2SiMe_3 or -CH_2CMe_3) in toluene at ambient temperature (1.10g in 15mL) was added neat Me_3P (2.20 equivalents) by syringe. The solution turned

cloudy immediately and was left stirring for two days. After this time the solvent was removed *in vacuo* to give the product as a white solid which was recrystallised from acetone to give colourless plates when R= $-CH_2SiMe_3$ or white needles when R= $-CH_2CMe_3$. As indicated by their ^{31}P, ^{13}C and ^{1}H NMR spectra (vide infra) the products are both pure *trans*- isomers.

Anal.

Calcd. ($C_{10}H_{29}ClP_2PtSi$): C, 25.56; H, 6.22; Cl, 7.54. Found: C, 25.57; H, 6.25; Cl, 7.71.

Calcd. ($C_{11}H_{29}ClP_2Pt$): C, 29.11; H, 6.44. Found: C, 28.90; H, 6.41.

^{31}P NMR (36.21MHz, d-chloroform): -

R= $-CH_2SiMe_3$; -14.60 p.p.m., -529.5Hz (t, $^{2}J_{(Pt-P)}$=2764.7Hz).

R= $-CH_2CMe_3$; -13.62 p.p.m., -494.0Hz (t, $^{2}J_{(Pt-P)}$=2933.1Hz).

^{1}H NMR (90MHz, d-chloroform): -

R= $-CH_2SiMe_3$; 0.02 (t, $^{4}J_{(Pt-H)}$ =2.4Hz) [CH_3]; 0.36 (tt, $^{2}J_{(Pt-H)}$ =91.8Hz, $^{3}J_{(P-H)}$ =18.8Hz) [Pt-CH_2]; 1.49 (tt, $^{3}J_{(Pt-H)}$ =27.4Hz, $^{2}J_{(P-H)}$ =7.0Hz) [P-CH_3].

R= $-CH_2CMe_3$; 1.03 (t, $^{4}J_{(Pt-H)}$ =4.2Hz) [CH_3]; 1.53 (tt, $^{3}J_{(Pt-H)}$ =28.4Hz, $^{2}J_{(Pt-H)}$ =7.0Hz) [P-CH_3].

^{13}C NMR (62.9MHz, d-chloroform):-

R= $-CH_2CMe_3$; 13.84 (m, $^{1}J_{(P-C)}$ =36.5Hz, $^{2}J_{(Pt-C)}$ =39.8Hz), [H_3**C**-P]; 15.50 (tt, $^{1}J_{(Pt-C)}$ =748.5Hz, $^{2}J_{(P-C)}$ =4.4Hz), [Pt-**C**H_2]; 34.09 (t, $^{3}J_{(Pt-C)}$ =48.2Hz), [-C-**C**H_3]; 35.86 (t, $^{2}J_{(Pt-C)}$ =24.0Hz), [-CH_2-**C**-CH_3].

R= $-CH_2SiMe_3$; -14.94 (tt, $^{1}J_{(Pt-C)}$=650.7Hz, $^{2}J_{(P-C)}$=4.7Hz), [Pt-**C**H_2]; 2.92 (t, $^{3}J_{(Pt-C)}$ =31.4Hz), [-Si-**C**H_3]; 13.39 (m, $^{1}J_{(P-C)}$ =38.3Hz, $^{2}J_{(Pt-C)}$=38.9Hz), [H_3**C**-P].

Preparation of HCl/1,4-dioxane solution.

1,4-Dioxane was dried over 4A molecular sieves and then distilled from sodium/benzophenone. HCl gas was passed over a portion of this distillate to give a concentrated solution of HCl in 1,4-dioxane, which was then diluted with a further portion of distillate until a 0.18M solution was obtained. This solution was stored in the dark under nitrogen.

Protonolysis of $(Me_3P)_2Pt(CH_2SiMe_3)Cl$ and $(Me_3P)_2Pt(CH_2CMe_3)Cl$ by $HCl_{(1,4\text{-dioxane})}$.

$(Me_3P)_2Pt(CH_2SiMe_3)Cl$ (ca. 6mg) or $(Me_3P)_2Pt(CH_2CMe_3)Cl$ (ca. 8mg) were dissolved in a mixture of d_6-benzene and 1,4-dioxane (75:25 v/v). The ^{31}P NMR of these solutions indicated that the stereochemistry of the complexes was *trans-* in solution.

^{31}P NMR (36.21MHz, 75% d_6-benzene and 25% 1,4-$C_4H_8O_2$): -

R= $-CH_2CMe_3$; -14.54 ppm (t, $^1J_{(Pt\text{-}P)}$ =2935.3Hz).

R= $-CH_2SiMe_3$; 15.45 ppm (t, $^1J_{(Pt\text{-}P)}$ =2773.6Hz).

The same amounts of each complex were now dissolved up in d_6-benzene under N_2 and enough of a 0.18M solution of HCl in 1,4-dioxane was added to give a 75:25 v/v mixture of d_6-benzene and 1,4-dioxane. In each case, a white solid started to precipitate out almost immediately, which was filtered off, washed with cold hexane (2 x 0.5mL) and dried *in vacuo* . Elemental analysis of these white solids showed them to be $(Me_3P)_2PtCl_2$.

Anal. Calcd: C, 17.23; H, 4.34.

Found (Product from $(Me_3P)_2Pt(CH_2\text{-}SiMe_3)Cl$): C, 17.31; H, 4.23.

Found (Product from $(Me_3P)_2Pt(CH_2CMe_3)Cl$): C, 18.01; H, 4.41.

The ^{31}P NMR spectra of the supernatant solutions revealed 1:4:1 'triplets'. The large $^1J_{(Pt\text{-}P)}$ coupling constants indicate *trans-*

products.

^{31}P NMR (36.21MHz, 75% d_6-benzene and 25% 1,4-$C_4H_8O_2$): Product from R= $-CH_2CMe_3$ -16.61 ppm (t, $^1J_{(Pt-P)}$=2401.3Hz). Product from R= $-CH_2SiMe_3$ -16.67 ppm (t, $^1J_{(Pt-P)}$ =2403.6Hz).

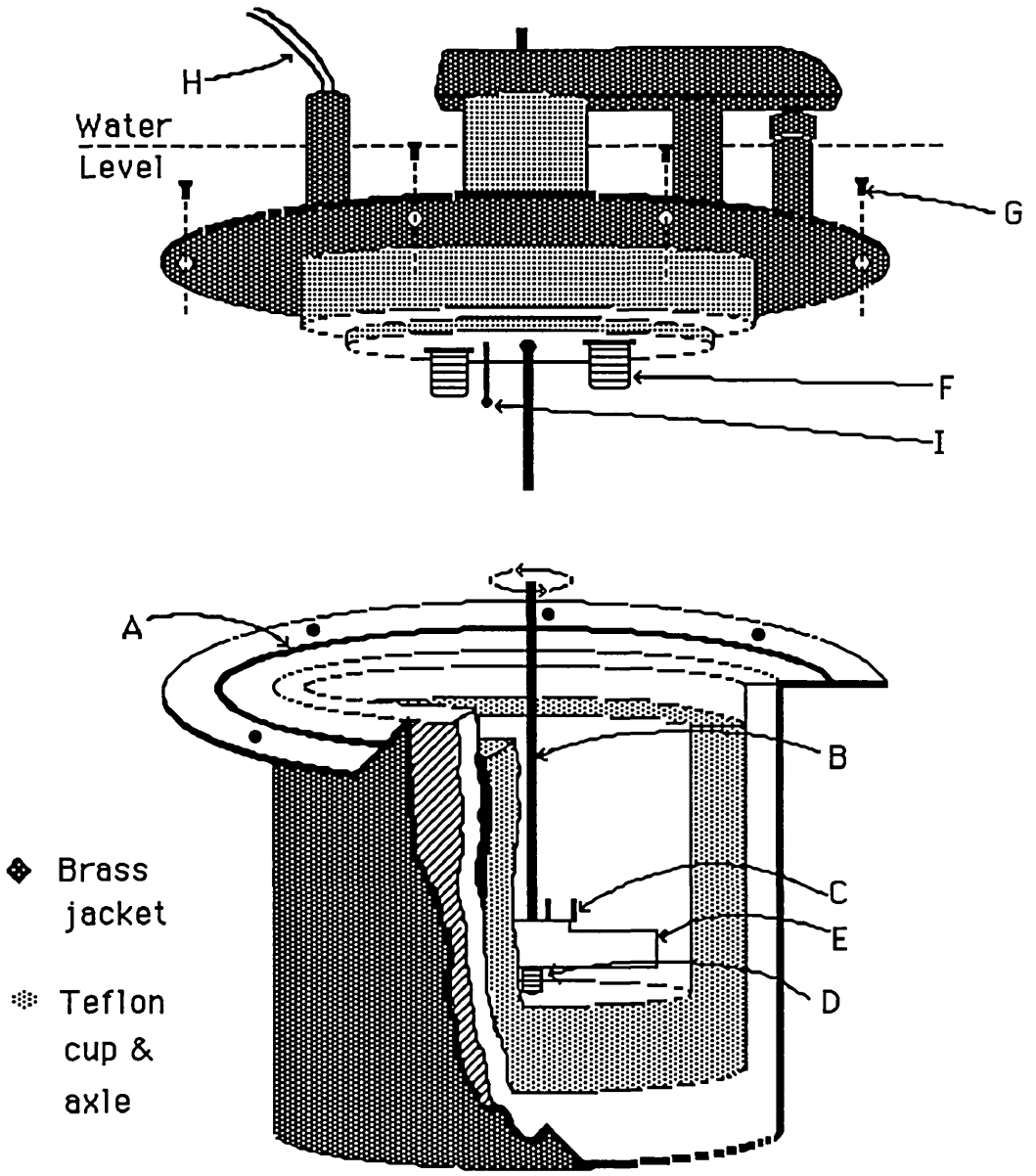
3.3. APPARATUS

The hydrolysis reactions were carried out in a solution calorimeter modified to cope specifically with our reactions. The dimensions of the calorimeter were as follows: height 55mm, diameter 45mm, wall thickness 4mm, and internal capacity 35ml. This small internal capacity made it possible to measure, with reasonable accuracy, the heats of hydrolysis of our reactions using small quantities of the expensive organoplatinum complexes.

The calorimeter was designed in order to minimise the amount of heat loss (see Fig. 3.10.) It consisted of a Teflon cup, surrounded by expanded mica insulation (Vermiculite), all enclosed within a brass jacket. Convection currents were reduced by allowing no large air gaps between the layers of these three materials. The calorimeter lid consisted of a Teflon axle which passed through the brass lid of the jacket. The lid was fastened tightly to the base of the calorimeter by six brass screws (G) with a water-tight seal being obtained by using a silicone O-ring (A). The whole set-up (as shown in Fig. 3.10.) was then immersed in a thermostatted water bath maintained at 25.0°C.

Also built into the calorimeter was a stainless steel stirrer (B) equipped with a Teflon blade (E), above which protruded four stainless steel spikes (C). This stirrer was secured in the bush

Fig. 3.10. **Calorimeter.**



(D) in the base of the Teflon cup. The stirrer had the dual purpose of agitating the reaction mixture at a constant rate and of breaking the glass ampoules containing the complex by way of the four raised spikes. The stirrer shaft ran through the Teflon axle and was coupled to an overhead stirrer motor.

From the underside of the calorimeter lid protruded a glass-bead thermistor (I) and two Nylon ampoule holders (F). The

thermistor was connected to the electrical circuit by means of two leads (H).

The calorimeter was water-tight when the brass lid was secured so long as the water level was below the level of the top of the Teflon axle.

Electrical circuit

The thermistor was incorporated as one of four arms of a Wheatstone Bridge circuit, the other three arms consisting of two fixed resistances and one variable resistance (Fig. 3.11.) This variable resistance had a range of 0 - 9999 Ω and could be varied by as little as 1 Ω to balance the bridge. Galvanometer, G, was a moving spot galvanometer and the power source was specially built to give a constant output current (400mA) and e.m.f. (5.75V)

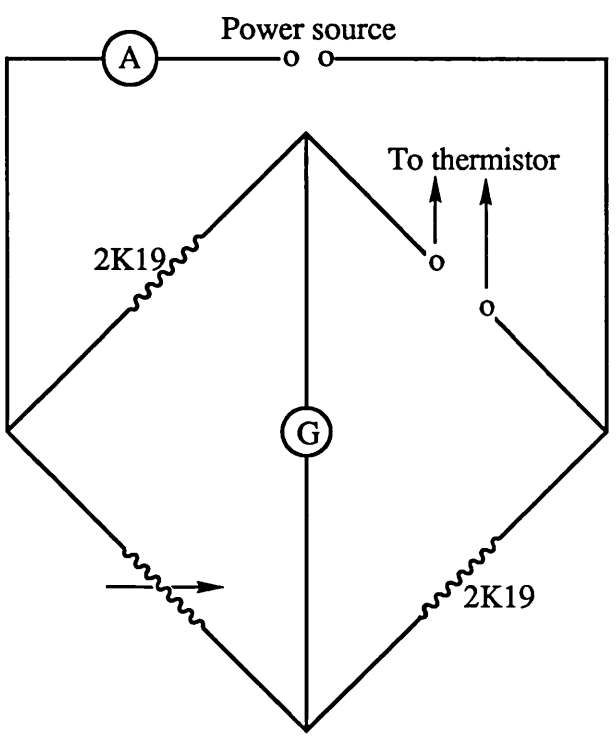


Fig. 3.11. **Electrical Circuit used to Measure the Resistance of the Thermistor.**

as the resistance of the thermistor depended to some degree on the current passing through it.

Temperature Characteristics of Thermistor

The thermistor was immersed in water at 29.00° C which was then allowed to cool slowly to 24.00° C. The resistance of the thermistor was measured at regular intervals together with the corresponding temperature (° C). The temperature was measured using a mercury thermometer accurate to 0.05° C.

A plot of the thermistor resistance (R) versus the water temperature (T° C) was not perfectly linear. A plot of lnR versus T did, however, display linear correspondence (Fig. 3.12.) Hence the correlation of R and T is: -

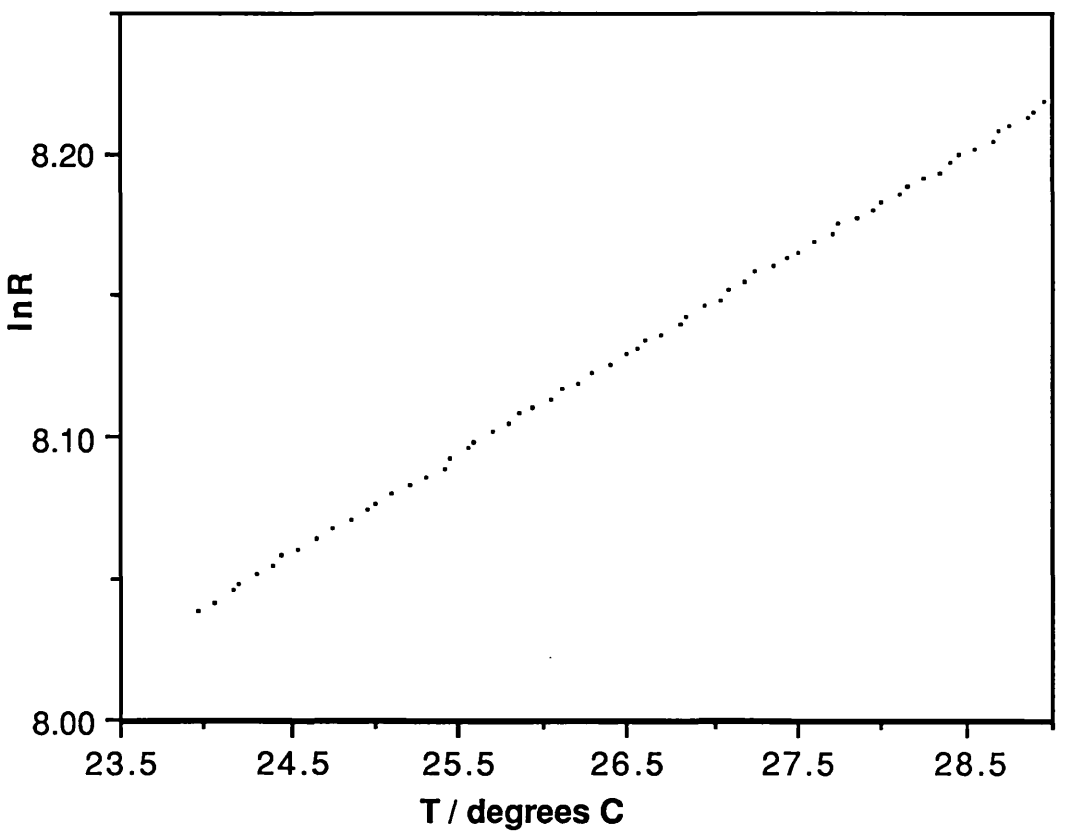


Fig. 3.12. **Temperature Characteristics of Thermistor.**

$T = A\ln R + B$ where A and B are constants characteristic of this particular thermistor.

Linear regression analysis of the data indicated: -

$\ln R = 3.55 \times 10^{-2} T + 7.19 \Rightarrow$

$T = 28.15 \ln R - 202.34$ . . . . . Equation 3.1.

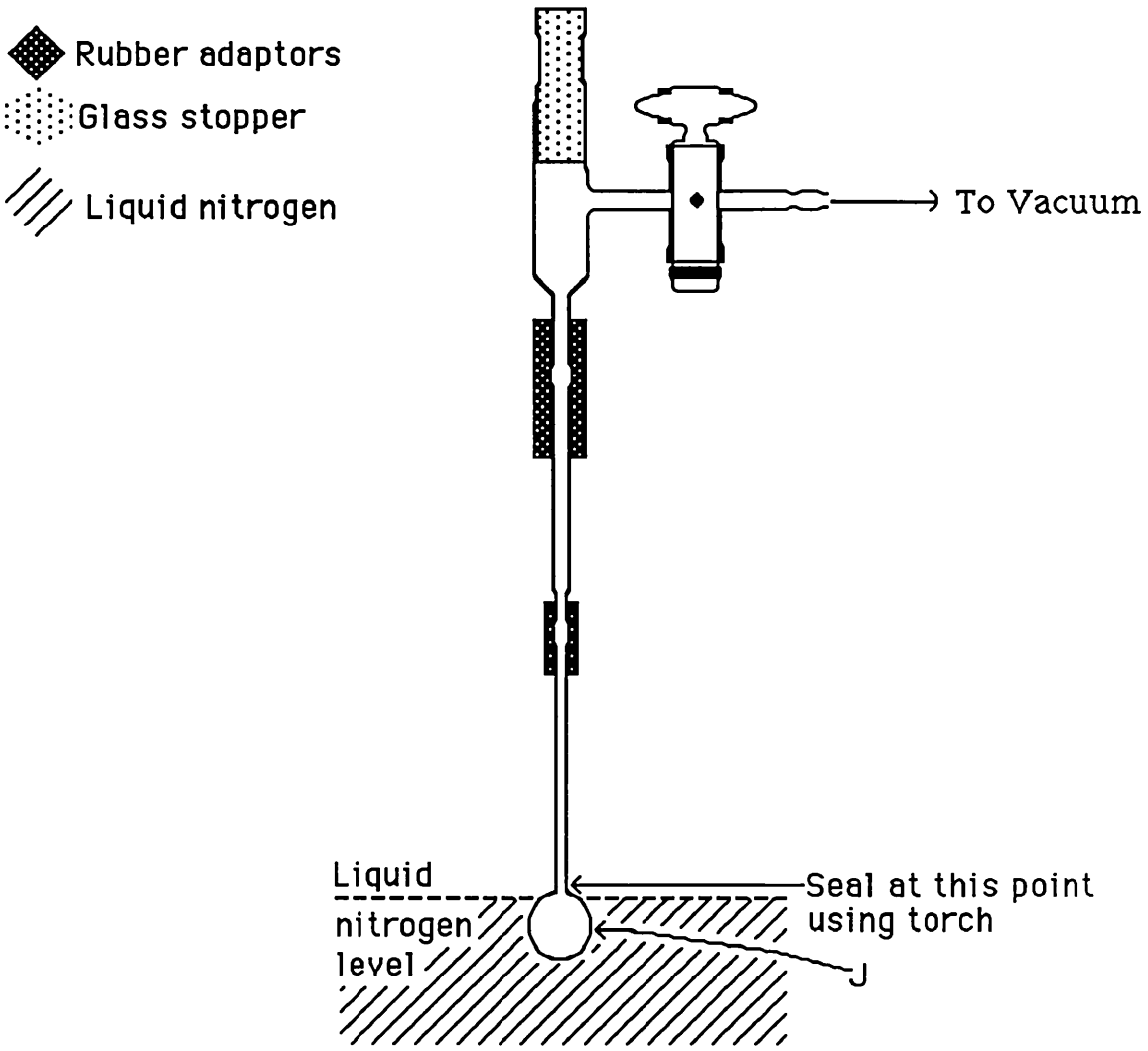
Bulb sealing

Blowing hot hollow glass tubing of the correct dimensions (ca. 4.5mm o.d. and 2.5mm i.d.) produced thin-walled bulbs (ca. 11.0mm o.d.) The thickness of the bulb walls were tested non-destructively by dropping the bulb onto a flat wooden surface from a height of 1cm and listening to the sound produced.

Clean dry bulbs were precisely weighed, filled with the required amount of sample and sealed *in vacuo* using the apparatus depicted in Fig. 3.13. The reason for sealing the bulbs at the base of the neck was to minimise the evacuated volume above the compound, into which some of the sample might be sucked on breaking (rather than all of it falling into the dioxane).

The bulb containing the compound was allowed to reach ambient temperature and the bulb, compound and remains of the neck reweighed together to allow calculation of the weight of compound in the bulb.

Fig. 3.13. **Apparatus for sealing bulbs.**



Calculation of ΔH.

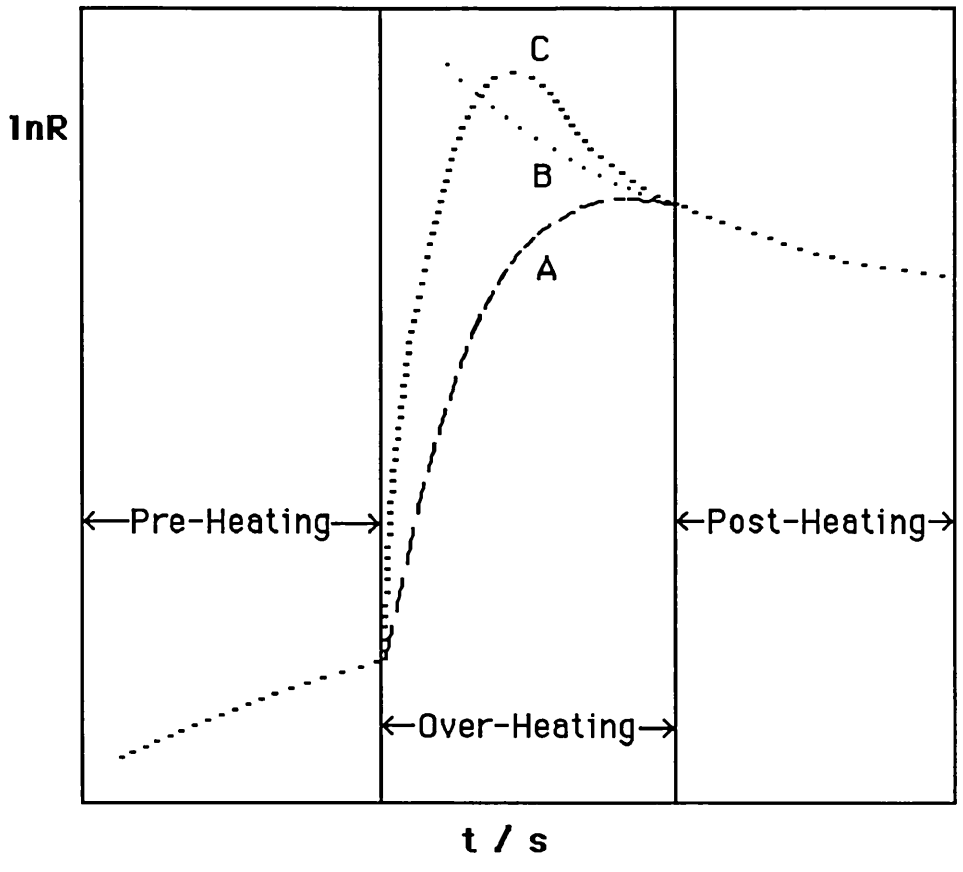
In a typical run the Teflon cup of the calorimeter was filled with 33.0mL of the HCl solution in dioxane. The bulb containing the compound was inserted into the Nylon ampoule holder and the lid then firmly secured onto the body of the calorimeter. The whole calorimeter was immersed in a water bath at 25.0° C and the solution stirred at a constant speed for twenty to forty minutes (depending on ambient temperature).

The thermistor resistance was monitored and after about ten readings, the bulb was broken and the temperature change and cooling curve (or warming curve if the process is endothermic) of the solution followed, using the resistance of the thermistor, for at least fifteen minutes.

A plot of the thermistor temperature (lnR) versus time displayed three different periods for an exothermic reaction (Fig. 3.14.); the pre-heating period, the over-heating period and the post-heating period (for an endothermic reaction they might be renamed appropriately). The pre-heating period represents the calorimeter and its contents approaching bath temperature (exponentially) before the bulb was broken. The post-heating period ensues after the reaction has occurred, where the calorimeter and its contents again approach the bath temperature exponentially. There is also a period between these two phases, starting just after the bulb has been broken, and lasting for various lengths of time (up to 10 minutes) where the cooling curve is not exponential.

In Fig. 3.14. the typical variation of the measured thermistor temperature (C) and the expected wall temperature (A), which is required in order to calculate the heat loss or gain, are shown. Consistent results are obtained if curve A is taken to be the mirror image of curve C, upto its maximum point, in curve B (the extrapolation of post-heating curve) and then linear down to the break point of the bulb.

The thermistor temperature and the wall temperature are the same when the calorimeter is at equilibrium which occurs only in the pre- and post-heating periods. During the over-heating



A - Expected Wall Temperature

B - Extrapolation of Post-Heating Period

C - Thermistor Temperature

Fig. 3.14. **Typical Plots of Thermistor and Wall Temperatures against Time for a Reaction Step.**

period the wall temperature lags behind the thermistor temperature due to the rapid heat change. As equilibrium is reattained, the wall temperature again approaches the thermistor temperature and the post-heating period is entered.

The reason that measurements were continued for at least fifteen minutes after the bulb was broken was to ensure that at least some measurements were on the exponential post-heating

part of this curve.

Newton's Law of Cooling (Equation 3.2.):-

$dT/dt = -k(T - T_o)$ . . . . . Equation 3.2.

where k is the Newton's Constant of the calorimeter.

was applied using values of the calorimeter wall temperature for T and T_o. This equation applies for systems near equilibrium which are undergoing slow change and therefore may be used for the pre-heating and post-heating periods but not during the over-heating period. As only data in the pre- and post-heating periods were used, the thermistor temperature could be substituted for the wall temperature in this Equation 3.2.

Calculating R_o

Tangents to the cooling curve at several points in the pre- and post-heating periods were obtained. Combining Equations 3.1. and 3.2:-

$dlnR/dt = (dR/dt) \times (dlnR/dR) = -k(lnR - lnR_o)$

$1/R \times dR/dt = -k(lnR - lnR_o)$ . . . . Equation 3.3.

For each calorimetric run, measured values of R, t and dR/dt (the gradient of the tangent) for both the pre- and post-heating curves allows calculation of R_o and k from Equation 3.3. Extrapolation of these curves to the time labelled t_f is, hence, possible.

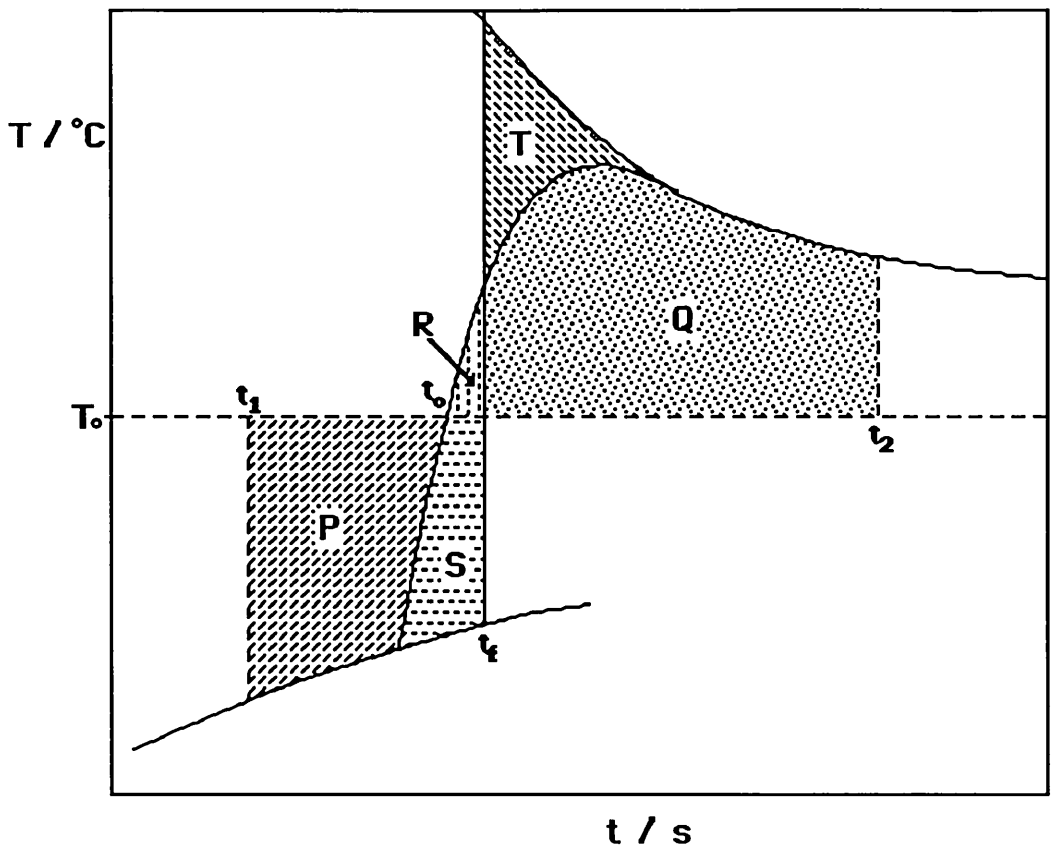


Fig. 3.15. **Typical Plot of T versus Time for a Reaction Step.**

Estimation of t_f

A vertical line at t_f in Fig. 3.15. corresponds to the hypothetical infinitely fast reaction, with the same ΔH as the real reaction, in which thermal equilibrium between the calorimeter wall and the solution is obtained instantaneously. There would hence be no heat loss or gain during the actual course of the reaction and $\Delta H_{reaction} = -K\Delta T = -K'\Delta \ln R$. An accurate estimation of t_f was necessary in order to find the $\Delta \ln R$ of this instantaneous reaction.

For the real reaction monitored between t_1 and t_2, the increase in heat when $T<T_o$, q_1, is given by the integration of

Equation 3.2. between t_o and t_1.

$$q_1 = -K.k\int_{t_0}^{t_1}(T-T_0)dt = -K.k.P$$

Similarly, the increase in heat when $T>T_o$, q_2, is given by integration between t_2 and t_o.

$$q_2 = -K.k\int_{t_0}^{t_2}(T-T_0)dt = -K.k\,(Q+R)$$

For the hypothetical reaction:-

$$\Delta H = \Delta H_{reaction} + P + S - Q - T$$

For the real reaction:-

$$\Delta H = \Delta H_{reaction} + P - Q - R$$

The ΔH of the hypothetical and real reactions are equivalent if R + S = T so the value of t_f is varied until this is true.

Calculation of R_f and R_i

From our knowledge of R_o and t_f, a value for R_f discounting the over-heating effects can be found. A plot of $\ln(\ln R - \ln R_o)$ against t is linear in the post-heating period but not linear in the over-heating period. By ignoring this over-heating period and extrapolating the linear section back to t_f, a reasonably accurate value for $\ln R_f - \ln R_o$, and hence for R_f may be obtained.

The value of R at the start of the hypothetical reaction, R_i,

can be similarly determined by simple extrapolation of $\ln(\ln R_o - \ln R)$ against t upto t_f. As the pre-heating curve is completely exponential before the bulb is broken, there is no difficulty in determining this value. The value of $\Delta \ln R$ or $\Delta \ln(R_f - R_i)$ which is proportional to ΔT and hence (for the constant heat capacity of the calorimeter and its contents) ΔH may be determined.

3.4. RESULTS

The reaction steps whose $\Delta \ln R$ values were measured are shown below:-

1 $Et_2NH_{(l)} + HCl_{(soln)} \rightarrow Et_2NH.HCl_{(c)}$

2 *trans*-$(Me_3P)_2Pt(CH_2CMe_3)Cl_{(c)} + HCl_{(soln)} \rightarrow$ *trans*-$(Me_3P)_2PtCl_{2(soln)} + Me_4C_{(l)}$

3 *trans*-$(Me_3P)_2Pt(CH_2SiMe_3)Cl_{(c)} + HCl_{(soln)} \rightarrow$ *trans*-$(Me_3P)_2PtCl_{2(soln)} + Me_4Si_{(l)}$

4 $Me_4C_{(l)} + HCl_{(soln)} \rightarrow Me_4C_{(soln)}$

5 $Me_4Si_{(l)} + HCl_{(soln)} \rightarrow Me_4Si_{(soln)}$

The similarity in reaction steps 2 and 3 and also 4 and 5 are obvious. From reaction steps 2 - 3 - 4 + 5, reaction step 6 is obtained. In doing this manipulation, it is assumed that the heats of vaporisation of the two organoplatinum complexes are similar. Also the heats of vaporisation of Me_4Si and Me_4C must be similar:-

6 *trans*-$(Me_3P)_2Pt(CH_2CMe_3)Cl_{(c)} + Me_4Si_{(l)} \rightarrow$ *trans*-$(Me_3P)_2Pt(CH_2SiMe_3)Cl_{(c)} + Me_4C_{(l)}$

Table 3.1.

$Et_2NH_{(l)}+HCl_{(soln)} \rightarrow Et_2NH.HCl_{(s)}$

ΔlnR	mmoles
29.403	1.272
32.022	1.313
40.458	1.560
42.859	1.658

trans- $(Me_3P)_2Pt(CH_2CMe_3)Cl_{(s)}+HCl_{(soln)} \rightarrow$ *trans-* $(Me_3P)_2PtCl_{2(soln)}$

ΔlnR	mmoles
16.172	0.961
19.136	1.096
24.783	1.338
30.611	1.684

trans- $(Me_3P)_2Pt(CH_2SiMe_3)Cl_{(s)}+HCl_{(soln)} \rightarrow$ *trans-* $(Me_3P)_2PtCl_{2(soln)}$

ΔlnR	mmoles
21.497	1.082
26.887*	1.538
27.240	1.304
32.089	1.557
41.188	1.936

$(CH_3)_4C_{(l)}+HCl_{(soln)} \rightarrow (CH_3)_4C_{(soln)}$

ΔlnR	mmoles
5.652	3.423
6.852	4.681
8.940	5.565
7.615	4.165
9.335	6.547

$(CH_3)_4Si_{(l)}+HCl_{(soln)} \rightarrow (CH_3)_4Si_{(soln)}$

ΔlnR	mmoles
2.551	3.527
3.492	4.062
5.215	5.183
6.372	4.832
7.531	5.142

* Data point ignored as more than 2 standard deviations from best-fit line.

The ΔlnR values for measurements on individual reaction steps (1-5) are shown above (Table 3.1.) For each reaction step at least four measurements were obtained. From Table 3.1:-

$\Delta lnR(1)mmol^{-1} = 24.8 \pm 1.4$

$\Delta lnR(2)mmol^{-1} = 17.8 \pm 0.8$

$\Delta lnR(3)mmol^{-1} = 20.7 \pm 0.6$

$\Delta lnR(4)mmol^{-1} = -1.6 \pm 0.2$

$\Delta lnR(5)mmol^{-1} = -1.1 \pm 0.3$

$\Delta lnR(6)mmol^{-1} = -2.4 \pm 1.1$

From reaction step 1, ΔlnR = 24.8 but $\Delta H^{o} = -141.3 \pm 5.0$ kJ mol^{-1}. So there is a scaling factor of -5.69×10^{3} between ΔlnR and ΔH^{o}. Using this scaling factor, $\Delta H^{o}(6) = 13.7 \pm 6.0$ kJ mol^{-1}. This means that $E(Pt\text{-}CH_2CMe_3) - E(CH_2SiMe_3) \approx 14 \pm 6$ kJ mol^{-1}.

3.5. DISCUSSION

Related observations.

Some relative metal-carbon bond strengths of compounds containing alkyl groups with and without β-Si atoms have been measured previously. A proportion of this work has featured direct calorimetric measurement of metal-carbon bond strengths, mostly on neopentyl and trimethylsilylmethyl complexes (Table 3.2.) For the homoleptic alkyls studied, the metal-carbon bond strengths are likely to be quite accurate. But for the complexes with other supporting ligands, it is felt that the accuracy of the

Table 3.2.

Previously Determined Metal-Carbon Bond Strengths for Neopentyl and Trimethylsilylmethyl Complexes.

Compound	$E(M\text{-}C)_{gas}$
$Cp^*_2Th(CH_2CMe_3)_2$	302 (16)[58]
$Cp^*_2Th(CH_2SiMe_3)_2$	336 (14)[58]
$Cp^*_2Th(CH_2CMe_3)(O\text{-}t\text{-}C_4H_9)$	322 (16)[58]
$Cp^*_2Th(CH_2SiMe_3)(O\text{-}t\text{-}C_4H_9)$	346 (14)[58]
$Cp_3Th(CH_2CMe_3)$	326 (13)[59]
$Cp_3Th(CH_2SiMe_3)$	360 (15)[59]
$(Me_3SiC_5H_4)_3U(CH_2SiMe)_3$ [a]	164 (10)[61]
$Cp^*_2U(CH_2SiMe_3)_2$ [b]	307 (14)[60]
$Ti(CH_2CMe_3)_4$	184 (8)[62]
$Ti(CH_2SiMe_3)_4$	268 (8)[62]
$Zr(CH_2CMe_3)_4$	226 (8)[62]
$Zr(CH_2SiMe_3)_4$	314 (8)[62]
$Hf(CH_2CMe_3)_4$	243 (8)[62]
$Zn(CH_2CMe_3)_2$	175 [63]
$Zn(CH_2SiMe_3)_2$	195 [63]
py(saloph)Co-CH_2CMe_3	75 [72,73]

[a] $E(U\text{-}R)_{soln}$ [b] Average of both $E(U\text{-}R)_{gas}$

metal-carbon bond strengths determined is likely to be less, due to the difficulty of apportioning the heats of reaction to several dissimilar metal-ligand bonds; all that may accurately be determined is the relative order of the metal-carbon bond

strengths. These data show that for all the directly comparable pairs of neopentyl and trimethylsilylmethyl complexes, the metal-carbon bond for the trimethylsilylmethyl complex is stronger than that for the neopentyl complex.

The differences in the Th-C bond strengths could be due, however, to the greater steric demands of the neopentyl ligand around the metal.[15,46,47,74-79,82-85] Table 3.3. shows evidence from the literature that the coordinated neopentyl group is more bulky close to the metal centre than is the coordinated trimethylsilylmethyl group. Much of this evidence comes from the measurement of the degree of association of complexes in solution in benzene.

At least one author[76] has attributed the lower thermal stability of a neopentyl complex relative to the analogous trimethylsilylmethyl complex (in this case UR_8.3dioxan) to these steric differences. Such disparates could also be responsible for the weakness (relative to the trimethylsilylmethyl analogues) of the above U-CH_2CMe_3, Th-CH_2CMe_3, Ti-CH_2CMe_3, Zr-CH_2CMe_3, Hf-CH_2CMe_3 and Co-CH_2CMe_3 bonds, but are unlikely to be the cause of the weak Zn-CH_2CMe_3 bond in the linear zinc dialkyl.

Another general impression is the greater thermolytic inertness of compounds containing β-Si atoms over those containing β-C atoms[15,26,50] although this is not always the case[80,81]. This might arise in some part from the thermodynamics of greater Pt-C bond strengths in the former but is more likely to be a predominantly kinetic effect, as argued in Chapter 4.

One major reservation about Table 3.2. is that none of the compounds shown in Table 3.2. contain Group VIII metals, whereas

Table 3.3. **Comparison of Steric Hindrance in Analagous Neopentyl and (Trimethylsilyl)methyl Complexes.**

NEOPENTYL COMPLEXES	(TRIMETHYLSILYL)METHYL COMPLEXES	REFERENCE
Exchange of the mutually *trans*- trimethylphosphine ligands (*cis*- to the $-CH_2CMe_3$ group) with $P(CD_3)_3$ in *cis*- $L_4Os(H)(CH_2CMe_3)$ is more rapid than for the equivalent $-CH_2SiMe_3$ complex.	Exchange of the mutually *trans*- trimethylphosphine ligands is less rapid in *cis*- $L_4Os(H)(CH_2SiMe_3)$ than in the equivalent $-CH_2CMe_3$ complex.	45-47
$Al(CH_2CMe_3)_3$ is monomeric in solution in benzene.	$Al(CH_2SiMe_3)_3$ is a mixture of monomers and dimers in solution in benzene.	82,83
$Be(CH_2CMe_3)_2$ is a mixture of monomers and dimers in solution in benzene.	$Be(CH_2SiMe_3)_2$ is dimeric in solution in benzene.	80
$Mg(CH_2CMe_3)_2$ is trimeric in solution in benzene.	$Mg(CH_2SiMe_3)_2$ is polymeric and insoluble in benzene.	78
Solid $Mn(CH_2CMe_3)_2$ is tetrameric.	Solid $Mn(CH_2SiMe_3)_2$ is an infinite polymer.	79
$(CH_2CMe_3)(Cl)Hf[N(SiMe_3)_2]_2$ but not $(CH_2CMe_3)_2Hf[N(SiMe_3)_2]_2$ has been isolated.	Both $(CH_2SiMe_3)(Cl)Hf[N(SiMe_3)_2]_2$ and $(CH_2SiMe_3)_2Hf[N(SiMe_3)_2]_2$ have been isolated.	76-77

most of the best understood rearrangements are for Group VIII metal compounds. So uptil now, for Group VIII metals we have had to rely on more indirect evidence of the relative metal-carbon bond strengths.

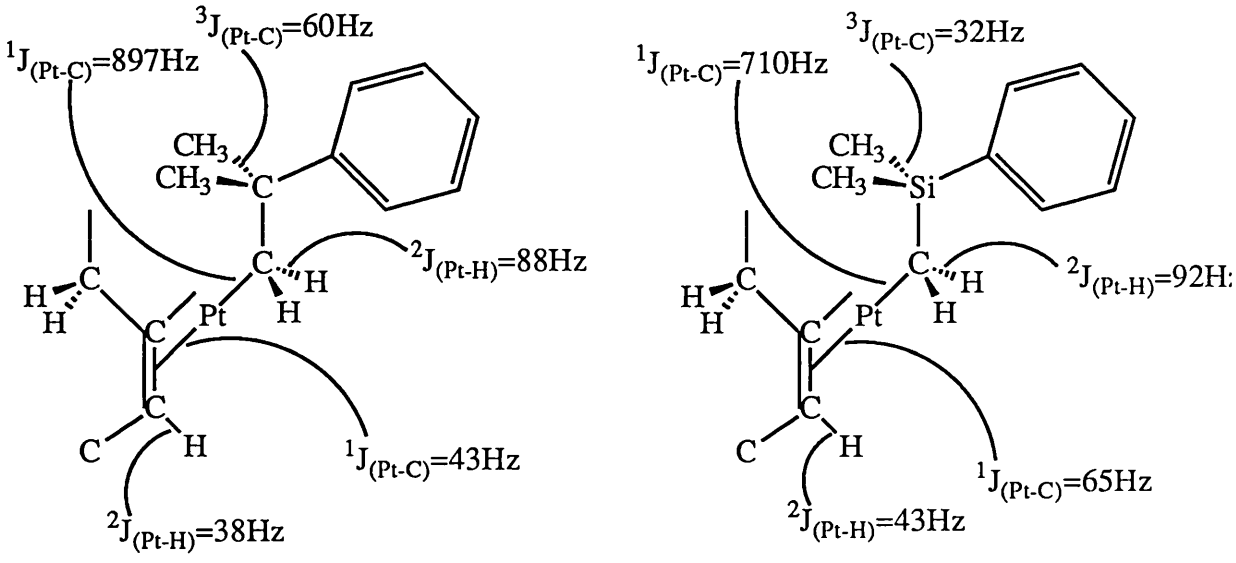


Fig. 3.16. **Comparative NMR Characteristics for (cod)Pt(CH_2CMe_2Ph)$_2$ and (cod)Pt(CH_2SiMe_2Ph)$_2$.**

Crystal structures have been obtained for the two analogous compounds (cod)Pt(CH_2CMe_2Ph)$_2$ and (cod)Pt(CH_2SiMe_2Ph)$_2$.[13] This has shown the Pt-C(alkyl) bond lengths in the two compounds to be very similar; 2.110 (9) and 2.084 (8) Å for the former and 2.060 (12) and 2.053 (10) Å for the latter; implying that the difference in the Pt-C bond strengths between the two compounds is small.

At first sight it would seem that the Pt-CH_2 bonds in (cod)Pt(CH_2SiMe_2Ph)$_2$ are slightly stronger than the Pt-CH_2 bonds in (cod)Pt(CH_2CMe_2Ph)$_2$ because of the slight shortening of the former as compared to the latter. Yet this seems to be in direct

contradiction to the platinum-carbon coupling constants for the same bonds ($^1J_{(Pt-C)}$ is 897Hz for neophyl and 710Hz for sila-neophyl. Fig. 3.16.) which seems to indicate the opposite order of relative bond strengths in the two compounds.

So we may say that either the platinum-carbon bond lengths are a good indication of platinum-carbon bond strengths or else platinum-carbon coupling-constants are a good measure of platinum-carbon bond strengths. Actually the truth may be that neither are ideal indicators of bond strength. Bond lengths will depend to a large extent on the steric requirements of the alkyl group. As the coordinated neophyl group is more bulky close to the platinum atom than the sila-neophyl group[15,46,47,74-77] the Pt-C bond length would have been expected to be longer in the neophyl complex than in the sila-neophyl complex. This same bulkiness of the alkyl groups may force a rehybridization around the β-C or Si and so alter the amount of s- and p-character in the Pt-C bond, factors upon which Pt-C coupling constant depend greatly.

At this point it should be pointed out that β-C atoms giving rise to larger Pt-CH_2 coupling constants than their β-Si analogues is quite a general phenomenon. For example, the pair of model compounds chosen for our solution calorimetry studies exhibited this phenomenon. Figs. 3.18. and 3.17. show the resonances due to the methylene carbon (as a triplet of triplets) in the proton-decoupled ^{13}C NMR spectra of the trimethylsilylmethyl and neopentyl complexes. From these the $^1J_{(Pt-C)}$ can be measured as 650.7Hz (for X=Si) and 748.5Hz (for X=C); the quintet in Fig.3.17. is due to the phoshine methyls and occurs at a similar shift in the spectrum of the trimethylsilylmethyl complex.

Fig. 3.17.

^{13}C-{^{1}H} n.m.r. of methylene carbons for *trans* -$(Me_3P)_2Pt(CH_2CMe_3)Cl$ in $CDCl_3$

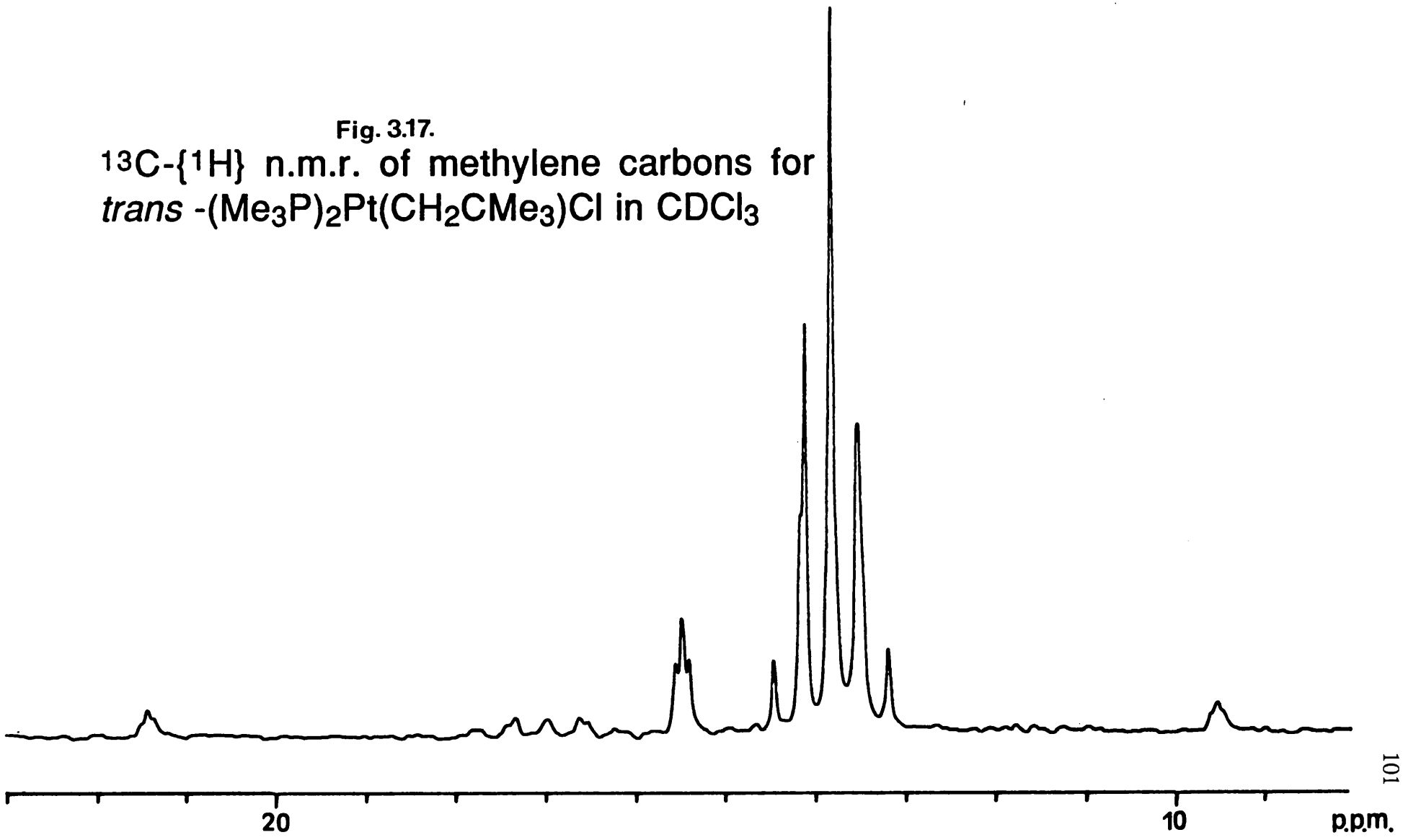
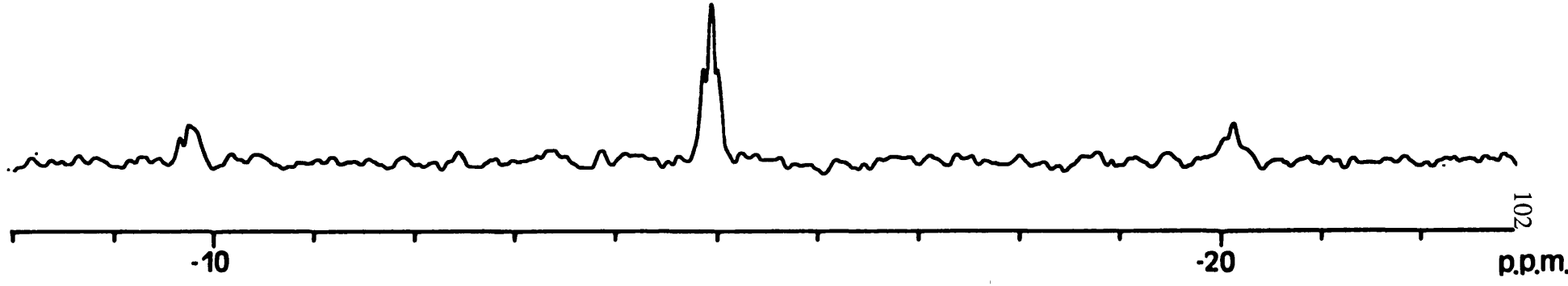


Fig 3.18.

^{13}C-{^{1}H} n.m.r. of methylene carbons for *trans* -$(Me_3P)_2Pt(CH_2SiMe_3)Cl$ in $CDCl_3$



Present Calorimetric Results.

Our calorimetric results indicate that the Pt-C bond in the neopentylplatinum complex is stronger than the same bond in the trimethylsilylmethylplatinum complex by 8-20 kJ mol^{-1}. The order of these relative bond strengths are the reverse of that for every previously reported pair of M-C bond strengths in analagous neopentyl and trimethylsilylmethyl complexes. This could be because, as mentioned earlier, this is the first system measured where M is a Group VIII metal.

As the greater stability of trimethylsilylmethyl complexes over neopentyl complexes may not be due to the former having the greater metal-carbon bond strengths, we feel that it may be a kinetic effect (Chapter 4) arising from a greater *trans*- effect of the neopentyl group. Whether this greater *trans*- effect is at least partially due to the greater steric hindrance around the platinum centre caused by the neopentyl group is not known.

CHAPTER FOUR

Relative *Trans*-Effects and *Trans*-Influences of the Neopentyl and Trimethylsilylmethyl Ligands in *Trans*-$(Me_3P)_2Pt(CH_2SiMe_3)Cl$ and *Trans*-$(Me_3P)_2Pt(CH_2CMe_3)Cl$.

4.1. INTRODUCTION

In an effort to understand the general thermolytic lability of complexes with β-C atoms compared with their β-Si analogues, the Pt-C bond strengths in the two complexes *trans*-$(Me_3P)_2Pt(CH_2CMe_3)Cl$ and *trans*-$(Me_3P)_2Pt(CH_2SiMe_3)Cl$ were investigated (*vide supra*). It was found that *trans*-$(Me_3P)_2Pt(CH_2CMe_3)Cl$ had a Pt-C bond strength significantly greater than that of *trans*-$(Me_3P)_2Pt(CH_2SiMe_3)Cl$. In other words, the thermodynamic trend is the reverse of that expected in lability.

An alternative explanation is that these differences are kinetically induced by the disparate *trans*-effects of the Me_3SiCH_2- and Me_3CCH_2- ligands. An attempt was made to quantify this difference in the two organoplatinum analogues by measuring the rate of substitution of the chloro-substituent by methoxide anion in methanol solution.

The relative *trans*-influences of the two alkyl ligands were also determined by measuring the platinum-chlorine stretching frequency [υ(Pt-Cl)].

4.2. EXPERIMENTAL

General and Instrumental.

IR and ^{31}P NMR spectra were measured as in Chapter 1. UV-vis spectra were measured in solution in MeOH on a Philips PU 8740 UV/VIS scanning spectrophotometer using matched quartz cells and MeOH (HPLC Grade) as a reference.

Measurement of Pt-Cl Stretching Frequencies.

The IR spectra of samples of $(Me_3P)_2Pt(CH_2SiMe_3)Cl$ and $(Me_3P)_2Pt(CH_2CMe_3)Cl$, prepared as in Chapter Three, were measured between 2000 and 220cm^{-1}.

IR (cm^{-1}):-

$(Me_3P)_2Pt(CH_2SiMe_3)Cl$; υ(Pt-Cl) 280s, $\upsilon(P\text{-}C)_{sym}$ 675s[86], 1423m, 1300m, 1284s, 1276s, 1235s, 1020m, 974s, 946vs (br), 850s, 825s, 770m, 740s, 675s, 607w, 538m, 349s, 315w, 265s, 254s, 248w, 244w, 234w, 221w.

$(Me_3P)_2Pt(CH_2CMe_3)Cl$; υ(Pt-Cl) 262m, $\upsilon(P\text{-}C)_{sym}$ 675m[86], 1422m, 1354m, 1304w, 1287m, 1279m, 1241m, 1152m, 951vs (br), 858m, 745m, 735s, 342w, 244w, 232w, 223w.

Measurement of UV-vis Spectra.

UV-vis spectra of 3.0 x 10^{-4}M methanol solutions of $(Me_3P)_2Pt(CH_2SiMe_3)Cl$ and $(Me_3P)_2Pt(CH_2CMe_3)Cl$ were measured between 210 and 900nm. The two spectra were very similar showing two bands and a shoulder. Each compound had an intense band centred at about 210nm. The exact wavelength and molar extinction coefficient are not known as the band leads off the edge of the spectrum. The second band occurs at 247.2nm (ε = 8400) for $(Me_3P)_2Pt(CH_2SiMe_3)Cl$ and at 250.4nm (ε = 5300) for $(Me_3P)_2Pt(CH_2CMe_3)Cl$. This band has a shoulder in both compounds, 270nm (ε = 4300) for $(Me_3P)_2Pt(CH_2SiMe_3)Cl$ and 280 (ε = 1000) for $(Me_3P)_2Pt(CH_2CMe_3)Cl$.

Reaction of $(Me_3P)_2Pt(CH_2SiMe_3)Cl$ and $(Me_3P)_2Pt(CH_2C$-$Me_3)Cl$ with $NaOBu^t$.

3.50mL of 3.0 x 10^{-4}M solutions (1.05μmol) of $(Me_3P)_2Pt(CH_2$-$CMe_3)Cl$ or $(Me_3P)_2Pt(CH_2SiMe_3)Cl$ in methanol were added to solid $NaOBu^t$ (105μmol, 10.1mg) in a UV cell (the volume of the solution and hence the absolute concentrations of reactants clearly change slightly on addition to the $NaOBu^t$.) The time of addition was noted and the UV-vis spectrum (220-320nm) measured at three minute intervals. The spectra are shown in Figs. 4.1. and 4.2. respectively.

For $(Me_3P)_2Pt(CH_2CMe_3)Cl$ the intense band centred at about 210nm increased in intensity (or shifted to longer wavelength) and the peak at 250.4nm disappeared. In its place appeared a new peak at 273.6nm. From the rate of increase of the absorbance of this peak, we could tell that the reaction was complete after about 10 minutes (Fig. 4.1.)

The $(Me_3P)_2Pt(CH_2SiMe_3)Cl$ complex behaved similarly, the 210nm peak growing or shifting, the 247.2nm peak disappearing and a new peak appearing at 265.2nm. However the increase in absorbance of this peak continued well after ten minutes and even after 18 minutes the reaction was still incomplete (Fig. 4.2.)

In solution in MeOH both $NaOBu^t$ and $KOBu^t$ rapidly and quantitatively form MeO^- and it is the latter which attacks the organoplatinum complexes (*vide infra.*) However $KOBu^t$ was easier to handle than than NaOMe and its greater relative molecular mass allowed more accurate determination of the concentrations of MeO^- solutions. Hence $KOBu^t$ was used to generate the MeO^- *in situ* in all the kinetic runs.

From the above qualitative data it appears that the rate of

attack of $^{-}$OMe on $(Me_3P)_2Pt(CH_2CMe_3)Cl$ was greater than its rate of attack on $(Me_3P)_2Pt(CH_2SiMe_3)Cl$.

Products of Reaction of $^{-}$OMe with $(Me_3P)_2Pt(CH_2SiMe_3)Cl$ and $(Me_3P)_2Pt(CH_2CMe_3)Cl$.

^{31}P NMR studies on the reactions of $(Me_3P)_2Pt(CH_2SiMe_3)Cl$ and $(Me_3P)_2Pt(CH_2CMe_3)Cl$ with OMe^- in d_4-methanol showed the formation of two products (both of them *trans-* and visible as 1:4:1 triplets) from each of the organoplatinum precursors.

Trans-$(Me_3P)_2Pt(CH_2SiMe_3)Cl$ [^{31}P NMR, (d_4-MeOH) -10.81 ppm, t, $^1J_{(Pt-P)}$=2760 Hz] reacted with eight equivalents of $KOBu^t$ (or NaOMe) to give two triplets at -8.98 ppm (t, $^1J_{(Pt-P)}$=2909 Hz) and -17.90 ppm (t, $^1J_{(Pt-P)}$=2647 Hz). The triplet at -8.98 ppm appeared first but after about one hour stopped increasing in intensity. As a small amount of insoluble white solid started to precipitate out after about one hour it may be that this triplet at -8.98 ppm is due to this white solid. The other triplet at -17.90 ppm started to appear later but its intensity overtook that of the triplet at -8.98 ppm after about one and a half hours.

Trans-$(Me_3P)_2Pt(CH_2CMe_3)Cl$ [^{31}P NMR, (d_4-MeOH) -9.77 ppm, t, $^1J_{(Pt-P)}$=2929 Hz) reacted with eight equivalents of $KOBu^t$ (or NaOMe) to give two triplets at -8.73 ppm (t, $^1J_{(Pt-P)}$= 3059 Hz) and -18.32 ppm (t, $^1J_{(Pt-P)}$=2747 Hz). Again the triplet at -8.73 ppm appeared first but stopped increasing in intensity after about half an hour with concomitant production of a trace of an insoluble white solid. The other triplet at -18.32 ppm started to appear later but its intensity overtook that of the triplet at -8.73 ppm after about one hour.

Measurement of Kinetics of Reaction of $^{-}$OMe with $(Me_3P)_2Pt(CH_2SiMe_3)Cl$ and $(Me_3P)_2Pt(CH_2CMe_3)Cl$.

The reaction was monitored by UV-vis spectroscopy because ^1H NMR was unsuitable due to the large excess of $KOBu^t$ required. Additionally, the reaction was too fast to be followed by ^{31}P NMR [as the acquisition time for viable signal-to-noise ratios was several half-lives in the reaction of $(Me_3P)_2Pt(CH_2CMe_3)Cl$).]

The wavelengths at which the reactions were observed were 265.2 nm for $(Me_3P)_2Pt(CH_2SiMe_3)Cl$ and 273.6 nm for $(Me_3P)_2Pt(CH_2CMe_3)Cl$. Pseudo-first order conditions were imposed throughout and all runs were carried out at 20±1°C.

Standard stock 2.80 x 10^{-3} M [(0.40 x 10^{-3} x 0.50)/3.50] solutions of $(Me_3P)_2Pt(CH_2SiMe_3)Cl$ and $(Me_3P)_2Pt(CH_2CMe_3)Cl$ were made up in methanol. A similar standard stock solution of $KOBu^t$ in methanol was made up. Its concentration was (z x 0.40 x 10^{-3} x 3.50)/3.00 where z is the molar excess of $KOBu^t$ (values of z used were 50, 100, 150 and 200.) These stock solutions were prepared fresh every day and were used within a few hours of their making.

3.00mL of the standard $KOBu^t$ solution was pipetted into one of the UV cells. To this was added by pipette 0.50mL of the solution of the organoplatinum complex, the reaction mixture shaken and placed into the spectrometer (which takes 30 seconds) and the reaction followed for at least three half-lives. At each concentration of $KOBu^t$ (or MeO^-) the reaction was repeated at least once.

To calculate k_{obsd} (*vide infra*) the absorbances of the reaction mixtures at infinite time and at the instant that the reactants were mixed were required. The former was

Table 4.1.

Measured Values for k_{obsd} for the Reaction of MeO^- with *Trans*-$(Me_3P)_2Pt(CH_2EMe_3)Cl$ (where E=Si or C) at 20±1°C.

$(Me_3P)_2Pt(CH_2CMe_3)Cl$

$[MeO^-]$ / M	$10^3 k_{obsd}$ / s^{-1}
0.020	6.522
0.020	7.119
0.040	9.149
0.040	9.748
0.060	12.035
0.060	11.319
0.080	12.955
0.080	12.506

$(Me_3P)_2Pt(CH_2SiMe_3)Cl$

$[MeO^-]$ / M	$10^4 k_{obsd}$ / s^{-1}
0.020	7.857
0.020	8.005
0.040	10.347
0.040	10.624
0.040	7.233*
0.060	13.159
0.060	13.583
0.080	16.272
0.080	15.362

* Data point ignored as more than 2 standard deviations from best-fit line.

straightforward; after each run was completed for at least three half-lives, the reaction mixture was left in the spectrometer for a further four half-lives and the final absorbance taken to be A_∞. A_0 was estimated by adding the 0.50mL of the organoplatinum complex to 3.00mL of pure methanol in the UV cell and measuring its absorbance. This method can only give a good estimate of A_0

as it ignores any absorption due to the Bu^tOH (formed from $KOBu^t$ and MeOH.)

4.3. RESULTS

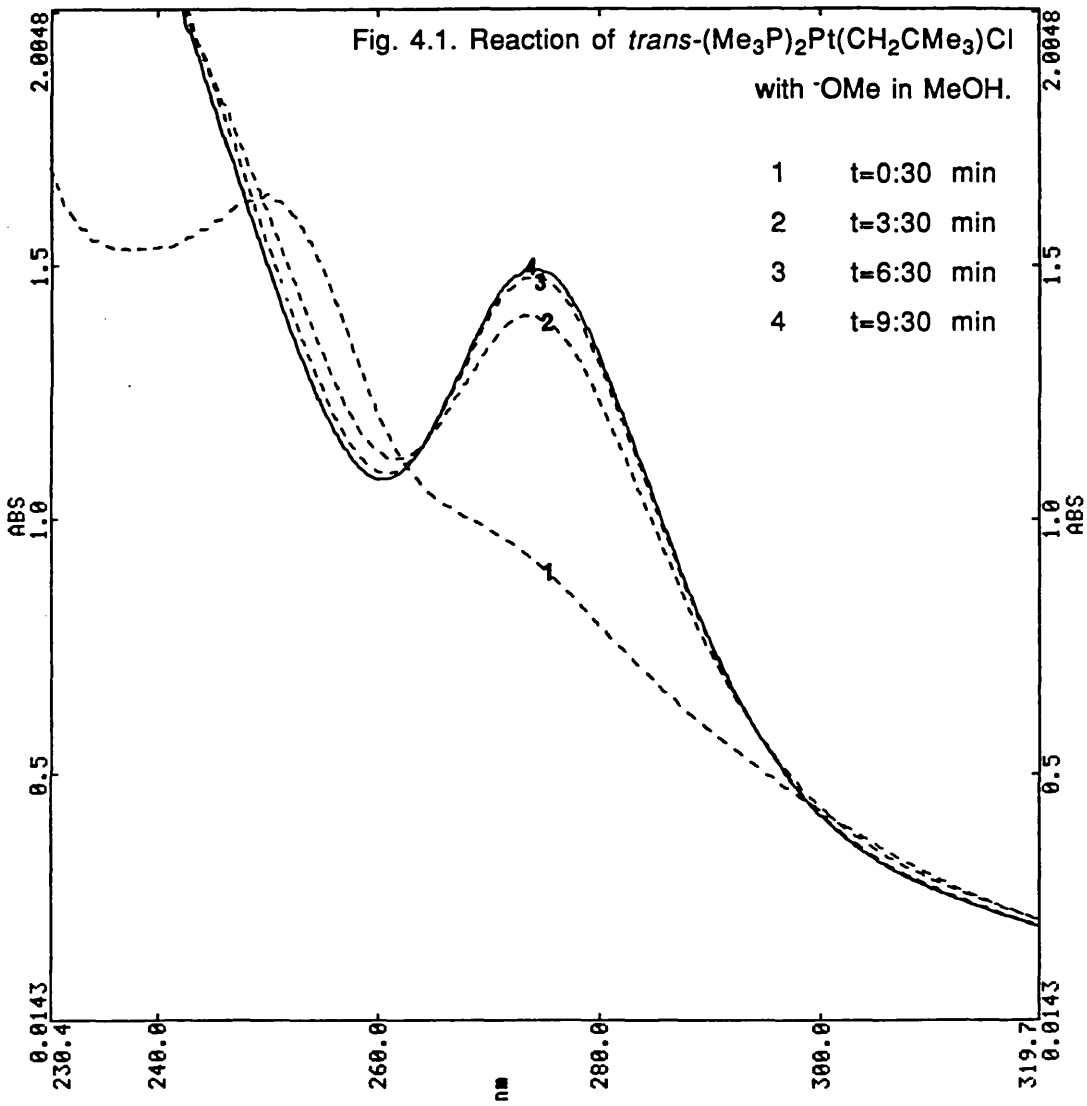
By following the reactions of the organoplatinum complexes with MeO^- on an NMR scale we detected two products for each reaction (both of which, by ^1H and ^{31}P NMR, still contain one alkyl group and two *trans-* phosphines) whose concentrations vary with time (over a period of many hours.) But when following the reaction by UV-vis spectroscopy the reactions are complete within one and a half hours to give products with UV-vis spectra very similar to the starting organoplatinum complexes.

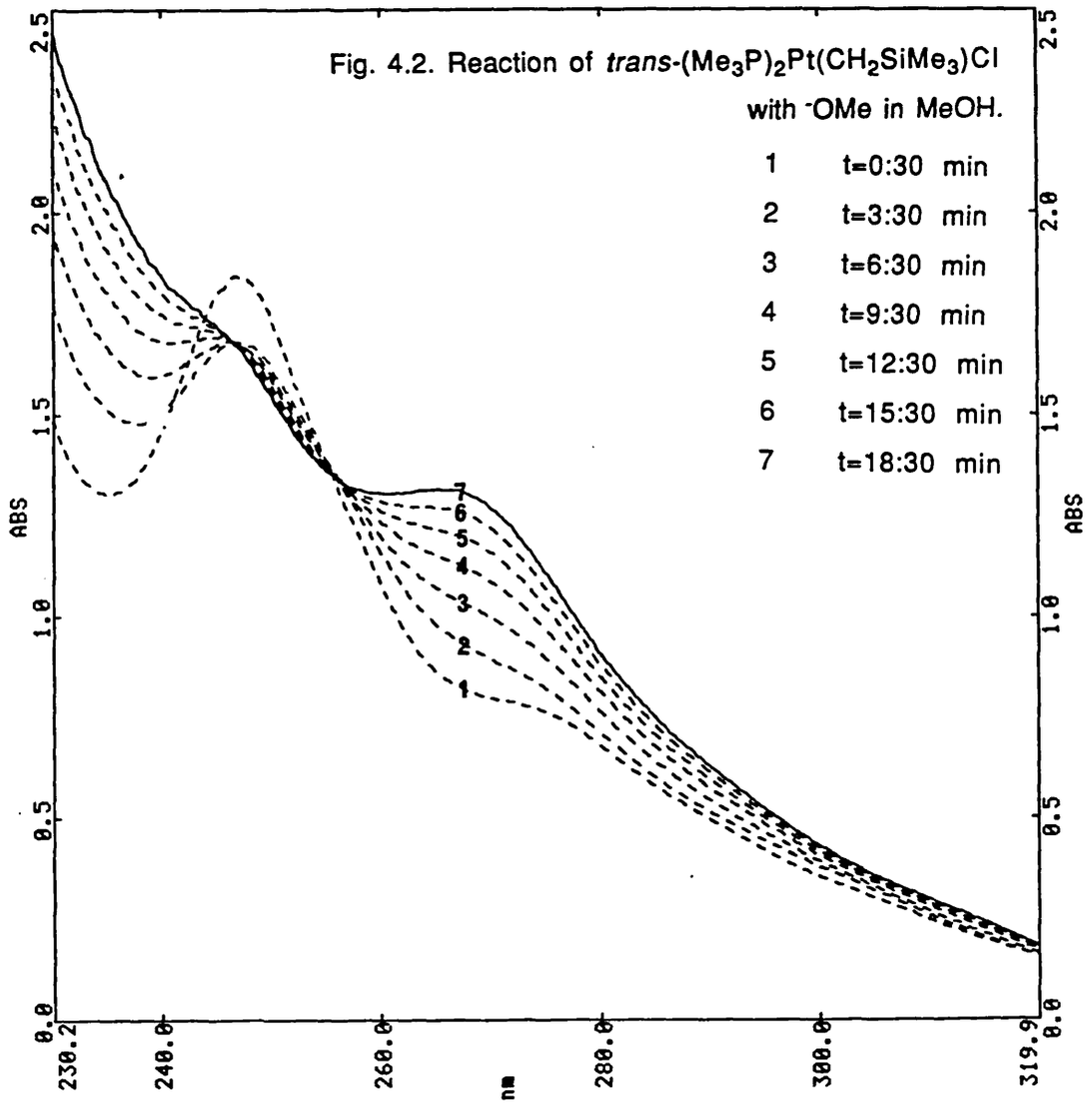
The reactions that we have followed by kinetics occur in very dilute solution and with a large excess of MeO^- and do not neccessarily give two products each, as they do in concentrated solution and with a lower excess of MeO^- on an NMR scale.

The kinetic data obtained was analysed below as if the reaction of MeO^- with the organoplatinum complexes were simple substitutions. If the organoplatinum complexes had reacted under the conditions of the kinetic runs to give two different complexes each, then the results would still be meaningful as, with the alkyl and two *trans-* phosphines present in the products, it would seem that substitution of MeO^- had occurred initially at the chloride with a subsequent rearrangement.

$$X + OMe^- \rightarrow Y + Cl^-$$

where X = *trans*-$(Me_3P)_2Pt(CH_2EMe_3)Cl$ and Y is an unknown product.


Fig. 4.1. Reaction of trans-(Me3P)2Pt(CH2CMe3)Cl
with -OMe in MeOH.
1 t=0:30 min
2 t=3:30 min
3 t=6:30 min
4 t=9:30 min
ABS
2.0048
1.5
1.0
0.5
0.0143
230.4
240.0
260.0
280.0
300.0
319.7
nm


Fig. 4.2. Reaction of *trans*-$(Me_3P)_2Pt(CH_2SiMe_3)Cl$
with ^-OMe in MeOH.
1 t=0:30 min
2 t=3:30 min
3 t=6:30 min
4 t=9:30 min
5 t=12:30 min
6 t=15:30 min
7 t=18:30 min
ABS
nm
230.2
240.0
260.0
280.0
300.0
319.9
0.0
0.5
1.0
1.5
2.0
2.5

$$-d[X]/dt = k_{obsd}[X]$$

$\Rightarrow$ $\int(d[X]/[X]) = -\int k_{obsd}dt$ (integrating between t and 0)

$\Rightarrow$ $\ln([X]_t/[X]_o) = -k_{obsd}t$

As $[X]_t = [X]_o - [Y]_t$

$\Rightarrow$ $\ln\{([X]_o - [Y]_t)/[X]_o\} = -k_{obsd}t$

Now if A_x is the absorbance due to X and A_y the absorbance due to Y: -

$$A_t = A_x + A_y$$

Using a 1cm path length: -

$A_x = -\varepsilon_x[X]_t$ and $A_y = -\varepsilon_y[Y]_t$

$\Rightarrow$ $\varepsilon_x = -A_o/[X]_o$ and $\varepsilon_y = -A_\infty/[X]_o$

$$A_t = (A_o[X]_t/[X]_o) + (A_\infty[Y]_t/[X]_o)$$

$\Rightarrow$ $A_t - A_o = \{(A_o[X]_t) + (A_\infty[Y]_t) - (A_o[X]_o)\}/[X]_o$

$\Rightarrow$ $A_t - A_o = \{(A_\infty[Y]_t) - A_o([X]_o - [X]_t)\}/[X]_o$

$\Rightarrow$ $A_t - A_o = \{(A_\infty[Y]_t) - (A_o[Y]_t)\}/[X]_o$

$\Rightarrow$ $[Y]_t = [X]_o(A_t-A_o)/(A_\infty-A_o)$

Plotting $-\ln\{([X]_o-[Y]_t)/[X]_o\}$ against t for various concentrations of MeO^- gave straight lines (for at least three half-lives) of gradient k_{obsd}.

A plot of k_{obsd} against [$^-$OMe] for both the compounds gave straight lines which did not pass through the origin. This implies that attack on the organoplatinum complexes is by both MeO^- and

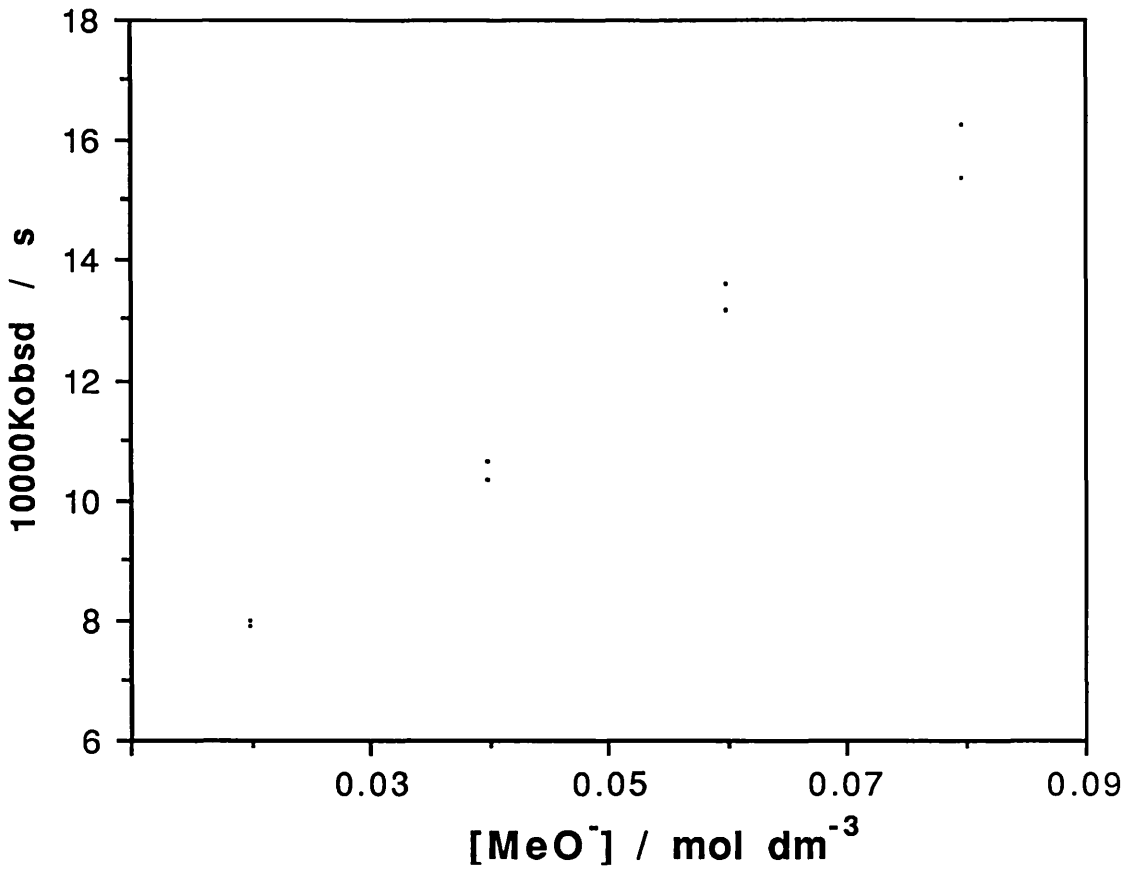


Fig. 4.3. **Graph of 10^4 k_{obsd} against [$^-$OMe] for the Reaction with $(Me_3P)_2Pt(CH_2SiMe_3)Cl$.**

MeOH. Such a two-term rate law is characteristic[87] of associative nucleophilic substitution reactions in square-planar metal complexes. k_{obsd} has contributions from attack by two different nucleophiles:-

$k_{obsd} = k_1 + k_2[OMe^-]$ where $k_1 = k_s[MeOH] = 26k_s$

k_1 and k_2 for both substitution reactions are derived from the intercepts and gradients of Figs. 4.3. and 4.4. These are shown in Table 4.2. The significance of both k_1 and k_2 for the reaction of $(Me_3P)_2Pt(CH_2CMe_3)Cl$ with MeO^- being approximately ten times

greater than for the same reaction with $(Me_3P)_2Pt(CH_2SiMe_3)Cl$ is that both MeO^- and MeOH nucleophilicly attack the former more rapidly than the latter.

The standard deviations in k_1 and k_2 for $(Me_3P)_2Pt(CH_2SiMe_3)Cl$ are smaller than for $(Me_3P)_2Pt(CH_2CMe_3)Cl$. This is due to the fact that the reaction of $(Me_3P)_2Pt(CH_2CMe_3)Cl$ with MeO^- in methanol is near to the limits of this experimental method. The slower reaction of $(Me_3P)_2Pt(CH_2SiMe_3)Cl$ with MeO^- in methanol shows much smaller standard deviations.

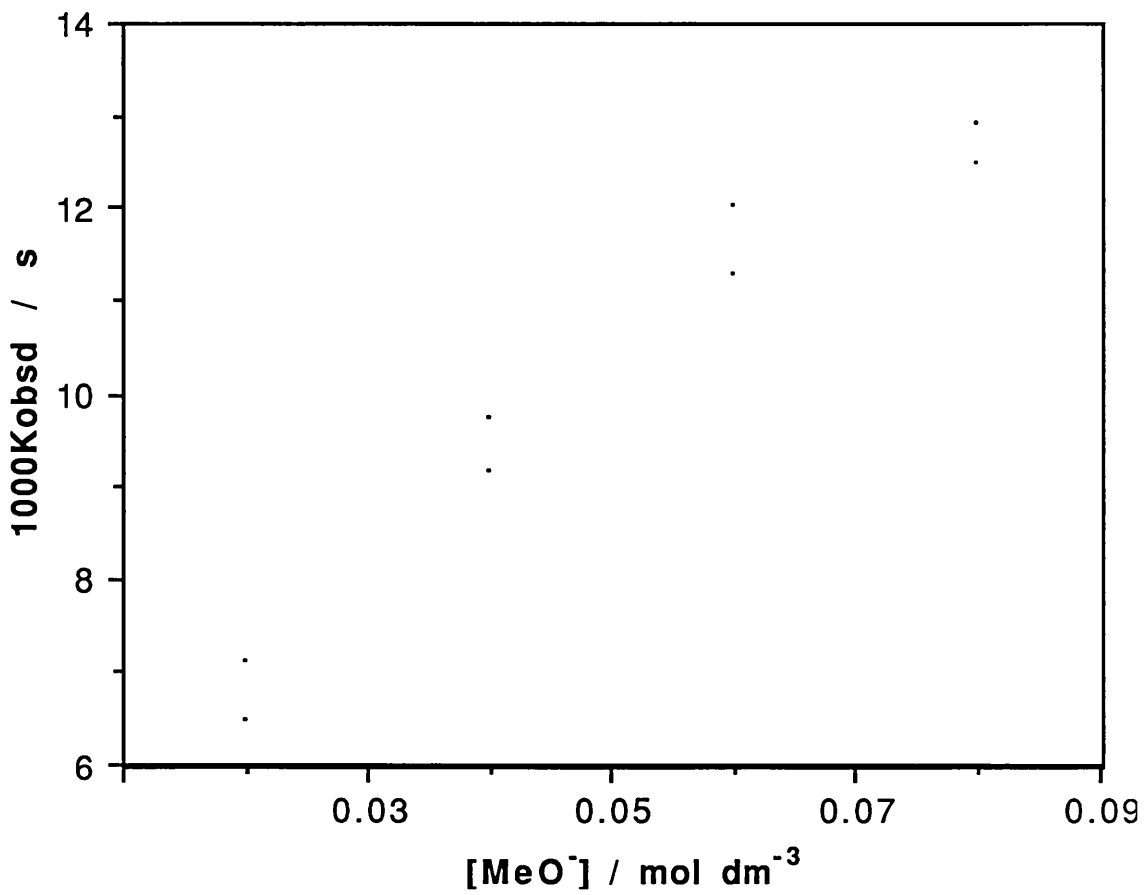


Fig. 4.4. **Graph of 10^3 k_{obsd} against [$^-$OMe] for the Reaction with $(Me_3P)_2Pt(CH_2CMe_3)Cl$.**

Table 4.2.

Measured k_1 and k_2 Values and their Standard Deviations at 20±1°C for the Reaction of MeO^- with *Trans*-$(Me_3P)_2Pt(CH_2EMe_3)Cl$ (where E = Si or C).

	$(Me_3P)_2Pt(CH_2CMe_3)Cl$	$(Me_3P)_2Pt(CH_2SiMe_3)Cl$
k_1	$5.18 \times 10^{-3}\ s^{-1}$	$5.27 \times 10^{-4}\ s^{-1}$
σ_1	0.54×10^{-3}	0.24×10^{-4}
k_2	$9.98 \times 10^{-2}\ M^{-1}s^{-1}$	$1.33 \times 10^{-2}\ M^{-1}s^{-1}$
σ_2	0.99×10^{-2}	0.04×10^{-2}

4.4. DISCUSSION

Only one Pt-Cl stretching frequency is expected in the IR spectrum of *trans*-$(Me_3P)_2Pt(CH_2EMe_3)Cl$. This peak was found at $280cm^{-1}$ when E = Si and at $262cm^{-1}$ when E = C, which may be compared with the *trans*-monoalkylmonochloroplatinum complexes in Table 4.3.

It has previously been observed[91] that ligands coordinated to a metal by a σ-C atom tend to have a high *trans*-influence as manifested by low platinum-chlorine stretching frequencies. We may see that in our two model complexes the $-CH_2CMe_3$ and $-CH_2SiMe_3$ ligands are no exception to this.

Table 4.3.

Platinum-Chlorine Stretching Frequencies in various *Trans*-Organoplatinum Complexes.

Complex	υ (cm^{-1})	Reference
$(Et_3P)_2PtMeCl$	274	88
$(Ph_2MeP)_2PtMeCl$	272	89
$(Et_3P)_2PtPhCl$	270	88
$(Ph_2MeP)_2Pt(CF_3)Cl$	302	89
$(Ph_2MeP)_2Pt(C_2F_5)Cl$	302, 315[a]	89
$(Ph_2MeP)_2Pt(CH_2SMe)Cl$	282	90
$(Ph_3P)_2Pt(CH_2SMe)Cl$	272	90

[a] Peak split by solid state effects

If the platinum-chlorine stretching frequency can be taken as a measure of the platinum-chlorine bond strength, then the order of the *trans*- influences of the two alkyls is $-CH_2CMe_3 > -CH_2SiMe_3$. Insertion of $-C_6H_5$, $-CH_3$ and other alkyl ligands in Table 4.3. into this series, remembering that for these complexes the platinum-chlorine stretching frequencies were measured in complexes containing other phosphines as supporting ligands (the platinum-chlorine stretching frequency is only slightly dependent on the nature of the *cis*- ligands[91]) now gives the *trans*-influence series shown: -

$$-CH_2CMe_3 > -C_6H_5 \geq -CH_3 > -CH_2SMe \geq -CH_2SiMe_3 > -CF_3 \geq -C_2F_5$$

This series should not be regarded as being invariant for all metal complexes. Obviously the strength of the *trans*-influence of a ligand depends to some extent on the environment in which it finds itself; on the nature of the metal, the other ligands and the coordination geometry. As well as the difference in phosphine ligands in the above series, other factors indicate that the series may not be too rigorous: -

i) The difference in the platinum-chlorine stretching frequencies between the two end members of the above series (-CH_2CMe_3 and -C_2F_5) is only 50cm^{-1} when compared to the possible range in frequencies of over 100cm^{-1} in similar complexes of the type *trans*-$(PEt_3)_2PtXCl$[91] where X is not necessarily a σ-C donor ligand.

ii) The change in relative molecular mass of the alkyl group causes the P_2PtR- group to also change in mass slightly and so alter the platinum-chlorine stretching frequency to a small extent, regardless of any change in the platinum-chlorine bond strength. This factor is likely to be very small for the -CH_2CMe_3, -CH_2SiMe_3 and -C_6H_5 complexes where the alkyl groups have similar relative molecular masses.

Measurements of the relative *trans*-influences of the neopentyl and trimethylsilylmethyl ligands in *cis*-$(R'_3P)_2Pt(CH_2EMe_3)_2$ (by $^1J_{(Pt-P)}$) and $(cod)Pt(CH_2EMe_3)_2$ (by $^1J_{(Pt-C)}$) have also been measured. Similarly the relative *trans*-influences of the neophyl and sila-neophyl ligands in $(cod)Pt(CH_2EMe_2Ph)_2$ have been measured. These data all have the alkyl group with the β-Si atom exerting a greater *trans*-influence than the group with the β-C atom.

There has been some other recent work to show that an

alkyl group with a β-Si atom has a greater *trans*-effect than its non-substituted analogue. This investigation[13] has involved measuring the rate of substitution of d_0-PPh_3 by d_{15}-PPh_3 *trans*- to the neophyl and sila-neophyl groups in *cis*-$(Ph_3P)_2Pt(CH_2CMe_2Ph)(CH_2SiMe_2Ph)$. The phosphine *trans*- to the neophyl group has been established to undergo substitution at the greater rate, in broad agreement with the observations here.

It seems that, in planar tetracoordinate platinum (II) complexes, the presence of a β-C (as opposed to a β-Si) atom in the alkyl chain both weakens and labilises the *trans*- bond. This labilising effect may contribute to the greater inertness of trimethylsilylmethyl and sila-neophyl complexes relative to their neopentyl and neophyl analogues.

REFERENCES

1. D. C. Griffiths and G. B. Young, *Polyhedron* , 1983 , **2** ,1095.
2. D. C. Griffiths, L. G. Joy, A. C. Skapski, D. J. Wilkes and G. B. Young, *Organometallics* , 1986 , **5** , 1744.
3. D. C. Griffiths and G. B. Young , *Organometallics* , 1989 , **8** , 875.
4. S. I. Black and G. B. Young, *Polyhedron* , 1989 , **8** , 585.
5. E. Carmona, F. Gonzalez, M. L. Poveda, J. L. Atwood and R. D. Rogers, *J. Chem. Soc., Dalton Trans.*, 1980 , 2108.
6. E. Carmona, F. Gonzalez, M. L. Poveda, J. L. Atwood and R. D. Rogers, *J. Chem. Soc., Dalton Trans.*, 1981 , 777.
7. E. Carmona, F. Gonzalez, M. L. Poveda and J. M. Marin, *Synth. React. Inorg. Met.-Org. Chem.*, 1982 , **12** , 185.
8. E. Carmona, M. Paneque, M. L. Poveda, R. D. Rogers and J. L. Atwood, *Polyhedron* , 1984 , **3** , 317.
9. E. Carmona, P. Palma, M. Paneque, M. L. Poveda, E. Gutierrez-Puebla and A. Monge, *J. Am. Chem. Soc.* , 1986 , **108** , 6424.
10. E. Carmona, M. Paneque, M. L. Poveda, E. Gutierrez-Puebla and A. Monge , *Polyhedron* , 1989 , **8** , 1069.
11. S. K. Thomson and G. B. Young, *Polyhedron* , 1988 , **7** , 1953.
12. B. C. Ankianiec and G. B. Young, *Polyhedron* , 1989 , **8** , 57.
13. B. C. Ankianiec. Ph. D. Thesis. University of London.
14. G. W. Parshall, *J. Am. Chem. Soc.* , 1974 , **96** ,2360.
15. T. H. Tulip and D. L. Thorn, *J. Am. Chem. Soc.*, 1981 , **103** , 2448.
16. S. E. Himmel and G. B. Young, *Organometallics* , 1988 , **7** , 2440.
17. P. M. Maitlis and F. G. A. Stone, *Chem. Ind.* , 1962 , 1865.

18. J. Lau and R. Sustmann, *Tet. Lett.*, 1985 , **26** , 4907.
19. R. Sustmann and J. Lau, *Chem. Ber.*, 1986 , **119** , 2531.
20. T. Ito, H. Tsuchiya and A. Yamamoto, *Bull. Chem. Soc. Jpn.*, 1977 , **50** , 1319.
21. F. Ozawa, T. Ito and A. Yamamoto, *J. Am. Chem. Soc.*, 1980 , **102** , 6457.
22. F. Ozawa and A. Yamamoto, *Chem. Lett.*, 1981 , 289.
23. F. Ozawa, T. Ito, Y. Nakamura and A. Yamamoto, *Bull. Chem. Soc. Jpn.*, 1981 , **54** , 1868.
24. G. Oehme and A. Modler, *Z. Anorg. Allg. Chem.*, 1979 , **449** , 157.
25. R. Tooze, K. W. Chiu and G. Wilkinson, *Polyhedron* , 1984 , **3** 1025.
26. B. Wozniak, J. D. Ruddick and G. Wilkinson, *J. Chem. Soc. (A)* 1971 , 3116.
27. M. Bochmann, G. Wilkinson and G. B. Young, *J. Chem. Soc., Dalton Trans.*, 1980 , 1879.
28. G. Yoshida, H. Kurosawa and R. Okawara, *J. Organomet. Chem.*, 1976 , **113** , 85.
29. K. Miki, Y. Kai, N. Yasuoka and N. Kasai, *J. Organomet. Chem.*, 1979 , **165** , 79.
30. P. Diversi, D. Fasce and R. Santini, *J. Organomet. Chem.,* 1984 **268** , 285.
31. J. R. Doyle, P. E. Slade and H. B. Jonassen, *Inorg. Synth.*, **6** , 218.
32. E. C. Constable, *Polyhedron* , 1983 , **2** , 551.
33. R. D. Gillard, *Coord. Chem. Rev.*, 1975 , **16** , 67.
34. N. Serpone, *Coord. Chem. Rev.*, 1983 , **50** , 209.
35. R. D. Gillard, R. J. Lancashire and P. A. Williams, *Transition*

Met. Chem., 1979 , **4** , 115.

36. K. R. Seddon, J. E. Turp, E. C. Constable and O. Wernberg, *J. Chem. Soc., Dalton Trans.*, 1987 , 293.
37. P. B. Hitchcock, K. R. Seddon, J. E. Turp, Y. Z. Yousif, J. A. Zora, E. C. Constable and O. Wernberg, *J. Chem. Soc., Dalton Trans.*, 1988 , 1837.
38. D. W. Clack, L. A. P. Kane-Maguire, D. W. Knight and P. A. Williams, *Trans. Met. Chem.*, 1980 , **5** ,376.
39. D. W. Clack and R. D. Gillard, *Trans. Met. Chem.*, 1985 , **10** , 419.
40. P. A. Lay, *Inorg. Chem.*, 1984 , **23** , 4775.
41. E. C. Constable, *Inorg. Chim. Acta.*, 1986 , **117** , L33.
42. H. Bredereck, R. Gompper and H. Herlenger , *Chem. Ber.*, 1958, **91** , 2832.
43. T. D. Heyes and J. C. Roberts, *J. Chem. Soc.*, 1951 , 328.
44. R. K. Harris, 'Nuclear Magnetic Resonance Spectroscopy'. Longman Group UK Ltd, 1983.
45. J. F. Eastham and S. C. Watson, *J. Organomet Chem.*, 1967 , **9** 165.
46. a) P. J. Desrosiers, R. S. Shinomoto and T. C. Flood, *J. Am. Chem. Soc.*, 1986 , **108** , 1346.
    b) P. J. Desrosiers, R. S. Shinomoto and T. C. Flood, *J. Am. Chem. Soc.*, 1986 , **108** , 7964.
47. T. G. P. Harper, R. S. Shinomoto, M. A. Deming and T. C. Flood, *J. Am. Chem. Soc.*, 1988 , **110 ,** 7915.
48. J. A. Statler, G. Wilkinson, M. Thornton-Pett and M. B. Hursthouse, *J. Chem. Soc., Dalton Trans.,* 1984 , 1731.
49. J. W. Bruno, T. J. Marks and L. R. Morss, *J. Am. Chem. Soc.*, 1983 , **105** , 6824.

50. J. W. Bruno, G. M. Smith, T. J. Marks, C. K. Fair, A. J. Schultz and J. M. Williams, *J. Am. Chem. Soc.,* 1986 , **108** , 40.

51. R. A. Andersen, R. A. Jones and G. Wilkinson, *J. Chem. Soc., Dalton Trans.,* 1978 , 446.

52. L. Andreucci, P. Diversi, G. Ingrosso, A. Lucherini, F. Marchetti, V. Adovasio and M. Nardelli, *J. Chem. Soc., Dalton Trans.,* 1986 , 477.

53. P. Foley and G. M. Whitesides, *J. Am. Chem. Soc.*, 1979 , **101** , 2732.

54. P. Foley, R. DiCosimo and G. M. Whitesides, *J. Am. Chem. Soc.*,1980 , **102** , 6713.

55. S. S. Moore, R. DiCosimo, A. F. Sowinski and G. M. Whitesides, *J. Am. Chem. Soc.*, 1981 , **103** , 948.

56. S. K. Thomson and G. B. Young, *Organometallics,* 1989 , **8** , 2068.

57. T. Behling, G. S. Girolami, G. Wilkinson, R. G. Somerville and M. B. Hursthouse, *J. Chem. Soc., Dalton Trans.*, 1984 , 877.

58. C. M. Fendrick and T. J. Marks, *J. Am. Chem. Soc.*, 1984 , **106** , 2214.

59. D. C. Sonnenberger, L. R. Morss and T. J. Marks, *Organometallics,* 1985 , **4** , 352.

60. J. W. Bruno, H. A. Stecher, L. R. Morss, D. C. Sonnenberger and T. J. Marks, *J. Am. Chem. Soc.*, 1986 , **108** , 7275.

61. L. E. Schock, A. M. Seyam, M. Sabat and T. J. Marks, *Polyhedron* , 1988 , **7** , 1517.

62. M. F. Lappert, D. S. Patil and J. B. Pedley, *J. Chem. Soc., Chem. Comm.*, 1975 , 830.

63. I. E. Gümrükçüoglü, J. Jeffrey, M. F. Lappert, J. B. Pedley and A. K. Rai, *J. Organomet. Chem.*, 1988, **341** , 53.

64. S. J. Ashcroft and C. T. Mortimer, *J. Chem. Soc. (A)* , 1967 , 930.

65. R. L. Brainard, T. M. Miller and G. M. Whitesides, *Organometallics* , 1986 , **5** , 1481.

66 R. L. Brainard, W. R. Nutt, T. R. Lee and G. M. Whitesides, *Organometallics* , 1988 , **7** , 2379.

67. J. W. Bruno, T. J. Marks and V. W. Day, *J. Am. Chem. Soc.*, 1982 , **104** , 7357.

68. C. M. Fendrick and T. J. Marks, *J. Am. Chem. Soc.*, 1986 , **108**, 425.

69. G. M. Smith, J. D. Carpenter and T. J. Marks, *J. Am. Chem. Soc.*, 1986 , **108** , 6805.

70. G. Alibrandi, D. Minniti, R. Romeo, P. Uguagliati, L. Calligaro and U. Belluco, *Inorg. Chim. Acta* , 1986 , **112** , L15.

71. J. X. McDermott, J. F. White and G. M. Whitesides, *J. Am. Chem. Soc.* , 1976 , **98** , 6521.

72. T. T. Tsou, M. Loots and J. Halpern, *J. Am. Chem. Soc.*, 1982 **104** , 623.

73. J. Halpern, *Polyhedron* , 1988 , **7** , 1483.

74. R. A. Andersen, *J. Organomet. Chem.*, 1980 , **192** , 189.

75. R. A. Andersen, *Inorg. Chem.* , 1979 , **18** , 2928.

76. E. R. Sigurdson and G. Wilkinson, *J. Chem. Soc., Dalton Trans.*, 1977 , 812.

77. R. A. Andersen and G. Wilkinson, *J. Chem. Soc., Dalton Trans.*, 1977 , 809.

78. R. A. Andersen, E. Carmona-Guzman, J. F. Gibson and G. Wilkinson, *J. Chem. Soc., Dalton Trans.*, 1976 , 2204.

79. G. E. Coates and B. R. Francis, *J. Chem. Soc. (A)* , 1971 , 1309.

80. M. R. Collier, M. F. Lappert and R. Pearce, *J. Chem. Soc.,*

Dalton Trans., 1973 , 445.

81. P. J. Davidson, M. F. Lappert and R. Pearce, *J. Organomet. Chem.*, 1973 , **57** , 269.
82. O. T. Beachley Jr. and L. Victoriano, *Organometallics* , 1988 , **7** , 63.
83. J. Z. Nyathi, J. M. Ressner and J. D. Smith, *J. Organomet. Chem.* , 1974 , **70** , 35.
84 O. T. Beachley Jr., C. Tessier-Youngs, R. G. Simmons and R. B. Hallock, *Inorg. Chem.* , 1982 , **21** , 1970.
85. O. T. Beachley Jr. and C. Tessier-Youngs, *Organometallics,* 1983 , **2** , 796.
86. D. M. Adams, J. Chatt and B. L. Shaw, *J. Chem. Soc.*, 1960 , 2047.
87. F. Basolo and R. G. Pearson, 'Mechanisms of Inorganic Reactions'. J. Wiley and Sons, New York, 1958.
88. D. M. Adams, J. Chatt, J. Garratt and A. D. Westland, *J. Chem. Soc. (A)* , 1964 , 734.
89. M. A. Bennett, H. K. Chee and G. B. Robertson, *Inorg. Chem.*, 1979, **18** , 1061.
90. G. Yoshida, H. Kurosawa and R. Okawara, *J. Organomet. Chem.*, 1977 , **131** , 309.
91. T. G. Appleton, H. C. Clark and L. E. Manzer, *Coord. Chem. Rev.*, 1973 , **10** , 335.